



UNIVERSITY OF BIRMINGHAM

REDUCTION OF ANTIMICROBIAL RESISTANCE THROUGH ANTIMICROBIAL STEWARDSHIP

A research project submitted by

Claire Freddie Saxby

as part of the requirement for the degree of

Master of Research

July 2020

Supervised by

Dr Rebecca Drummond (University of Birmingham)

Professor Morgan Alexander (University of Nottingham)



Word count = 24 833

Contents

ACKNOWLEDGMENTS **4**

ABSTRACT **5**

ABBREVIATIONS **7**

1 INTRODUCTION **10**

1.1 A BRIEF HISTORY 10

1.2 THE PROBLEM OF RESISTANCE 13

1.3 ANTIMICROBIAL STEWARDSHIP 14

1.4 MECHANISMS OF RESISTANCE IN BACTERIA 15

1.5 CIPROFLOXACIN 17

1.6 RESISTANCE IN FUNGI 19

1.7 LINK TO MY RESEARCH 20

2 THE DETRIMENTAL EFFECT OF VANCOMYCIN ON THE MURINE IMMUNE RESPONSE TO *CANDIDA ALBICANS* 22

2.1 ABSTRACT 22

2.2 SIGNIFICANCE STATEMENT 22

2.3 INTRODUCTION 23

2.4 MATERIALS AND METHODS 25

2.4.1 Mice and *C. albicans* infection model 25

2.4.2 Culture of *C. albicans* 26

2.4.3 Tissue burdens 27

2.4.4 Flow cytometry 27
2.4.5 Bone marrow derived macrophages 28
2.4.6 Measuring mitochondrial function 28
2.4.7 Measuring ability of macrophages to kill *C. albicans* cells . 29
2.4.8 Protein extraction 30
2.4.9 Western blotting 31
2.4.10 Stastical analysis 33
2.5 RESULTS 34
2.5.1 Health and spread of fungi within the murine body on infection with *C. albicans* 34
2.5.2 Small intestine digests 36
2.5.3 Mitochondrial response to *C. albicans* infection *in vitro* . . 39
2.5.4 Killing ability of macrophages *in vitro* 41
2.5.5 LC3-associated phagocytosis protein expression 42
2.6 DISCUSSION 43
2.7 CONCLUSION 48

3 BIOINFORMATICS 49

3.1 ABSTRACT 49
3.2 SIGNIFICANCE STATEMENT 49
3.3 INTRODUCTION 50
3.3.1 The numbers 50
3.3.2 Resistance of *C. difficile* 50
3.3.3 Infection 51
3.3.4 Ribotypes 53
3.3.5 Sequence types 54
3.4 METHODS 56

3.5 RESULTS AND DISCUSSIONS 58
3.5.1 Quality of the raw data 58
3.5.2 Mapping the genome 61
3.5.3 *De novo* assembly 63
3.5.4 MLST results 65
3.5.5 SNPS 66
3.5.6 Isolate 07-00080 69
3.5.7 Presence of common resistance genes 69
3.5.8 The pangenome 72
3.5.9 Toxin genes 74
3.6 CONCLUSIONS 76

4 THE NEXT 3 YEARS **77**
4.1 MONOMERS 77
4.2 BIOFILMS 79
4.3 BACKGROUND SCIENCE – SOME IMPORTANT POLYMER PROPERTIES 80
4.3.1 Molecular weights 80
4.3.2 The glass transition 82
4.4 SUCCESS WITH URINARY CATHETERS 84
4.5 BLOOD CONTACTING CATHETERS 86
4.6 THE AIM OF THE PHD 96
4.6.1 Impact of this project 98

Appendices **100**

A Phylogenetic tree produced by the original paper **101**

BIBLIOGRAPHY **120**

ACKNOWLEDGEMENTS

My thanks for help in these projects initially go to Dr Rebecca Drummond (University of Birmingham), Professor Morgan Alexander, Professor Paul Williams and Professor Kim Hardie for their guidance over the year, and to everyone in the labs that I have worked in. These projects have been funded by the Wellcome Trust, who have also provided much training, and my thanks goes to them.

My thanks also goes to Rachel Kealy for her continuous support since we met in the dining hall queue in freshers week of our undergraduate degrees over 4 years ago, and to many others who have supported me througout my studies.

Final thanks goes to my family. Mum and Dad for their support through out my studies, and for dealing with many a tear-filled phone call.

Finally to Granny and Grandad, who made me realise how important this work is - I hope I've made you proud.

ABSTRACT

This thesis focuses on the reduction of antimicrobial resistance through the use of antimicrobial stewardship. Antimicrobial stewardship aims to responsibly use antimicrobials, while also preserving treatment options for patients of the future. The inappropriate use of antibiotic agents has been linked to *Clostridioides difficile* infections, longer stays in hospitals, higher hospital costs and nephrotoxicity [1], as well as the increased risk of subsequent fungal infections.

In chapter 2, the effects of a specific antibiotic, vancomycin, on the murine immune system is investigated. It has been observed that patients treated with vancomycin have an increased risk of developing candidiasis, leading to possible further treatment with anti-fungal agents. By understanding the effect of vancomycin treatment on the immune system, and how this increases the risk of candidiasis, the development of candidiasis can be prevented, meaning antifungal treatments are no longer necessary. Reduction in antimicrobial usage is one of the key components of antimicrobials stewardship. In an *in vivo* mouse model, vancomycin treatment is shown to reduce gut macrophage numbers, and major histocompatibility complex class II (MHCII) expression. However, no statistically significant differences could be seen in the response of *in vitro* bone marrow derived macrophages to *Candida albicans* infection with or without prior treatment with vancomycin.

In chapter 3, the genomic sequences of 57 clinical isolates of *C. difficile* ribotype 027 are re-analysed. *C. difficile* is commonly linked to prior treatment with antibiotic agents, with the ribotype 027 being a highly antibiotic resistant strain of the pathogen. By mapping the spread of the pathogen between people and locations, measures can be implemented to reduce the spread. This will lead to a lower incidence of *C. difficile* infection, therefore fewer patients requiring antibiotics to treat this infection. It is found in this study that multiple isolates contain no variations in their core genomes. While previous studies have identified

that the isolates are fluoroquinolone resistant, this could not be confirmed in this analysis. Evidence has been found within the genomes to suggest that a mobile genetic element, Tn6215, may be responsible for the observed erm(B) resistance gene found in some of the isolates.

In chapter 4, a proposed PhD project is set out, investigating new polymer coatings to prevent biofilm formation on blood-contacting catheters. Pathogens within a biofilm are tolerant to the host immune system, meaning that antimicrobial agents are required to treat the infection. However, the biofilm phenotype also increases the tolerance of the pathogen to antimicrobial agents, meaning higher doses are required. Often the catheter must be removed, in order to remove the biofilm from the patient. Since these catheters are used to deliver life saving drugs, a new catheter is placed. This process is both painful for the patient and leads to increased difficulty in the placement of subsequent lines.

ABBREVIATIONS

APS = Ammonium persulphate

ATG = Autophagy related proteins

BSA = Bovine serum albinum

CFU = Colony forming units

CLABSI = Central line associated blood stream infection

CVC = Central venous catheter

CVC-BSI = Central venous catheter blood stream infection

CDI = *Clostridioides difficile* infection

DHR = Dihydrohodamine-123

EDTA = Ethylenediaminetetraacetic acid

FBS = Fetal bovine serum

GI = Gastro-intestinal

HACDI = Healthcare associated CDI

HAI = Healthcare associated infections

HIV/AIDS = Human immunodeficiency virus/acquired immune deficiency syndrome

HRP = Horseradish peroxidase

ICU = Intensive care unit

LAP = LC3 – associated phagocytosis

LC3 = Microtubule-associated protein 1A/1B-light chain 3

LC3B = LC3-phosphatidylethanolamine conjugate

MALDI-ToF = Matrix-assisted laser desorption/ionisation time of flight

MGE = Mobile genetic element

MHCII = Major histocompatibility complex class II

MLST = Multi-locus sequence typing

MVG = Mito-View Green

M_n = Number averaged molecular weight

M_ν = Viscosity averaged molecular weight

M_w = Weight averaged molecular weight

M_z = z-averaged molecular weight

NCBI = National center for biotechnology information

NO = Nitric oxide

OEG = Oligo(ethylene glycol)

PBS = Phosphate buffer solution

PCR = Polymerase chain reaction

PE = Phosphatidylethanolamine

PI3K = Phosphoinositide 3-kinase complex

PI3P = Phosphatidylinositol-3-phosphate

PVDF = Polyvinylidene difluoride

ROS = Reactive oxygen species

SDS = Sodium dodecyl sulphate

SANS = Small angle neutron scattering

SCFA = Short-chain fatty acids

SDS-PAGE = Sodium dodecyl sulphate -polyacrylamide gel electrophoresis

SNPs = Single nucleotide polymorphisms

SPR = Surface plasmon resonance

SRA = Sequence read archive

ST = Sequence type

TEMED = Tetramethylethylenediamine

TPN = Total parenteral nutrition

WHO = World Health Organisation

Monomer abbreviations

AODMBA = (R)-α-acryloyloxy-β,β–dimethyl-γ-butyrolactone

BA = Butyl acrylate

BMA = Benzyl methacrylate

CyDMA = Cyclododecyl methacrylate

DEGMA = Di(ethylene glycol) methyl ether methacrylate

EDGPEA = Ethylene glycol dicyclopentenyl ether acrylate

IBMA = Isobornyl methacrylate

IBnA = Isobornyl acrylate

iDMA = Isodecyl methacrylate

TEGMA = Tri(ethylene glycol) methyl ether methacryate

TMCHMA = 3,3,5 – trimethylcyclohexyl methacrylate

tBCHMA = Tertbutylcyclohexyl methacrylate

tBCHA = Tertbutylcyclohexyl acrylate

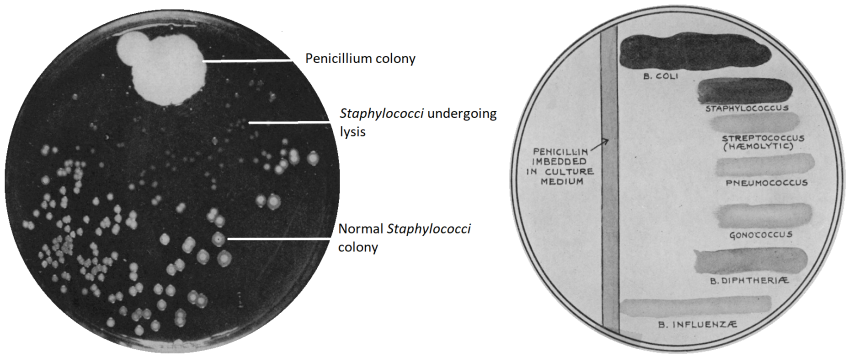
INTRODUCTION

1.1 A BRIEF HISTORY

Even in the ancient world, evidence of the use of antimicrobials can be found. For example, human skeletons dating from AD 350 - 550 from Nubia show traces of tetracyclines, indicating the presence of tetracyclines in the diet of these individuals [2]. While it cannot be deduced from this whether tetracycline was used for medical purposes, there is also evidence that people of the ancient world (including those of Egypt and Rome) placed mouldy bread onto wounds to aid healing - something which we now know is due to the presence of penicillin. This cure is also mentioned in the Eber's papyrus dating from 1550 BC [3], the earliest recorded medical document.

The first recorded hospital use of a drug to treat a bacterial infection was pyocyanase in 1899 [3, 4] , which was extracted from the bacteria found in the bandages of injured patients. One of the earliest methodical experiments designed to discover a new 'antibiotic' treatment was conducted in 1904 by Ehrlich to find a treatment for syphilis [4, 5]. The systematic screening of compounds by testing on syphilis-infected rabbits led to a treatment that was marketed under the name of Salvarsan [3]. Another key event in the early history of antibiotics was Fleming's discovery of Penicillin in 1928 [4]. Fleming identified that, staphylococcal colonies had become transparent and were undergoing lysis (figure 1.1a) in regions surrounding a large colony of contaminating mould (identified by its morphology as a penicillium) [6]. Fleming also reported a new method of examining the inhibitory power of his new antibacterial substance by using a strip of agar impregnated with the antibacterial agent within an agar plate and streaking the bacteria to be tested at right angles (figure 1.1b) [6]. Following these three important discoveries, came the start of the 'golden age of antibiotics' dur-

ing which a new class of antibiotic was discovered almost yearly, extracted from easy-to-cultivate fungi [7]. Once these sources were exhausted, the flow of antibiotic slowed [7] (figure 1.2).



(a) **(b)**

Figure 1.1 ***Images from [6].*** *(a)Modified image, showing the lysis of Staphylococci in locations near to a colony of Penicillium. (b) Determining the effect of penicillin on various microbes by imbedding penicillin in the culture media.* Balantidium coli *and* B. influenzae *show no growth inhibition as a result of penicillin in the culture medium, while* Staphylococcus, Streptococcus, Pneumococcus, Gonococcus, *and* B. diphtheriae *show regions of inhibition near to the penicillin imbedded strip. The presence of the penicillin within the strip will cause a concentration gradient of the penicillin across the media, allowing the determination of relative minimum inhibitory concentrations (MICs).*

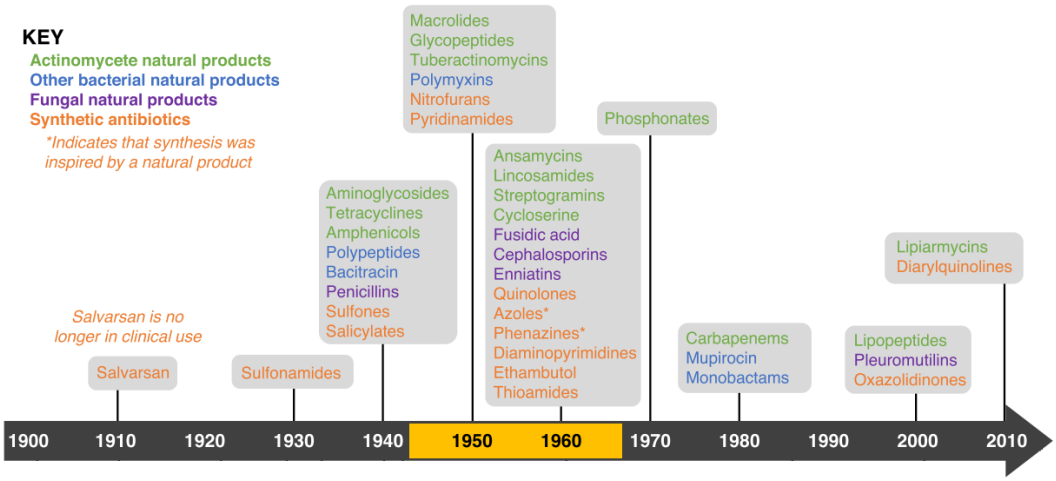


Figure 1.2 ***Time line of the history of antibiotic agents, adapted from [7].*** *The highlighted yellow area is the antibiotic golden age. For more detail on the classes of antibiotics used clinically, see table 1.1.*

The timeline of antifungal agents (figure 1.3) is much more recent than the timeline of antibiotic agents, with the first active and safe antifungal agents being developed almost 20 years after the first antibiotic agent, and the most prolific

period in antifungal discovery occurring over 40 years after the antibiotic golden age.

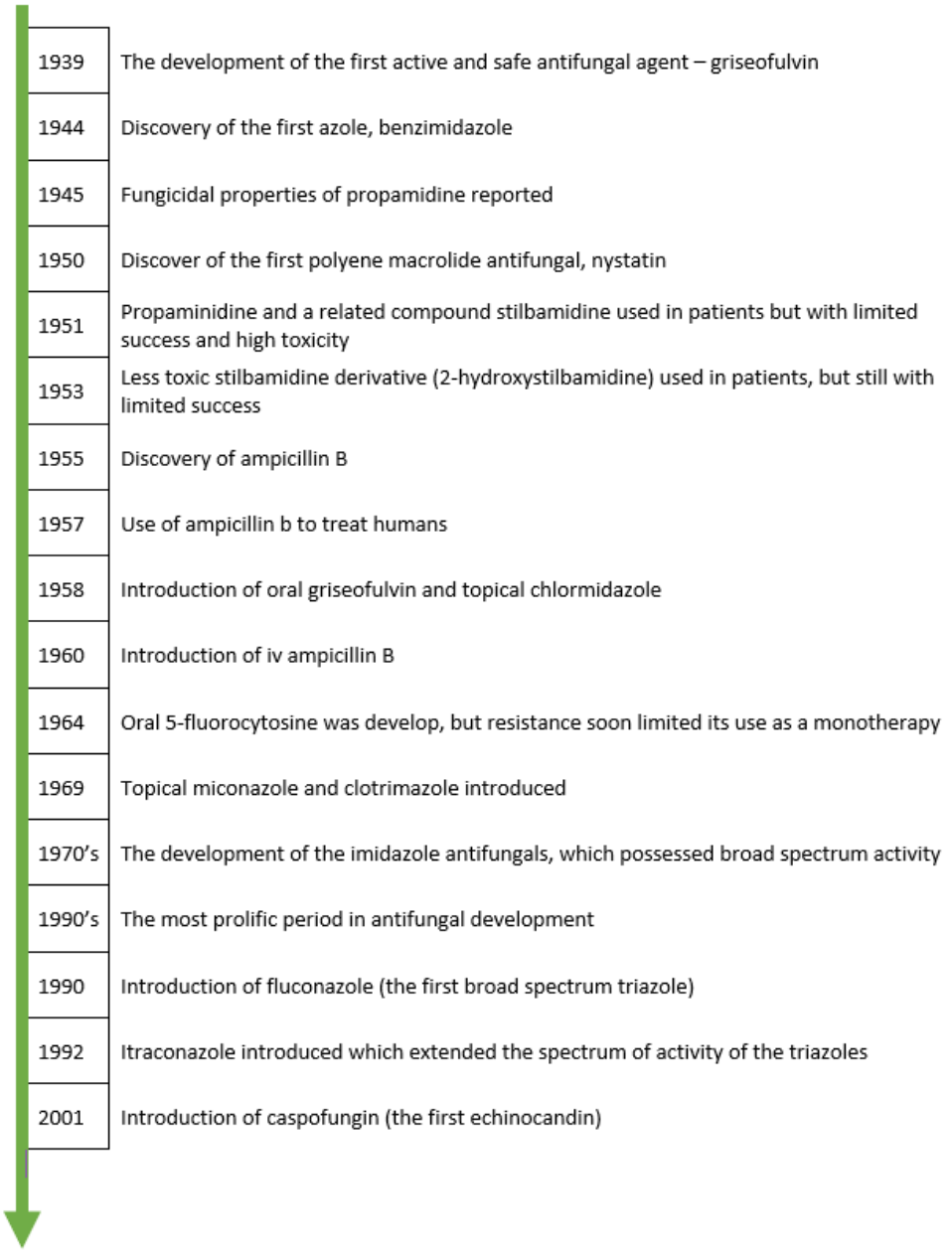


Figure 1.3 ***Time line of the history of antifungal agents, based on information from [8, pp161-162].***

1.2 THE PROBLEM OF RESISTANCE

Microbes have now become resistant to multiple drugs, with the rate of drug development not keeping up with the rate of resistance occurring to existing drugs [9]. The resistance to antimicrobial agents is of great medical importance, with the UK government predicting that, unless action is taken, there will be 10 million deaths globally each year caused by anti-microbial resistant infections by 2050 [10, 11], exceeding the annual deaths from cancer (figure 1.4).

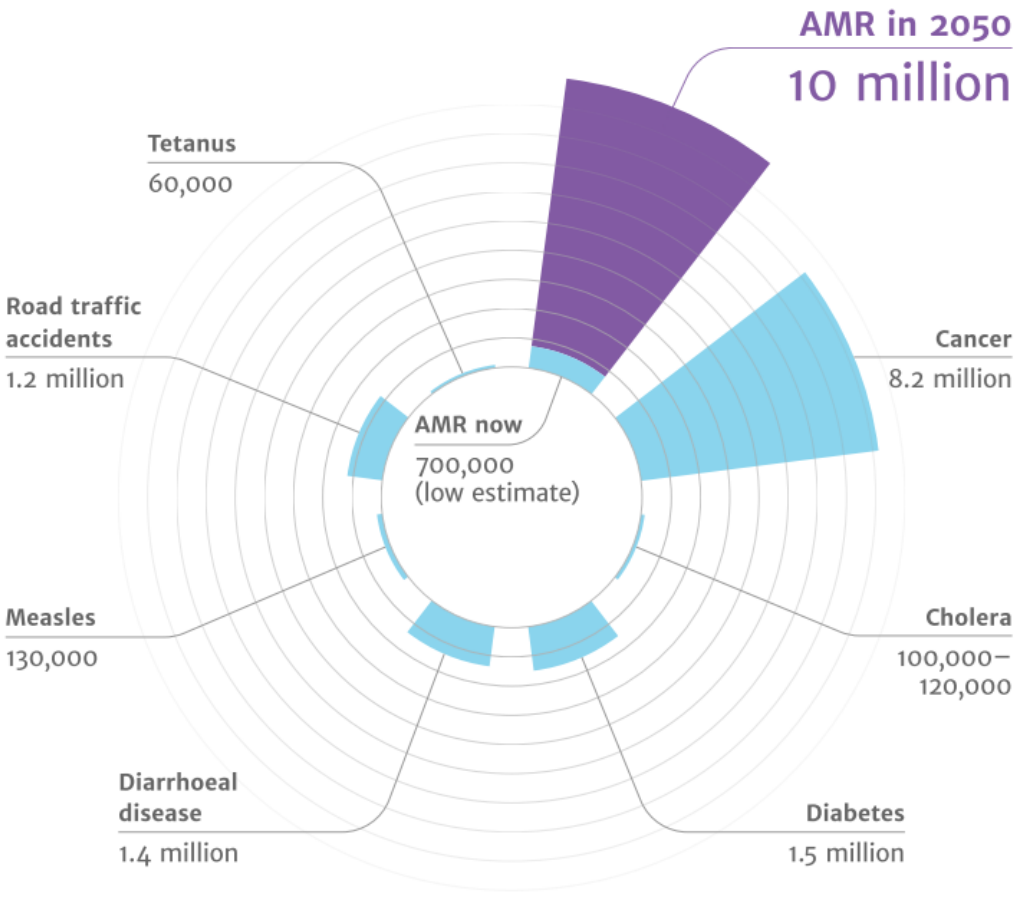


Figure 1.4 ***Comparison of deaths caused by different diseases, in comparison to deaths caused by antimicrobial resistance (AMR) and the predicted number of deaths caused by AMR in 2050*** *[12].*

This is not only of medical importance, but also financial, with the associated cost being $100 trillion [10, 11]. A 2017 study [13] showed that antibiotic-resistant infections were associated with increased in-hospital mortality and readmissions/visits to the emergency department (within 30 days of discharge) when

compared to infection by antibiotic-susceptible bacteria.

Antimicrobial treatment is essential for medical interventions that currently prolong life and improve its quality, such as chemotherapy and joint replacements [9]. Without adequate antimicrobial treatment being available, these interventions may not be available to future generations.

The effect of lack of treatment or vaccination of an infectious disease can be seen by the SARS-CoV-2 pandemic. While physical distancing will not reduce the spread of infections that are not air-borne, the spread of the virus does show the importance of proper cleaning regimes in preventing the spread of infections. In the future, pandemics may be caused by infective agents that are currently treatable but may cease to be as a result of the spread of antimicrobial resistance.

Development of new antimicrobial agents may not provide a long term solution, due to the trend of microbes becoming resistant to each new class of antimicrobials discovered [9] – a trend that, it can be assumed, will continue for any new classes of antimicrobial treatments. While continuing with current antimicrobial usage will result in the inability to treat infections, not treating patients with antibiotics would also increase the spread of infectious diseases, so a mid-ground must be met. This is where antibiotic stewardship comes in.

1.3 ANTIMICROBIAL STEWARDSHIP

Antimicrobial stewardship aims to use antimicrobial agents responsibly, to treat patients of today while preserving treatment options for patients of the future. While concerns about antibiotic resistance date back to Fleming in the 1940s [1], the first use of the term ‘antibiotic stewardship’ was in 1996 [14], and it is now being considered on a global scale, with the World Health Organisation (WHO) producing a policy package on World Health Day 2011 (for which the theme

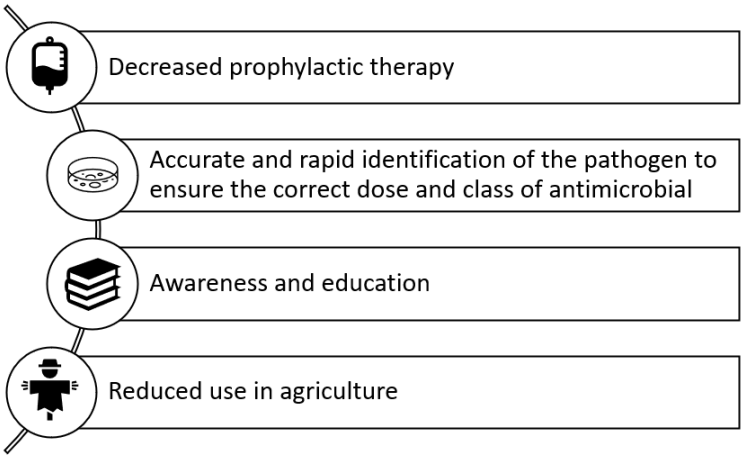


Figure 1.5 ***Various methods of antimicrobial stewardship that aim to reduce the development and spread of antimicrobial resistance.***

was antimicrobial resistance) to commit to a financed national plan to combat antimicrobial resistance [14]. The UK government has also produced a 5 year plan to tackle the problem, which includes optimising the use of antimicrobials in humans, agriculture, and animals [11]. Figure 1.5 shows some factors that are involved in antimicrobial stewardship.

1.4 MECHANISMS OF RESISTANCE IN BACTERIA

Resistance of bacteria to antibiotics can either be acquired or intrinsic. While intrinsic resistance is present in all bacterial cells within a certain species (for example as a result of the lack of the target site), acquired resistance is the result of mutations in DNA or the horizontal transfer of mobile DNA elements.

Antibiotics make use of the differences between eukaryotic cells and prokaryotic cells [1]. As different classes of antibiotics target different parts of the prokaryotic cell, there are different sets of mechanisms that cause resistance within bacterial cells (see table 1.1), however the mechanisms present in a specific bacterial cell will depend on the species of bacteria [1].

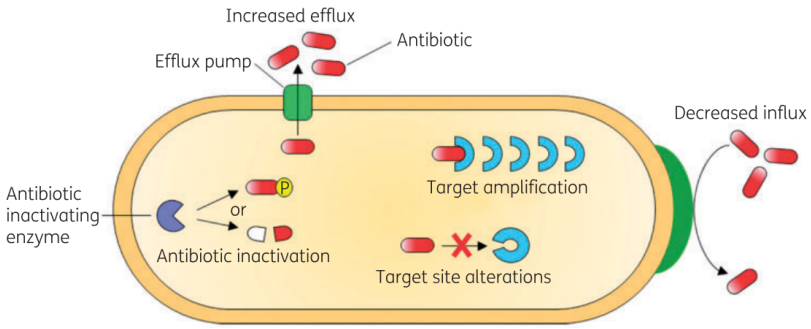


Figure 1.6 ***Diagram showing the main mechanisms of antibiotic resistance in bacteria*** *[15].*

The main methods by which bacteria are resistant to antibiotics in general are:

- Reduction in the accumulation of the drug within the cell,
- Changes to the target proteins to prevent the drug from binding,
- Producing enzymes that modify/destroy the drug,
- Producing proteins to protect the target proteins so the drug cannot bind.
- Amplification of the target protien

These mechanisms are shown in figure 1.6. The mechanisms of resistance to a specific class of antibiotics, the fluoroquinolones (and specifically ciprofloxacin), are explained in more detail in section 1.5. The section of ciprofloxacin is based on an essay written and presentation given in September 2019 as part of the Doctoral Training Programme.

Classes of antibiotics [16]	Target [17]	Mechanisms of resistance [17]	First reported in literature [7]	Clinically introduced [7]
Penicillins (beta lactams)	Peptidoglycan biosynthesis	Hydrolysis, efflux, and alterations of the target	1929	1943
Cephalosporins (beta lactams)	Peptidoglycan biosynthesis	Hydrolysis, efflux, and alterations of the target	1948	1964
Aminoglycosides	Translation	Phosphorylation, acetylation, nucleotidylation, efflux, and alteration of the target	1944	1946
Tetracyclines	Translation	Monooxidation, efflux, and alteration of the target	1948	1948
Macrolides	Translation	Hydrolysis, glycosylation, phosphorylation, efflux, and the alteration of the target	1952	1952
Fluoroquiolones	DNA replication	Acetylation, efflux, and alteration of the target	1962	1962

Table 1.1 ***The targets, resistance mechanisms, and important dates for clinical antibiotics.***

1.5 CIPROFLOXACIN

Ciprofloxacin (a type of fluoroquinolone antibiotic) works by attacking the topoisomerase IIA enzymes (DNA gyrase and topoisomerase IV) [18]. As both of these enzymes are located within the bacterial cell, the drug must penetrate the bacterial membrane. In *Escherichia coli* and *Staphylococcus aureus*, this occurs by simple diffusion, however active uptake by porins has been linked to the accumu-

lation of ciprofloxacin within other Gram-negative species of bacteria [19, p.570], meaning that a reduced expression of membrane porins in these bacteria will result in reduced accumulation of ciprofloxacin in the bacterial cell.

A strong reserpine-mediated growth inhibition in resistant bacteria when treated with ciprofloxacin has been reported [20] in *Streptococcus pneumoniae* and *S. aureus*. Reserpine is a known efflux pump inhibitor, so it can be concluded that efflux pumps play a role in resistance. However, another study has shown that efflux pumps are present in both ciprofloxacin-resistant and ciprofloxacin-susceptible strains of *S. pneumonia* [21], meaning that efflux pumps cannot be the sole cause of resistance in this species.

Through DNA sequencing of the genes coding for *gyrA*, *gyrB*, *parC*, and *parE*, it has been shown that amino acid substitutions are present in the target proteins of resistant bacteria [21].

Plasmid mediated resistance to ciprofloxacin was first confirmed in 1998 [22], when it was shown that the pMG252 plasmid confers resistance to multiple antibiotics, including ciprofloxacin. Following the discovery of this plasmid, other plasmids that cause resistance to ciprofloxacin have also been discovered [23]. These plasmids are of particular concern within antimicrobial resistance, as they allow transfer of resistance between species.

There appears to be conflicting reports as to whether quinolone resistance is associated with resistance to other antibiotics. In a study of 209 US clinical isolates [24], there was found to be no appreciable difference between the geometric mean ciprofloxacin MIC for penicillin resistant *S. pneumoniae* and penicillin susceptible *S. pneumoniae*. However, an earlier study [25] had tested 1856 *S. pneumoniae* strains from 15 centres in Western Europe and the USA, which shows that penicillin resistant strains of the bacteria have a slightly higher sensitivity to quinolones than penicillin sensitive strains. A study conducted in Spain [26]

tested 2882 *S. pneumoniae* strains, and found a correlation between the resistance to penicillin and ciprofloxacin ($p < 0.001$). Another study [27] tested 32 isolates that were non-susceptible to ciprofloxacin, obtained from Hong Kong, and found that they were all non-susceptible to penicillin, cefotaxime, and erythromycin. This variation is a result of there being three methods of resistance occurring in the bacterial cells; for example, the pMG252 plasmid encodes for resistance to multiple antibiotics, where as the presence of altered topoisomerase IIA enzymes would not confer resistance to any antibiotic that does not target this site.

1.6 RESISTANCE IN FUNGI

While antibiotic resistance is most well-known among the general population, resistance of fungi to antifungal agents is also of clinical concern. Only recently has it been shown that a reduction in the use of antifungal agents through a stewardship program does not result in the increased incidence of, or mortality from, hospital acquired candidemia [28]. This is an important finding, as it means that antimicrobial stewardship can be applied to the use of antifungal agents. It can be argued that, because of the smaller number of antifungal agents available in comparison to antibiotic agents, and their use as prophylaxis/empirical treatment (due to difficulties in rapid diagnosis [29]), antifungal resistance is going to become a more important part of any antimicrobial stewardship program. There is also an increasing number of cases of fungal infection [30], with multi-drug resistant *Candida spp* and Azole resistant *Aspergillus fumigatus* becoming increasingly prevalent [29]. A 2013 study by the United States department of health and human sciences attributes 3,400 of the 46,000 annual cases of *Candida spp* infections to strains that are resistant to Fluconazole [31].

In comparison to resistance in bacteria, resistance in fungi is usually the result of repeated, independent evolution events in multiple species, rather than by horizontal transfer through plasmids or phages [32]. Fungal cells show many strategies for resisting the effect of antifungal agents. Table 1.2 shows the methods of re-

sistance of *Candida spp* to various classes of antifungal agents.

Classes of antifungal	Target [33, 34]	Methods of resistance [32]
Polyenes	Ergosterol (a sterol that is fungal-specific)	Regulation of stress response pathways, absence of target
Azoles	Cytochrome P450 enzyme sterol 14α-demethylase	Target site conformational changes, target site overexpression, efflux pump overexpression, genomic plasticity
Echinocandins	The enzyme glucan synthase	Regulation of stress response pathways, target site conformational changes

Table 1.2 ***The target sites of the 3 main classes of antifungals used clinically, and mechanisms by which Candida spp become resistant.***

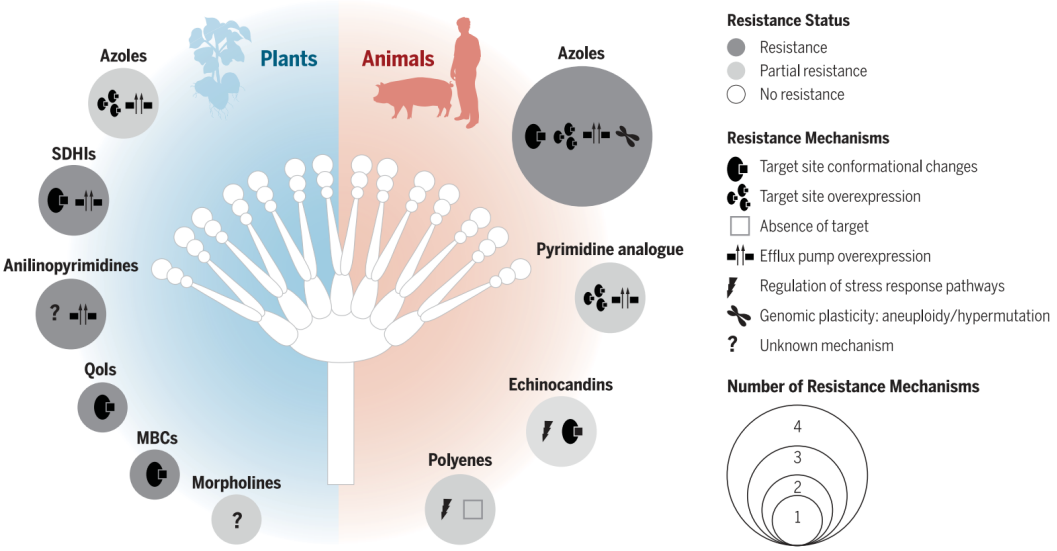


Figure 1.7 ***Mechanisms of resistance by fungi to plant and animal antifungal agents [32].***

1.7 LINK TO MY RESEARCH

An area of improvement suggested by the UK government [10, 11] to tackle antimicrobial resistance is to reduce the burden of infections, in order to reduce the prescribing of antimicrobials. The purpose of this thesis is to address methods of

reducing the burden of infections.

Chapter 2 describes research into how treatment with vancomycin affects the murine immune system, and how this increases the risk of developing systemic candidiasis. Knowledge of how antibiotic usage predisposes patients to fungal infections will reduce the burden of fungal disease in patients that are often already critically ill.

Chapter 3 describes a genomic research project, charting the spread of *C. difficile* throughout Germany. Understanding the spread of *C. difficile* infections will provide information that could be used in preventing the spread, and the associated infective burden. A 2013 report by the United States department of health and human sciences [31] has attributed 14,000 deaths each year to infection by *Clostridioides difficile*, leading to this disease being given an urgent treat level.

Chapter 4 lays out a proposed research project on polymer coatings of blood-contacting catheters in order to reduce the formation of biofilms. The prevention of biofilm formation on medical devices will reduce the burden of microbial disease from biofilm forming pathogens in patients that are already ill.

Chapter 2

THE DETRIMENTAL EFFECT OF VANCOMYCIN ON THE MURINE IMMUNE RESPONSE TO *CANDIDA ALBICANS*

2.1 ABSTRACT

This study investigates the effect of a specific antibiotic, vancomycin, on macrophage function. The *in vivo* mouse model shows that vancomycin reduces gut macrophage numbers, and their major histocompatibility complex class II (MHCII) expression; this is associated with increased presence of fungal cells within the gastrointestinal (GI) tract. *In vitro* studies were also used to determine the effects of vancomycin on reactive oxygen species (ROS) production and microtubule-associated protein 1A/1B-light chain 3 (LC3) associated phagocytosis (LAP) within macrophages, which have previously been shown to be disrupted by antibiotic treatment. The effect of vancomycin on the ability of macrophages to kill *Candida albicans* cells *in vitro* was also investigated, but no statistically significant effects could be seen.

2.2 SIGNIFICANCE STATEMENT

Candida albicans is part of the normal human commensal microbial flora, but can cause lethal systemic candidiasis. One reason why this occurs is because of the effect of antibiotics on the functioning of the immune system. This study uses *in vivo* and *in vitro* models to examine this effect.

2.3 INTRODUCTION

An estimated 1.5 million people die from invasive fungal infections yearly [35], while most people develop a superficial fungal infection at some point in their life [35]. The overall number of human fungal infections is increasing [30], partially due to increased numbers of immunosuppressed patients (e.g. due to increased life expectancy of HIV/AIDS patients). In 2016, 3.5 cases of candidaemia (blood stream *Candida spp* infection) were reported in England per 10,000 of the population [36], with *Candida albicans* being the most common cause. Commensal *C. albicans* found in the gastro-intestinal (GI) tract [37] can cause systemic infection in immunosuppressed patients with chemotherapy-associated damage to the GI-mucosal barrier [30]. Commensal *C. albicans* found on the skin [38, 39] can cause systemic infection when the skin of acutely ill intensive care patients is penetrated, such as by a central venous catheter [30]. There are many risk factors for the development of candidiasis [40], one of which is antibiotic usage [41].

It has been recently found that antibiotics can damage the immune response, however this is poorly understood. Known mechanisms are through changes to the microbiota [42], and alterations of the metabolism and reactive oxygen species (ROS) production of immune cells [43]. The mechanism(s) by which antibiotic usage increases the risk of fungal infections is not currently understood. This investigation focuses on the effect of vancomycin, as it has been found that vancomycin treatment is associated with a worse outcome from candidiasis (Drummond *et al*; unpublished). Other problems with vancomycin include nephrotoxicity and neutropenia [44], and the presence of *Vancomycin Resistant Enterococcus* [45].

Macrophages protect against *C. albicans* infections by phagocytosing yeast cells [46–49], and secreting pro-inflammatory cytokines and chemokines. Following phagocytosis, macrophages destroy the pathogen via several mechanisms, one of which is microtubule-associated protein 1A/1B-light chain 3 (LC3) associated phagocytosis (LAP). The process of LAP is shown in figure 2.1, and is reviewed

in more detail in [50]. LAP results in the binding of LC3B onto the phagosomal membrane, which has been shown to be necessary for lysosomal fusion [51], which provides the necessary compounds to destroy the pathogen. ROS are one of the necessary chemicals for the killing of phagocytosed cells. ROS can be produced by both the mitochondria and NADPH oxidase [52, 53].

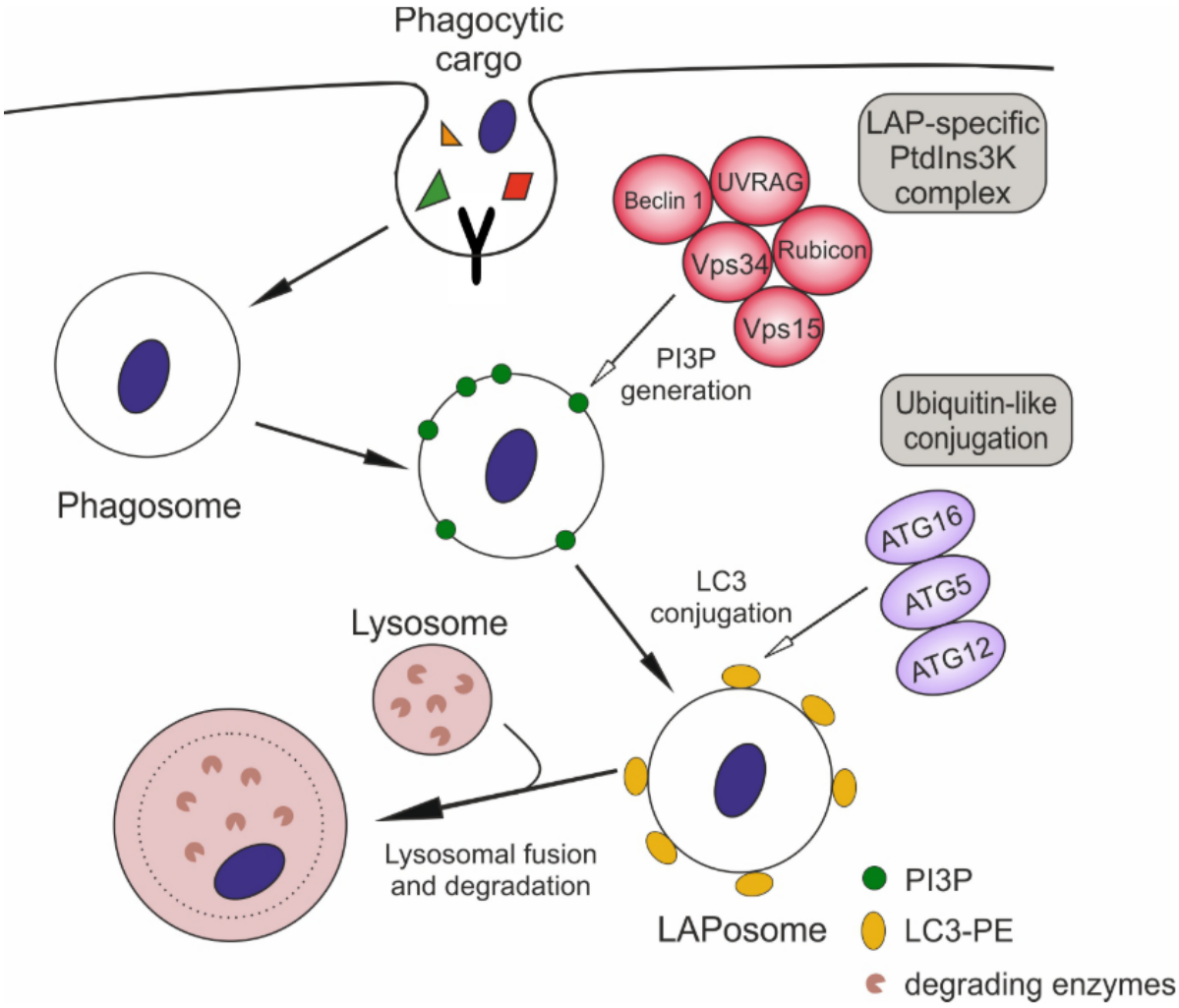


Figure 2.1 ***The process by which LC3-associated phagocytosis occurs [54].*** *In LAP, autophagy machinery [including the autophagy related (ATG) proteins] is used to destroy pathogenic material. Phagocytic cargo is internalised in a phagosome, which it decorated with phosphatidylinositol-3-phosphate (PI3P) created by the phosphoinositide 3-kinase complex (PI3K). PI3P is required for the recruitment of the ATG5-ATG12 and LC3-PE ubiquitin-like conjugation system (required for extension of the autophagosome in autophagy [55]) which covalently bond LC3 to phosphatidylethanolamine (PE) to form LC3-phosphatidylethanolamine conjugate (LC3B) conjugated onto the surface of the phagosome.*

In order for macrophages to phagocytose and kill pathogens, they undergo metabolic rewiring. Under homeostatic conditions, macrophages utilise glucose mainly through oxidative phosphorylation [56], however, activation results in a dampening of the mitochondrial function of the cells [57] and an increased reliance on the glycolysis and pentose phosphate pathways to provide necessary substrates for other biosynthetic pathways [58] (such as ROS production). The lack of efficiency in ATP-production is compensated for by an increase in glucose uptake [59].

Macrophages are of particular interest to this project, as they heavily populate the gut [60, 61], which, it has been suggested is the main point of entry for the fungal cells into the bloodstream [62]. Macrophages have a longer life span compared to other immune cells [63], so any damage caused to them by antibiotics will be experienced for a longer period of time post-treatment. This study aims to explore the effect of vancomycin on macrophage mitochondrial function, and response to *C. albicans* infection.

2.4 MATERIALS AND METHODS

2.4.1 Mice and *C. albicans* infection model

$8-10$ week old female $C57BL/6$ mice (Charles River), maintained at the Biomedical Services Unit at the University of Birmingham, were provided with food and water *ad libitum*. All experiments were approved by the local Animal Welfare and Ethical Review Board, and by the Home Office under Project Licence $PPL/PBE275C33$.

13 mice were treated for 4 weeks with 0.5 $mgml^{-1}$ vancomycin (Hospira) in the drinking water, refreshing the water twice weekly. Control mice were treated identically, but without vancomycin in the drinking water. 10 vancomycin-treated mice and 10 control mice were intravenously infected with 1×10^5 CFU of *C. al-*

*bicans SC*5314 per mouse, and monitored daily for weight loss and clinical symptoms (e.g. hunched posture, hypothermia, reduced movement).

Mice from the vancomycin-treated and control groups were randomly selected into the 7-day cohort (5 vancomycin-treated mice; 5 control mice) or the 23-day cohort (5 vancomycin-treated mice; 5 control mice). Mice were euthanised by cervical dislocation when their weight loss reached 30 %, when an advanced infection developed, or at the end point of their experiment (whichever came first). Mice in the 7-day cohort were used for tissue burden determination (see section 2.4.3), with the end point of the experiment being 7-days post-infection. Mice in the 23-day cohort were used for survival studies, with the end point of the experiment being 23-days post-infection. 3 vancomycin-treated mice and 4 control mice were not infected with *C. albicans*, and were euthanised to perform flow cytometry on their gut digests (see section 2.4.4).

An additional 7 control mice were euthanised so that bone marrow could be extracted for culturing bone marrow derived macrophages for *in vitro* experiments (mitochondrial staining, killing assays, and protein extraction).

The doses of vancomycin and *C. albicans* used were based on unpublished data from the Drummond lab.

2.4.2 Culture of *C. albicans*

C. albicans (SC5314) was cultured in YPD broth [1 % yeast extract (SIGMA), 2 % glucose (Gibco), and 2 % peptone (Fisher)] at 30 $^{\circ}C$ under gentle agitation ($180 - 200$ rpm) for $18 - 20$ hours. Fungal cells were spun down (2000 rpm, 5 minutes, 4 $^{\circ}C$), and the cell pellet resuspended (see below for concentrations) in phosphate buffer solution (PBS). *In vitro* experiments used 2 live yeast to each macrophage, or 10 heat-killed yeast (30 minutes at 70 $^{\circ}C$) to each macrophage.

2.4.3 Tissue burdens

Tissues (small intestines, caecum, colon, kidney) from 5 control mice and 5 vancomycin-treated mice were weighed and homogenised in 1 mL sterile PBS. Serial dilutions (neat to 1 : 1000) of the homogenate were plated onto YPD solid growth media [2 % peptone, 2 % glucose, 1 % yeast extract, 2 % bacteriological agar (OXOID)] supplemented with penicillin/streptomycin (to prevent the growth of commensal bacteria) and fungal colonies counted after incubation at 37 $°C$ for $\sim$ 18 hours. Spleen bacterial burdens were analysed in the same way, by plating onto Sheep Blood Agar (Remel), which was not supplemented with any antibiotics.

2.4.4 Flow cytometry

Small intestines (from 3 vancomycin-treated mice and 4 control mice) were removed and placed into phosphate buffer solution (PBS) on ice. Intestinal content was removed, and the intestines were cut laterally and gently cleaned in fresh PBS to remove any remaining contents. They were then cut into small squares ($\sim 1-2$ cm in length) and placed in 10 mL RPMI with 1.5 % fetal bovine serum (FBS) and 5 mM Ethylenediaminetetraacetic acid (EDTA). The intestines were then incubated at 37 $°C$ with shaking for 20 minutes. Intestines were vortexed and poured through a 100 μm filter. Intestine pieces were moved into a fresh tube containing 10 mL RPMI with 5 mM EDTA, vortexed, and filter/washed as above. Intestines were then digested in 10 mL of digest buffer [RPMI + 100 $\mu g ml^{-1}$ Collagenase IV (Gibco) + 100 $\mu g ml^{-1}$ dispase (Sigma) + 40$\mu g mL^{-1}$ DNase] at 37 $°C$ for 1 hour with shaking. The digested intestines were poured through a 40 μm filter, and washed through with FACS buffer [PBS + 0.5 % Bovine serum albumin (BSA) + 0.01 % sodium azide]. The filtrate was then spun down (1500 rpm, 5 minutes), resuspended in FACS buffer, and spun again. The cell pellet was then resuspended in PBS and stained with ZombieViolet live/dead dye (Biolegend) for 10 minutes on ice. Cells were then stained with fluorophore-conjugated antibodies in the presence

of Fc receptor block (anti-CD16/32, clone 93). The anti-mouse antibodies used in this study were: CD45::PE (30-F1) ; CD11b::APC Cy7 (REA592, Miltenyi Biotec); F4180::APC (BM8); CD19::PerCPcy5.5 (1D3/CD19); MHCII::PECy7 (M5/114.15.2) [all antibodies from BioLegend unless otherwise stated], each with a final concentration of $1 \mu g m L^{-1}$.

2.4.5 Bone marrow derived macrophages

Bone marrow macrophages were generated from the murine hind legs. Muscle and fat were removed aseptically and bones sterilised in 70 % ethanol. Bone marrow was flushed out with PBS (Gibco) supplemented with 2 mM EDTA (invitrogen), using a 25 G needle. The bone marrow was smashed through a 70 μm filter, spun down (1500 rpm, 5 minutes, 4 $^{\circ}C$), and resuspended in 20 mL RPMI Medium1640 (1X) with GlutaMAX and HEPES (Gibco) (for 2 bones, 1 leg) supplemented with 20 % FBS and 40 $ngmL^{-1}$ macrophage colony-stimulating factor (M-CSF). Vancomycin-treated macrophages were further supplemented with 20 $ngmL^{-1}$ vancomycin. Following 3 days of incubation (37 $^{\circ}C$, 5 % $CO-_2$) the media was replaced with fresh media (of the same composition). Macrophages were used for experiments after 5 days of differentiation. During differentiation, the samples were regularly checked for signs of contamination (e.g. cloudy media).

2.4.6 Measuring mitochondrial function

Bone marrow macrophages were lifted from their flasks by replacing the media with 12 mL of cold PBS/2 mM EDTA and incubating on ice for $5 - 10$ minutes, followed by the use of a cell scraper, and spun down (1500 rpm, 5 minutes, 4 $^{\circ}C$); the cell pellet was resuspended in RMPI/10 % FBS ($\pm$20 $ngmL^{-1}$ vancomycin). Cell concentration was determined using Trypan blue (dilution 1 : 20), and cells resuspended at 2×10^6 $cells/ml$. 1×10^5 macrophages were added to each well of a 96 well flat-bottom plate (Corning Incorporated), and the volume of media increased to 100 μL per well. The plate was incubated for $\sim$ 18 hours

(37 $°C$, 5 % CO_2) to allow macrophages to adhere, then macrophages were fed with 100 μL fresh media per well and incubation continued for $2-4$ hours. Media was then replaced with 50 μL of PBS supplemented with 10 % mouse serum (Biowest). 50 μL of either 4×10^6 $yeast/ml$ or PBS were added to each well, and the plate returned to 37 $°C$.

For mitochondrial mass measurements (using MitoView Green [MVG], BioLegend), the plate was incubated for 120 minutes, adding the stain (final concentration of 50 nM) after 90 minutes, and read at 490 nm excitation/516 nm emission. MVG stains the mitochondrial membrane in a potential-independent way, so the differences in fluorescence values observed show differences between the mitochondrial mass under the different conditions.

For mitochondrial ROS measurements (using MitoSOX red, M36008, Molecular Probes), the plate was incubated for 120 minutes, adding the stain (final concentration of 5 μM) after 110 minutes, and read at 510 nm excitation/580 nm emission.

For total ROS measurements (using dihydrohodamine-123 [DHR], Sigma) the plate was incubated for 90 minutes, adding the stain (final concentration of 100 μM) after 60 minutes, and read at 507 nm excitation/529 nm emission.

2.4.7 Measuring ability of macrophages to kill *C. albicans* cells

Bone marrow macrophages were prepared as above, and the killing assay was conducted in the presence of 10 % mouse serum (Biowest) (opsonised samples) or 10 % FBS (unopsonised samples). 50 μL of *C. albicans* with concentration of 4×10^6 $cells/ml$ were added to each well, and macrophages were incubated for 2 hours (37 $°C$). The plate was then spun (2000 rpm, 4 minutes), and the supernatant removed. 100 μL of 0.02 % Triton-X in water was added to each well, and

the plate spun again. The supernatant was removed, replaced by PBS, and the plate spun. This wash step was repeated once more. 100 μL of 1X Alamar Blue (Thermo) was added to each well, and the plate was incubated for $\sim$ 18 hours (37 $^{\circ}C$, 5 % CO_2). The plate was then read at 560 nm excitation/290 nm emission.

2.4.8 Protein extraction

Bone marrow derived macrophages were prepared as above in 24 well plates (Corning Incorporated) with 0.5×10^6 macrophages per well. Stimulation with 5×10^6 heat-killed yeast per well [$\pm$50 μM chloroquinine (Sigma)] occurred for 2 hours, then the media was replaced with RIPA buffer supplemented with 1X protease/phosphatase inhibitor cocktail (Sigma) and the cells incubated on ice for $5 - 10$ minutes to lyse the cells. Cell lysates were snap frozen on dry ice. Protein concentration was determined using the Pierce BCA kit following the manufacturers' instructions. In some cases, protein samples were concentrated prior to use. For this, lysates were mixed with an equal volume of methanol (VWR BDH Chemicals), and chloroform (Alfa Aesar) added with a volume 1/8 of the total volume of protein and methanol. The mixture was inverted and centrifuged at maximum speed in a microfuge for 3 minutes. The top liquid phase was removed, and the same volume of methanol added, and the lysate pelleted as before. The supernatant was removed, and the pellet dissolved in fresh RIPA buffer before re-determining protein concentration. Protein samples were mixed with an equal volume of sample buffer and heat treated at 95 $^{\circ}C$ for 5 minutes prior to loading onto 10 % or 20 % sodium dodecyl sulphate-polyacrylamide gels. Protein samples were separated by running SDS-polyacrylamide gel electrophorese (SDS-PAGE) at 130 V for $\sim$ 60 minutes, in fresh running buffer. See tables 1a (page 32) and 1b (page 33) for the composition of the gels and buffers used respectively.

2.4.9 Western blotting

Following separation of the proteins, the gels were transferred to 0.2 μm polyvinylidene difluoride (PVDF) Western blotting membranes (Roche Diagnostics GmbH) using fresh transfer buffer at 100 V (constant) for 90 minutes, with the tank in a tray of ice to prevent over-heating. Following transfer, the membrane was washed 3 times in wash buffer for approximately $5 - 10$ minutes per wash. The membrane was blocked for an hour at room temperature under gentle agitation, in blocking buffer. Following a further 3 rounds of washing (same as previous), the membrane was probed with primary antibody diluted in wash buffer overnight at 4 $^{\circ}C$ under gentle agitation. The primary antibodies used in this study were: anti-mouse LC3B (D11); rodent specific SQSTM1/p62; or anti-mouse beta-actin (8H10D10) (all from Cell Signalling Technology). Membranes were washed as above, and then incubated for one hour with a horseradish peroxidase (HRP) linked secondary antibody (Cell Signalling Technology) diluted in wash buffer and washed again 3 times. The membrane was imaged using the Amersham ECL Western Blotting Detection Reagents (from GE Healthcare). All antibodies were used at $1 : 1000$. See table 1b (page 33) for the composition of the buffers used.

COMPONENT	10% SEPARATION GEL	20% SEPARATION GEL	STACKING GEL
Acrylamide/Bis-acrylamide 30% solution (Sigma Life Science)	47.80%	65.97%	16.70%
Separating gel buffer	35.70%	35.70%	
Stacking gel buffer			12.70%
Distilled water	13.60%	7.00%	68.50%
SDS (PanReac AppliChem ITW Reagents)	0.14%	0.14%	0.10%
APS (Sigma)	1.40%	1.40%	1.00%
TEMED (PanReac AppliChem)	0.10%	0.10%	0.10%

Table 1a *Composition of the gels used in SDS-PAGE*. *Separating gel buffer was composed of 18.2 % Tris-base and 0.002 % SDS, with pH adjusted to 8.8. Stacking gel buffer was composed of 6.1 % Tris-base and 0.002 % SDS, with pH adjusted to 6.8. APS = ammonium persulphate. TEMED = tetramethylethylenediamine.*

COMPONENT	SAMPLE BUFFER	RUNNING BUFFER	TRANSFER BUFFER	WASH BUFFER	BLOCKING BUFFER
SDS (PanReac AppliChem ITW Reagents)	5.20%	0.10%	0.10%		
Glycerol stock	26.00%				
Phenol red	0.03%				
Tris-HCl	0.163 M		25 mM		
Beta-mercaptoethanol	15.00%				
Tris (MP)		0.3 % w/v		10 mM	10 mM
Glycine (Fisher)		1.5 % w/v	192 mM		
Methanol (VWR BDH Chemicals)			20%		
NaCl				100 mM	100 mM
Tween20 (Fisher BioReagents)				0.10%	0.10%
FBS					2%
BSA (Sigma-Alrich)					2%

Table 1b *Composition of the buffers using in SDS/PAGE and Western blotting*.

2.4.10 Stastical analysis

Data was analysed using GraphPad Prism 8.1.2. Normality was tested using the Shapiro-Wilk test. Data not normally distributed was analysed with a non-parametric Mann Whitney test. An unpaired T-test was used for data that was normally distributed. For weight loss data, a Two-Way ANOVA test was conducted, using the Sidak correction for multiple comparisons. For percentage survival data, a log-rank (Mantel-Cox) test was conducted. Western blot images were analysed using Image J software (version 1.52).

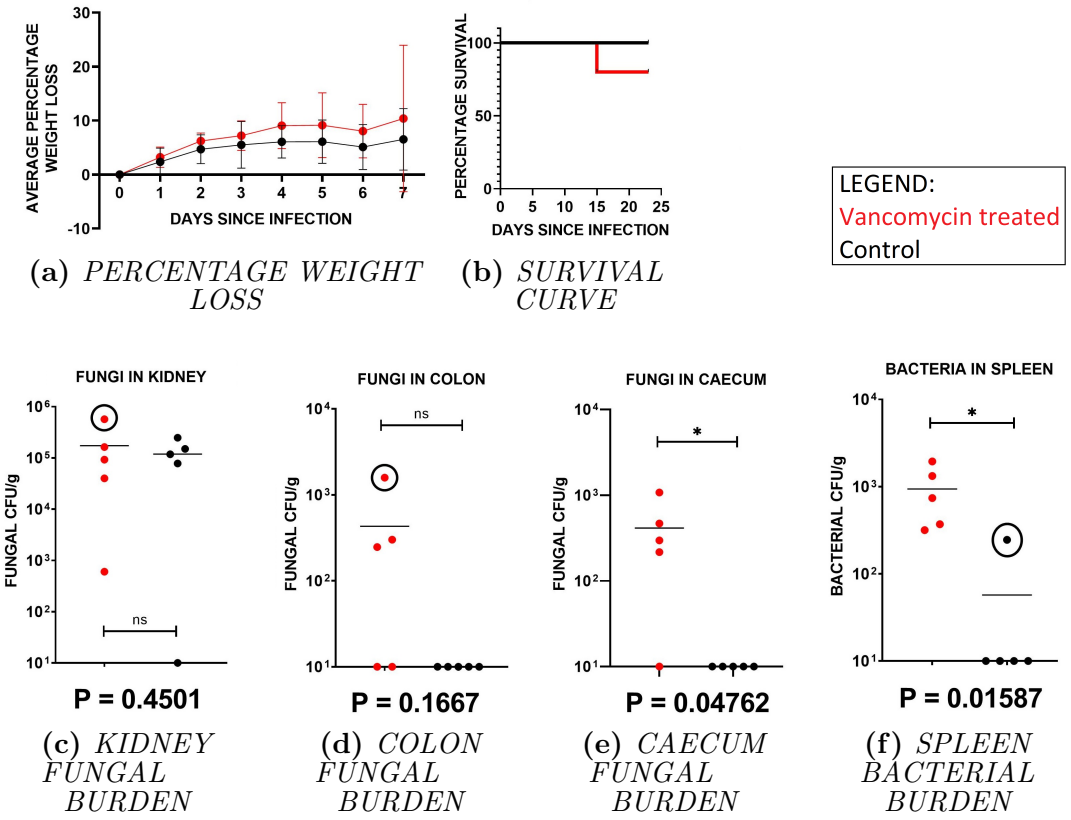
2.5 RESULTS

2.5.1 Health and spread of fungi within the murine body on infection with *C. albicans*

Since vancomycin has been shown to be a risk factor in humans for the development of Candidasis, we wanted to explore the mechanisms in a controlled animal model. 5 vancomycin-treated and 5 control mice were infected with *C. albicans*, their health monitored, and fungal burdens in the caecum, colon and kidney determined 7 days post-infection.

No statistically significant change was seen in the fungal burdens present in the kidney (figure 2.2c), which is of importance because this is the principle site of infection in this model [64]. Fungal cells were also detected in the colon and caecum of vancomycin treated mice, but were not detectable in control mice (figures 2.2d, figure 2.2e). This is of interest because immuno-competent mice are resistant to GI colonisation by *C. albicans* [65]. These results show that vancomycin treatment is causing the movement of fungal cells from the blood stream (as they were administered *intra-venously*) into the GI tract and the immune system of vancomycin-treated mice is unable to remove this fungi.

It was shown that there was a slight increase in percentage weight loss in mice pretreated with vancomycin following infection (figure 2.2a), however these mice showed no difference in survival at 7 days post infection (all mice survived 7 days). One vancomycin-treated mouse required euthanisation at 15 days post-infection (figure 2.2b). Vancomycin treatment in the absence of fungal infection does not affect the mice.



(a) *PERCENTAGE WEIGHT LOSS* (b) *SURVIVAL CURVE* (c) *KIDNEY FUNGAL BURDEN* (d) *COLON FUNGAL BURDEN* (e) *CAECUM FUNGAL BURDEN* (f) *SPLEEN BACTERIAL BURDEN*

Figure 2.2 ***Percentage weight loss in the first 7-days post-infection [a], percentage survival up to 23-days post-infection [b], fungal tissue burdens [c-e] and bacterial tissue burden [f] for vancomycin-treated (red) and control (black) mice following infection with* C. albicans**. *Mice were infected with* 1×10^5 *CFU* C. albicans, *with some mice having had prior treatment with vancomycin (0.5 mg/ml in drinking water for 4 weeks prior to infection). Percentage weight loss was monitored (n=10 for each group), and showed no statistically significant difference at any time point using a Two-Way ANOVA with Sidak's multiple comparisons test. Percentage survival was based on the mice not euthanised for the purpose of tissue burdens (n=5 for each group), and showed no statistically significant difference using the Log-rank (Mantel-Cox) test. Fungal tissue burdens in the kidney, colon, and caecum, and bacterial tissue burdens in the spleen were tested 7 days post-infection (n=5 for both groups). Each data point represents a single mouse, with outliers (identified by GraphPad QuickCalcs: Outlier calculator) circled. Outliers were not included in statistical analysis. P values for the kidney were determined using an unpaired parametric T-test. P values for the colon, caecum, and spleen were determined using non-parametric Mann-Whitney tests.*

Given that vancomycin appears to be allowing fungi to infect the GI tract, we wanted to explore whether there were any changes in the spleen caused by the prior-treatment of vancomycin, as this filters the blood. If vancomycin treatment is damaging the GI tract-blood barrier (therefore allowing fungi into the GI tract), there may also be bacteria passing into the blood from the GI tract, which may cause bacteria to be present in the spleen of the mice. To investigate this, the spleen bacterial burdens were determined from the same mice used above. Figure 2.2f shows that, with the exception of one outlier, bacteria were only found in the spleens of vancomycin treated mice. This implies that prior treatment with vancomycin is causing a subsequent bacterial infection.

2.5.2 Small intestine digests

Given the effect seen in the GI tract, we wanted to explore whether there were perturbations in the immune system in this location. Small intestines were removed from vancomycin-treated (n=3) and control (n=4) mice (who had not been infected with *C. albicans*), and flow cytometry was used to isolate different cell populations (figure 2.3). The cells from all the control mice were pooled together prior to analysis, as were the cells from all the vancomycin treated mice. Important values of cell populations taken from the flow cytometry analysis are shown in table 2.2. Although different numbers of mice were used with the flow cytometry analysis for vancomycin-treated and control mice, the differences between the values cannot be purely attributed to the difference in sample sizes, as can be seen in the 'per mouse' figures shown in table 2.3.

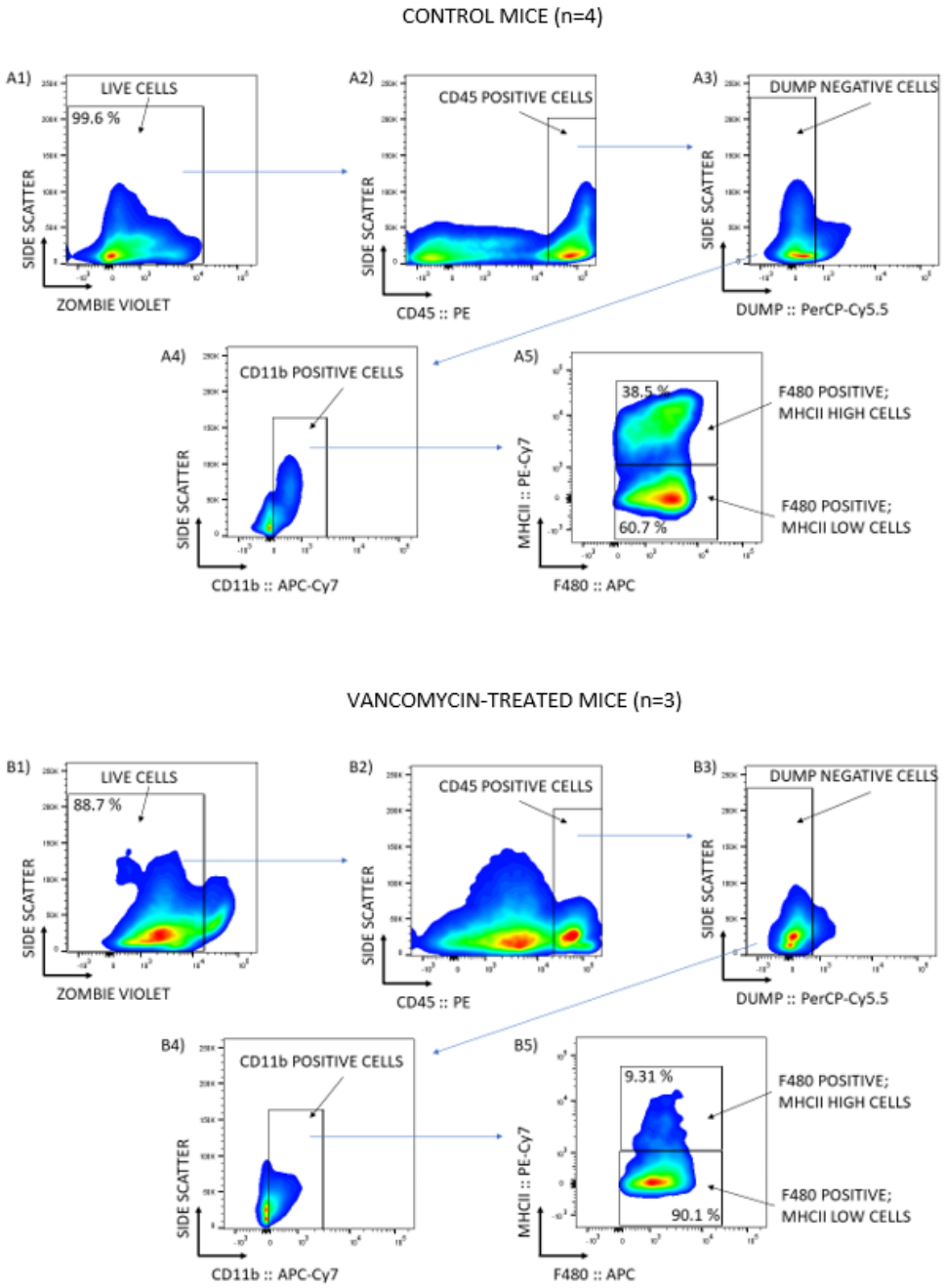


Figure 2.3 ***Flow cytometry analysis of gut macrophages isolated from control (A1-A5) and vancomycin-treated (B1-B5) mice.*** *Leukocytes were isolated from the small intestines and stained to identify macrophage populations (defined as CD45+CD3-CD19-CD11b+F480+). The dump channel contains any CD3+ or CD19+ cells. Macrophages were also separated into 2 populations based on their MHCII expression.*

	Control mice	Vancomycin-treated mice
Number of mice	4	3
Number of single cells isolated	143 654	36 362
Number of live single cells isolated	149 119	32 253
Number of live macrophages isolated	13 369	2 352
Number of live MHCII-high macrophages isolated	5 147	219
Number of live MHCII-low macrophages isolated	8 115	2 119

Table 2.2 ***Cell populations from flow cytometry analysis of gut macrophages isolated from control and vancomycin-treated mice***

	Control mice	Vancomycin-treated mice
Number of single cells isolated per mouse	37 414	12 120
Number of live single cells isolated per mouse	37 280	10 751
Number of live macrophages isolated per mouse	3 342	784
Number of live MHCII-high macrophages isolated per mouse	1 287	73
Number of live MHCII-low macrophages isolated per mouse	2 029	706

Table 2.3 ***Cell populations from flow cytometry analysis of gut macrophages isolated from control and vancomycin-treated mice expressed as an average per mouse***

The results show a decrease in the population size of macrophages in the small intestines of mice treated with vancomycin, with a majority of the decrease being in macrophages with a high expression of histocompatibility complex class II (MHCII). These macrophages are of importance, as the expression of MHCII is associated with activation of the macrophages, meaning that MHCII high macrophages are thought to be better able to deal with pathogens. There is also an increase in the number of dead cells in the samples from vancomycin treated mice in comparison to control mice. These results show that the treatment with vancomycin is having an effect on both the size and the composition

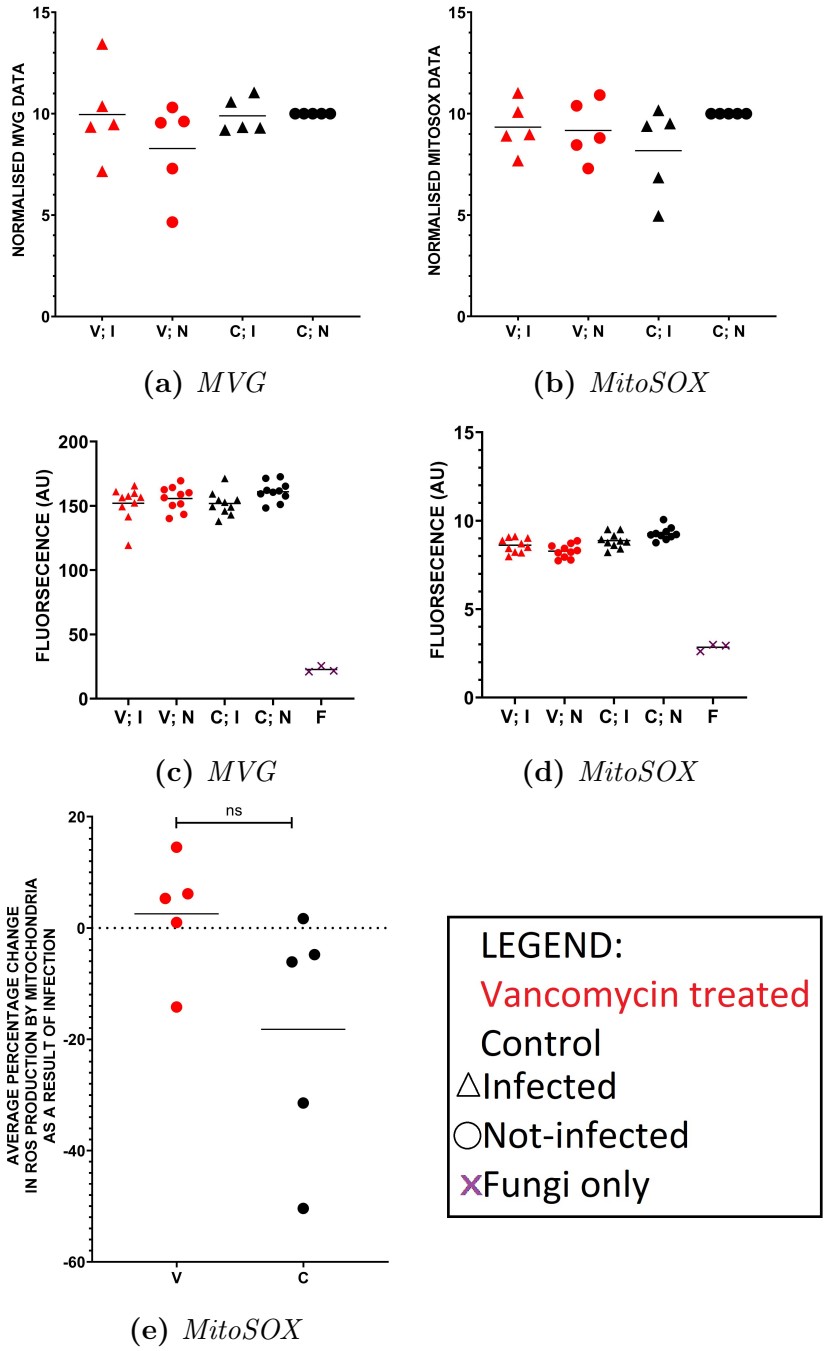
of the macrophage population within the small intestines.

2.5.3 Mitochondrial response to *C. albicans* infection *in vitro*

We also wanted to determine whether effects are seen *in vitro*. We firstly looked at whether vancomycin was having an effect on the production of ROS by the macrophages (an important chemical for killing pathogens), by both NADPH oxidase and the mitochondria. Bone marrow macrophages were either treated with vancomycin, or allowed to grow without antibiotic treatment, and staining assays were conducted to determine the ROS production. There was no significant effect of either vancomycin treatment or infection on the mitochondrial mass within the macrophages, as shown by the MVG staining (figure 2.4a).

MitoSOX staining (figures 2.4b and 2.4e) reveals that control macrophages experience a decrease in mitochondrial ROS production as a result of infection, whereas this is not seen in vancomycin treated macrophages. The difference, however, was not statistically significant. These results suggest that vancomycin treatment is preventing the alterations in mitochondrial functions that occur in control macrophages as a result of infection. Since the MVG assay shows no effect of vancomycin treatment or infection, this can be attributed to damage to the performance of the mitochondria.

Based on the DHR staining (figure 2.5a), it is difficult to draw any conclusions about the general ROS production within the macrophages, because the signal from the fungus alone was frequently similar to the signals from macrophages, even when heat killed fungi were used.

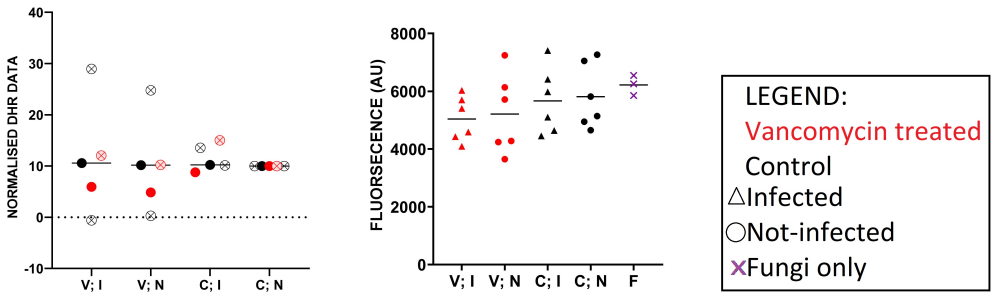


(a) *MVG* (b) *MitoSOX*

(c) *MVG* (d) *MitoSOX*

(e) *MitoSOX*

Figure 2.4 ***MitoSOX and MVG staining assay results for* in vitro *bone marrow macrophages***. *For the normalised mitochondrial staining assays (a-b),* 1×10^5 *vancomycin-treated (*$20\ ngmL^{-1}$ *in the media, red) or control (black) macrophages were infected with* 2×10^5 *of yeast cells (triangles) or remained uninfected (circles). Each data point in graphs a-b represents the average of results from* $n \geq 3$ *samples from bone marrow derived macrophages taken from a single mouse. The technical repeats for one biological replicate for MVG (c) and MitoSOX (d) are shown, with the fluorescence produced by fungi when they were exposed to the dyes in the absence of macrophages. MitoSOX results are also shown as a percentage change due to infection (e). P values for the effect of vancomycin on uninfected samples (MVG and MitoSOX) were determined using non-parametric Mann-Whitney tests. P values for the effect of vancomycin on infected samples (MVG and MitoSOX) and the change in ROS production by mitochondria were determined using an unpaired parametric T-test.* $P > 0.05$ *for all graphs.*



(a) *DHR* **(b)** *DHR*

Figure 2.5 ***DHR staining assay results for* in vitro *bone marrow macrophages***. *For the staining assays,* 1×10^5 *vancomycin-treated (20* $ngmL^{-1}$ *in the media, red) or control (black) macrophages were infected with* 2×10^5 *heat killed (red) or live (black) yeast cells. Hollow points show data where the yeast gave a similar reading to the macrophages. Each data point on graph A represents the average of results from* $n \geq 3$ *samples from bone marrow derived macrophages taken from a single mouse. The technical repeats for one biological replicate are shown, with the fluorescence produced by fungi when they were exposed to the dye in the absence of macrophages.*

2.5.4 Killing ability of macrophages *in vitro*

As well as the effect on ROS production, we also wanted to explore the effect of vancomycin on the ability of macrophages to kill *C. albicans*, by co-culturing bone-marrow macrophages (either treated with vancomycin or control) with *C. albicans* and determining the number of fungal cells alive after incubation for 2 hours. The results (figure 2.6) showed large variations between biological replicates, and no conclusions could be drawn.

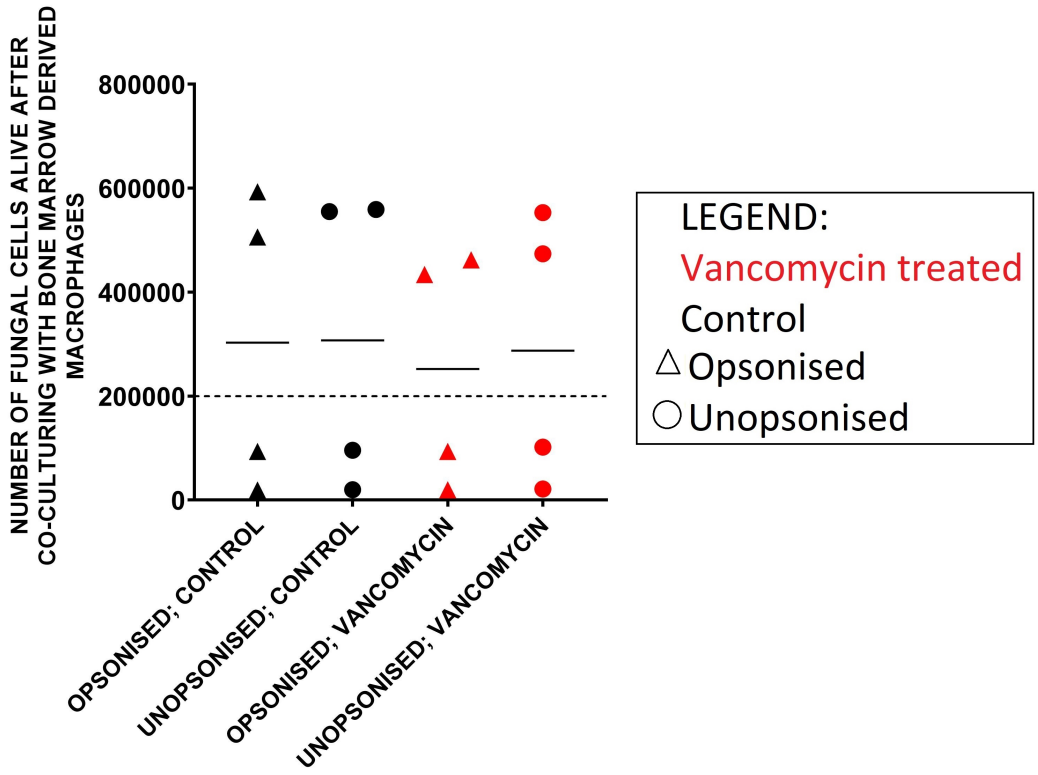


Figure 2.6 ***Killing assay results for* in vitro *bone marrow derived macrophages***. *1×10^5 vancomycin-treated (20 $ngmL^{-1}$ in the media, red) or control (black) macrophages were infected with 2×10^5 of yeast cells in the presence of either 10% mouse serum (opsonised; triangle) or 10% FBS (unopsonised; circles), and the number of fungal cells surviving after 2 hours of co-culture were determined. Each data point in the graph represents one biological replicate and is the average of results from $n \geq 3$ samples from bone marrow derived macrophages taken from a single mouse.*

2.5.5 LC3-associated phagocytosis protein expression

Vancomycin has been shown to affect LAP [66] which is an important process for the control of *C. albicans* infection [67], so this was also explored by extracting proteins from macrophages that had been infected with *C. albicans*. The results (figure 2.7) suggest that vancomycin caused a slight reduction in LC3B expression and a slight increase in P62 expression, however more repeats of this experiment are needed to back up this finding.

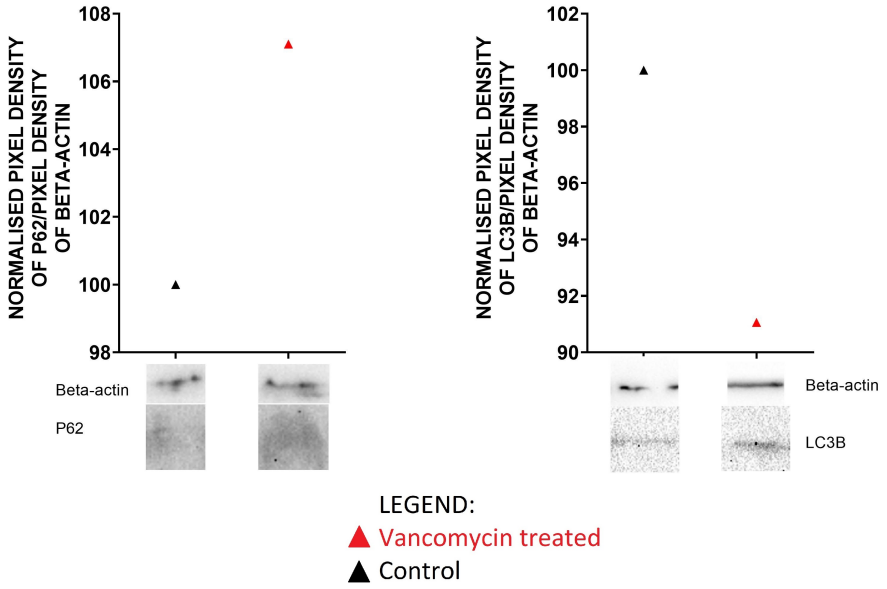


Figure 2.7 ***SDS-PAGE/Western blot results for*** **in vitro** ***bone marrow macrophages.*** *0.5×10^6 bone marrow macrophages (vancomycin treated [red] and control [black]) were co-cultured with 5×10^6* C. albicans *for 2 hours, and the proteins were extracted from the cells. Protein concentration were made to 1500 $\mu g/mL$ prior to addition of sample buffer, and 11.25 μg of proteins were loaded into each channel of the acrylamide gel. Each data point represents the result of a single SDS-PAGE. Results were expressed as a ratio of the beta-actin reading for the same condition, and then normalised to be a percentage of the control reading. P values could not be determined due to a lack of data points.*

2.6 DISCUSSION

Overall, these results show that vancomycin has an effect on the ability of the murine immune system to cope with a *C. albicans* infection *in vivo*, although no statistically significant effects of vancomycin treatment could be seen *in vitro*.

Within the fungal and bacterial *in vivo* graphs, all outliers have been left in to show the large variation between mice, however outliers have not been included in statistical analysis. It can be seen that most of the fungal burden variation occurs in the vancomycin treated mice, while there are no statistical outliers for the fungal burdens of control mice. This indicates that the variation can be attributed to the vancomycin treatment, potentially as a result of mice drinking different amounts of water and therefore acquiring different doses of vancomycin. To determine if this is the case, it would be necessary to use a different method

of administering vancomycin that is not mouse-dependent, such as oral gavage in which the vancomycin is delivered directly into the stomach of the mouse. Further experiments could be conducted to determine if the survival of vancomycin treated mice in comparison to control mice is altered at longer time durations, as only a short infection duration was used in this experiment. Fungal and bacterial tissue burdens could also be compared at longer time durations, as these may also show a difference between the vancomycin-treated and control mice.

Immuno-competent mice are resistant to GI-colonisation by *C. albicans*, meaning that an *intra-venous* method of administering the infection had to be used instead of administering the fungi through the oral route. The presence of fungal cells within the GI tract of the vancomycin-treated mice therefore shows that fungi are moving from the blood stream into the GI tract, and that the murine immune system is unable to remove this pathogen.

Bacteria that has been found in the spleens of vancomycin-treated mice has the potential of causing a fatal systemic bacterial infection. Since there was no introduction of bacteria during the study, it is highly likely that the bacteria found in the spleens was originally a commensal bacteria. Within the *in vivo* results, it has been shown that fungi have migrated from the blood stream into the GI tract, indicating damage to the GI tract-blood barrier within vancomycin-treated mice. It is therefore hypothesised that the bacteria that is found in the spleen was originally a commensal GI bacteria that migrated into the blood. One method to confirm this would be to run the same infection model on germ free mice (mice with no GI bacteria). If this hypothesis is correct, vancomycin treated germ free mice will not develop a bacterial infection after infection with *C. albicans*. An alternative method would be to run matrix-assisted laser desorption/ionisation time of flight (MALDI-TOF), in order to identify the species of the bacteria present in the spleen. MALDI-TOF is a method of mass spectrometry which uses ribosomes and other abundant bacterial proteins as biomarkers to allow quick and accurate identification of bacterial species [68]. This would allow the determination of whether the bacteria are typical gut commensals.

It is known that the presence of fungal and bacterial infections concurrently can alter the virulence of each of the pathogens [69]. For example, a mixed biofilm of *C. albicans* and *Staphylococcus aureus* results in *S. aureus* having a greater tolerance for vancomycin compared to *S. aureus* in a single species biofilm [70]. It has also been shown that the presence of a co-infection of *C. albicans* and *S. aureus* causes a significant increase in the cytokines and chemokines associated with the innate pro-inflammatory response in mice [71], and results in significantly lower survival rates. The decrease in survival caused by coinfection has also been reported for coinfection of *Streptococcus constellatus* and *Fusobacterium nucleatum* [72]. One vancomycin treated mouse within the experiments undertaken in this project experienced a significant, delayed weight-loss that required euthanisation at 15 days post-infection. It is possible that this was a result of a systemic bacterial infection, although no tests were conducted to confirm this.

MitoSOX data shows that control macrophages experience a decrease in mitochondrial ROS production on infection. This decrease in mitochondrial ROS production, however, is not seen in vancomycin treated macrophages. No published reports could be found to compare these results to. The difference between the mitochondrial ROS production in control and vancomycin treated mice suggests that vancomycin treatment is having an effect on how the macrophages alter their metabolism upon activation. To confirm this, more assays that analyse the metabolism would be needed, such as a Seahorse Assay which measures oxygen consumption and extracellular acidification to provide information on the mitochondrial and metabolic function of cells [73].

There is disagreement within the literature regarding changes in general ROS production that occurs as a result of *C. albicans* infection. Duan *et al* [74] suggests that stimulation with *C. albicans* results in increased ROS production in THP-1-derived macrophages (using DCFH-DA staining). In contrast, Wellington *et al* [75] report that *Candida spp* (including *C. albicans*) suppress general ROS production in *in vitro* phagocytes from the murine macrophage cell line J774.A1.

Spellberg *et al* [76] and Shin *et al* [77] report a suppression in nitric oxide (NO) generation from macrophages following stimulation by *C. albicans*. NO is known to be a form of ROS that can be used by macrophages to kill injested pathogens. In order to determine the effect of vancomycin treatment and/or *C. albicans* infection on the general ROS production, it will be necessary to optimise the DHR staining assay to ensure that the background is not obscuring the results being gained, such as by decreasing the incubation time [78–80] or washing the sample [81].

Differences in fungal burdens *in vivo* may also be a result of disturbances to LAP (a process that is known to be important in the macrophage response to *C. albicans*), so Western blot analysis was conducted on 2 of the LAP proteins (p62 and LC3B). Due to time spent optimising the Western blot assay and the luminescence imaging, only a single complete set of data was acquired. Difficulties were encountered in producing readable LC3B blots, so a number of different protein concentrations, gel compositions, and durations for SDS-PAGE had to be tried. This means that no statistical conclusions can be drawn.

An increase in P62 expression as a result of vancomycin treatment has previously been reported by Ha *et al* [66], and indicates that the vancomycin is blocking autophagy flux in the macrophages. This is in support of the result found during this project. However, it was also reported that LC3B expression increased for vancomycin treated macrophages in contrast to control macrophages [66]. The difference between this and the experimental results of this project may be due to errors in the data of figure 2.7, or may be a result of Ha *et al* [66] not using infected macrophages. Further repeats would be needed to determine a conclusion for these results.

The data from flow cytometry shows that there is a decrease in MHCII high macrophages within the gut of vancomycin-treated mice. MHCII is required for antigen presentation to the adaptive immune system, potentially leading to a dulled adaptive immune response in vancomycin-treated mice. The flow cytome-

try data also shows a reduction in the number of live cells within the gut digest.

The average number of macrophages per mouse (regardless of their MHCII presentation) reduced from 3,342 in control mice to only 784 in vancomycin treated mice. It has been previously reported that phagocytosis of *C. albicans* by macrophages can result in the death of the macrophage [82] by triggering pyroptosis [82] (a form of cell death) of the macrophages and by formation of hyphae [82] and by causing competition for glucose. [83]. More experiments are needed to determine if the killing of macrophages by *C. albicans* cells is affected by prior vancomycin treatment. This could be conducted by either flow cytometry of gut digests of *C. albicans* infected mice, or by an *in vitro* assay to determine the number of live macrophages after co-incubation with *C. albicans*.

The presence of fewer innate immune cells, and the potential lack of stimulation of adaptive immune cells could contribute to the inability of mice to clear the fungal infection from their GI tract. It would also allow the composition of the GI microbiome to alter [a known and common problem with antibiotic usage], which has the potential of allowing some bacterial populations to expand and become infective (possibly crossing into the blood stream and going on to infect the spleen). The combination of reduced live-cell numbers, and the reduction in stimulation of the adaptive immune system could account for why an effect is being seen *in vivo*, while there is no difference in killing ability *in vitro* (because an equal number of live cells were used for each *in vitro* experiment, and the role of the adaptive immune system was not examined as macrophages were the only murine cell used). This shows the main problem with conduction studies *in vitro* – they are not fully representative of the *in vivo* conditions.

To determine the effect of cell number, it would be necessary to determine the *in vivo* macrophages concentrations for both the control and vancomycin-treated mice, and use these concentrations (which will be different for both sets of mice) within the *in vitro* assays. The presence of other immune cells was removed for *in vitro* assays because these cells will also contribute a signal, so it will be more

difficult to determine the effect of stimulation of the adaptive immune system *in vitro*. Transgenic mice that express reporter molecules (such as green fluorescent protein) during cytokine production have been used within immunological research [84], and could be applied to study stimulation of the adaptive immune system *in vivo*.

2.7 CONCLUSION

In conclusion, while it has been shown that vancomycin is having an effect on the murine immune system, and specifically on macrophages, further studies are needed to determine the exact effect that is being caused. Of most interest would be to produce consistent killing assay results *in vitro* to determine whether macrophages are less able to deal with a *C. albicans* infection after treatment with vancomycin. Following from this, the effect of vancomycin on ROS production would be of interest, as there is disagreement in the literature within this field.

Currently, prophylaxis antifungal treatment is routinely given to intensive care patients [29]. Once the effect of antibiotics on the immune system is fully understood, this prophylaxis treatment can be limited to only those patients who are at particular risk (or antibiotic treatments with a lower risk of damage to the immune system could be used for these patients). This will reduce the requirement for antifungal treatment, and therefore reduce the selective pressure on fungi which promotes the spread of resistance.

BIOINFORMATICS

3.1 ABSTRACT

This analysis was based on data from a set of 57 clinical isolates of *Clostridioides difficile* (with ribotype 027) collected from hospitalised patients in 26 locations in Germany [85]. Samples were taken between 1990 and 2012. The paper used Bayesian phylogeographic analysis to determine the spatial and temporal dynamics of the spread of *C. difficile* throughout Germany, and discovered that fluoroquinolone resistant *C. difficile* was imported into Germany on at least 4 occasions.

This report focuses on re-analyzing the genomic sequences from the 57 clinical isolates, however it does not repeat the Bayesian phylogeographic analysis.

3.2 SIGNIFICANCE STATEMENT

Clostridioides difficile can cause severe, hospital acquired infections. It is estimated that *C. difficile* infections (CDI) cause 29,500 deaths annually (within 30 days of diagnosis) [86]. The development of a CDI is often associated with the prior use of antibiotics.

3.3 INTRODUCTION

Clostridioides difficile (formerly *Clostridium*) is a Gram-positive anaerobic bacillus [87] which can cause severe, hospital acquired infection. Within just 40 years of the first isolation of *C. difficile* in 1935, it was recognised as the main cause of antibiotic associate colitis and diarrhoea [87]. Over the past 20 years, there has been an increase in the prevalence of *C. difficile* infections [86]. While this is partially attributed to increased number and sensitivity of testing, it is also a result of the rapid spread of the polymerase chain reaction (PCR) ribotype 027 strain of bacteria.

3.3.1 The numbers

A 2019 meta-analysis [88], which included data from 41 different countries, estimated that the prevalence of health-care facility associated *C. difficile* infection (CDI) for patients of all ages was 2.24 per 1000 admissions per year or 3.54 per 10 000 patient days, accounting for 44.6% of gastro-intestinal (GI) infections and 4.9% of all healthcare associated infections (HAI) [89]. It is the elderly population that is particularly affected [88].

3.3.2 Resistance of *C. difficile*

Resistance of *C. difficile* to many antibiotics have been reported, as shown in table 3.1.

Antibiotic	Mechanism(s) of resistance	Target protein or gene
Cephalosporins	Antibiotic enzymatic destruction; alteration of the target	Putative beta-lactamases and PBPs
Macrolide-lincosamide-streptograminB	23s RNA methylases; RNA methyl transferase	*ermB* and *cfr*
Fluoroquinolones	Alteration of the target	*gyrA* and *gyrB*
Metronidazole	Metabolic pathway alterations; biofilm formation	
Vancomycin	Alteration of the target; biofilm formation	*murG*
Rifamycins	Alteration of the target	*rpoB*
Tetracycline	Ribosomal protection	*tetM*; *tet44*
Chloramphenicol	Chlorampenicol acetyltransferase	*catD*

Table 3.1 ***Resistance mechanisms of*** C. difficile to common antibiotics *[90].*

3.3.3 Infection

C. difficile is transmitted by the faecal-oral route, as shown in figure 3.1, and the development of CDI is often associated with antibiotic use. A study of 47 stool isolates of *C. difficile* from Iraqi hospitals by Hindi *et al* [91] showed that all of the isolates came from patients who had received at least one antibiotic, with over 80% of the isolates associated with patients who had taken more than 2 different antibiotics. This association is caused by the alterations in the commensal flora of the gut that results from antibiotic usage. This alteration allows *C. difficile* bacteria to proliferate [87].

Hospitals provide a major reservoir for *C. difficile*, with the bacteria being carried by both symptomatic patients and asymptomatic carriers [87]. Patients with symptomatic infections heavily contaminate their environment with spores that can persist despite regular cleaning [87]. It has been shown that asymptomatic carriers can act as a source of hospital-acquired CDI (HACDI) [93]. In addition to HACDI, community acquired CDI is becoming increasingly prevalent, and affects

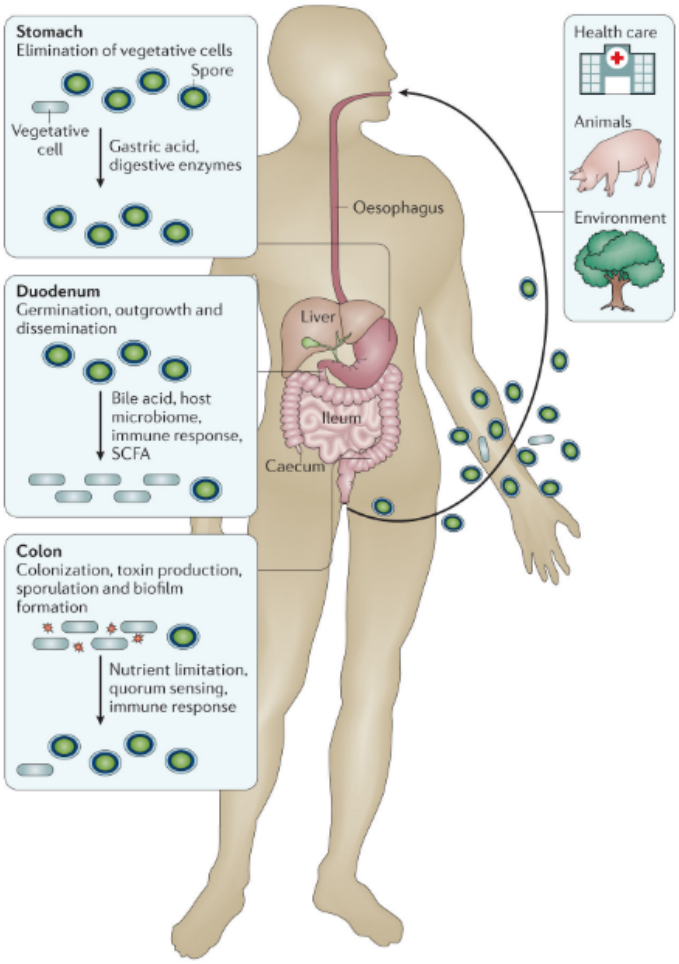


Figure 3.1 ***The life cycle of*** **C. difficile** ***within the human gastrointestinal tract [92].*** *Spores present in the faecal matter of infected individuals contaminate their environment and are ingested. Passage through the stomach removes most vegetative cells, so only spores pass into the duodenum, where they germinate. The* C. difficile *cells then colonize the colon and begin to produce toxins. Spores are also produced, and these leave the body in the faeces, allowing the cycle of infection to continue. SCFA = short-chain fatty acids.*

patients who are not currently classified as 'at risk' such as the young and those who have not recently received antibiotic treatment [86].

Symptoms of *C. difficile* infection (CDI) are caused by toxin produced by the *C. difficile cells*. Toxinogenic isolates usually simultaneously produce 2 toxins (A and B), which cause fluid secretion, inflammation, and mucosal damage [87]. The toxins act to disrupt the tight junctions and destroy the actin cytoskeletons in the enterocytes [86]. This can lead to severe complications, such as toxic mega-colon [92].

3.3.4 Ribotypes

C. difficile bacterial isolates can be classified in multiple ways, of which one method is ribotyping. Ribotyping involves classifying the isolates based on the sequence in the 16S-23S intergenic spacer region of their genome [94], which is the region of DNA between the 16S and 23S rRNA genes that is transcribed with the rRNA genes. Many ribotypes of *C. difficile* have been identified [95, 96].

Ribotype 027

C. difficile ribotype 027 has been shown to exhibit one of the highest antibiotic resistance profiles of all of the *C. difficile* ribotypes, with a 2020 study showing that over 40% of the tested ribotype 027 isolates being resistant to at least 3 classes of antibiotics [97]. All of the tested ribotype 027 isolates also showed high levels of resistance to moxifloxacin (a fluoroquinolone), however they were susceptible to vancomycin [97], one of the first line treatments for *C. difficile* infections.

The increased prevalence of this particularly resistant ribotype of *C. difficile* is of concern. In a 2020 study [97] 65.2% of the tested isolates were of ribotype 027, when 253 toxinogenic isolates of *C. difficile* from Poland were analysed. However, in the United Kingdom, between April 2008 and March 2018, there was a decrease in the prevalence of the PCR ribotype 027 isolates [98], in isolates sent to the *Clostridium difficile* Ribotyping Network as a result of hospitals experiencing increased frequency/severity/mortality/recurrence of CDI. This, therefore, does not account for all cases of CDI as there is no requirement for hospitals to report cases. A similar trend has also been seen in Texas [99]. While these trends are promising, studying the spread of ribotype 027 of *C. difficile* will provide knowledge to help in preventing the spread of any new highly virulent ribotypes, such as the ribotype 255. Ribotype 255 is a novel ribotype that has been identified in Texas and has a similar disease severity to ribotype 027, however it infects patients who are younger on average than those infected with ribotype 027 [99].

3.3.5 Sequence types

Another method of classifying *C. difficile* isolates is through the use of sequence types . The sequence types (STs) of different isolates are determined based on nucleotide sequences of house keeping genes, with each unique combination of alleles being assigned to a different sequence type. A 2010 study identified 40 sequence types for *C. difficile* isolates taken from stool samples [100]. A phylogenetic tree was produced to show the relationships between isolates from the different sequence types (figure 3.2). For most of the sequence types (32/40), each sequence type corresponded to a single PCR ribotype, however 8 of the sequence types corresponded to multiple PCR ribotypes. Table 3.2 shows the ribotypes associated with each sequence type. It was also noted that PCR ribotype was not always predictive of the sequence type, for example, the ribotype 014 was associated with both the sequence type 2 and sequence type 14 (see table 3.2).

ST	Ribotype	ST	Ribotype
1	027, 036	22	023
2	014, 020, 076, 220	26	039, 140
3	001, 009, 072, 115	27	067
4	137	32	153
5	023, 063	33	064
6	005	34	056
7	026	35	046
8	002, 159	36	011
9	081	37	017
10	015	38	060
11	078	39	085
12	003, 225	40	035
13	129	42	106, 118, 174
14	014	46	191
15	010	51	186
16	050	53	103
17	018	54	012
18	050	56	021
19	110	67	019
20	202	69	072

Table 3.2 ***Table showing the ribotypes that correspond to each sequence type (ST) for*** **C. difficile** *[100].*

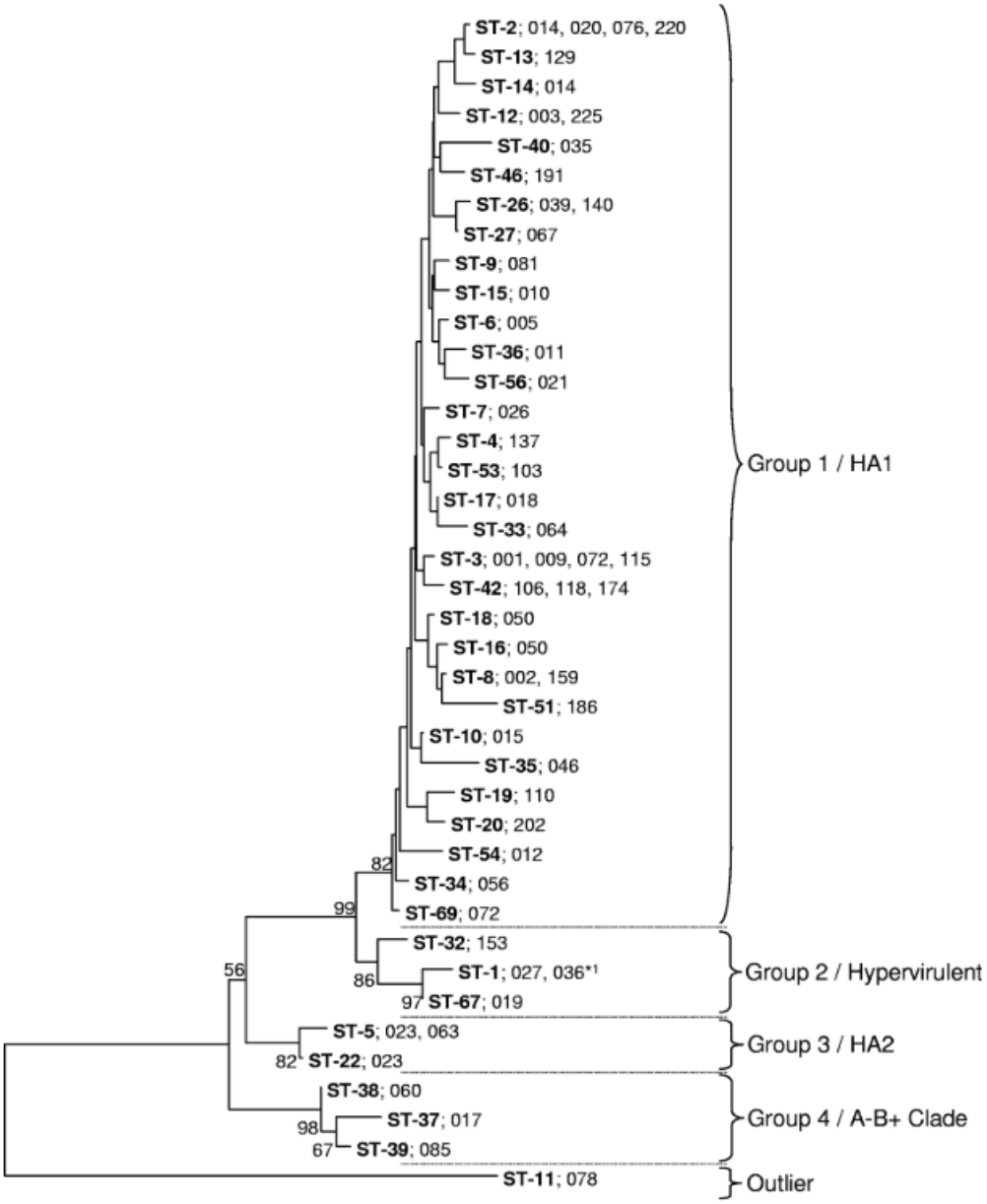


Figure 3.2 ***Phylogenetic tree constructed for the 40 sequence types of* C. difficile *detected, based on seven loci used in multi-locus sequence typing (MLST)*** *[100]. Based on the clades of the tree, the different sequence types can be classified into 4 main groups, which correspond to the groupings found in whole genome analysis. Bootstrap=1,000.*

3.4 METHODS

This analysis is based on genomic data taken from a research article that aimed to trace the spread of *C. difficile* Ribotype 027 in Germany [85]. Raw data was downloaded from the sequence read archive (SRA) onto the server using fastq-dump (version 2.10.0) using the accession number PRJEB9067 for the bioproject. This programme is part of the sra-toolkit (NCBI). The data used is available at `https://www.ncbi.nlm.nih.gov/biosample?Db=biosample&DbFrom=bioproject&Cmd=Link&LinkName=bioproject_biosample&LinkReadableName=BioSample&ordinalpos=1&IdsFromResult=288366`. The isolation year for each isolate is shown in table 3.3, along with the lineage (FQR1 or FQR2) assigned in the original paper that this analysis is based on. A work flow showing the processes used as part of this research is shown in figure 3.3.

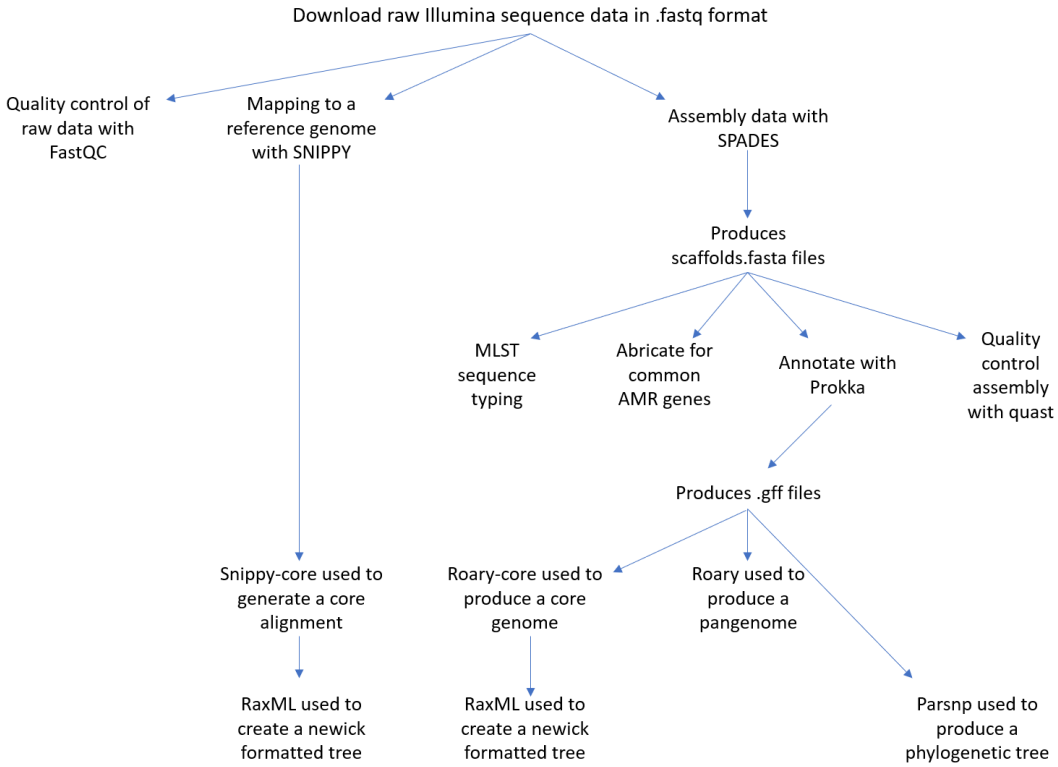


Figure 3.3 ***Work flow used for bioinformatics analysis.***

Isolate	Isolation Year	Lineage	Isolate	Isolation Year	Lineage
07-00080	2007	FQR2	10-00370	2010	FQR2
07-00089	2007	FQR2	10-00391	2010	FQR2
08-00070	2007	FQR2	10-00412	2010	FQR2
08-00201	2008	FQR2	10-00432	2010	FQR2
08-00233	2008	FQR2	10-00454	2010	FQR2
08-00267	2008	FQR2	10-00484	2010	FQR1
08-00411	2008	FQR2	12-00001	2008	FQR2
08-00495	2008	FQR2	12-00002	2009	FQR2
08-00669	2008	FQR2	12-00003	2011	FQR2
09-00022	2009	FQR2	12-00004	2011	FQR2
09-00072	1990	-	12-00005	2012	FQR2
09-00077	2008	FQR2	12-00006	2012	FQR2
09-00133	2009	FQR2	12-00007	2012	FQR2
09-00161	2009	FQR2	12-00008	2012	FQR2
09-00211	2009	FQR2	12-00009	2012	FQR2
09-00274	2009	FQR2	12-00010	2012	FQR2
09-00300	2009	FQR2	12-00011	2012	FQR2
09-00313	2009	FQR2	12-00012	2012	FQR2
09-00350	2009	FQR2	12-00013	2012	FQR2
09-00361	2009	FQR2	12-00014	2012	FQR1
09-00385	2009	FQR2	12-00015	2012	FQR2
09-00386	2009	FQR2	12-00016	2012	FQR2
09-00414	2009	FQR2	12-00017	2012	FQR1
10-00071	2010	FQR2	12-00018	2012	FQR1
10-00078	2010	FQR2	12-00019	2012	FQR1
10-00253	2010	FQR2	12-00020	2012	FQR2
10-00313	2010	FQR2	12-00021	2012	FQR2
10-00327	2010	FQR2	12-00022	2012	FQR2
10-00331	2010	FQR2			

Table 3.3 ***The year that each isolate was taken, and the lineage that it is assigned to in the original paper that the analysis is based on****. [85]*

FastQC (v0.11.8) was used to quality control the raw data files. *De novo* assemblies were then created using SPAdes (v3.13.1). Assemblies were quality controlled using QUAST (v5.0.2). Multi-locus sequence typing and screening for common resistance genes were conducted on the assemblies using mlst (2.17.6) and ABRicate (0.9.8) respectively. The assembled genomes were also annotated, using Prokka (1.14.0). From the assembled and annotated genomes, a pangenome was created using ROARY (3.12.0) [101]. ROARY was also used (by passing additional flags) to produce a core genome alignment from the assembled genomes. Using RaxML, this core genome alignment was formed into a phylogenetic tree. Parsnp (v1.2) was also used to produce a phylogenetic tree directly from the assembled, annotated genomes.

The raw data was also mapped against a reference genome (GenBank assembly number GCA_000027105.1) using SNIPPY (4.4.5). SNIPPY-core (4.4.5) was used to create a core genome alignment, from which RaxML was used to create a phylogenetic tree.

09-00072 (isolated in 1990) is used as an outgroup for rooting phylogenetic trees.

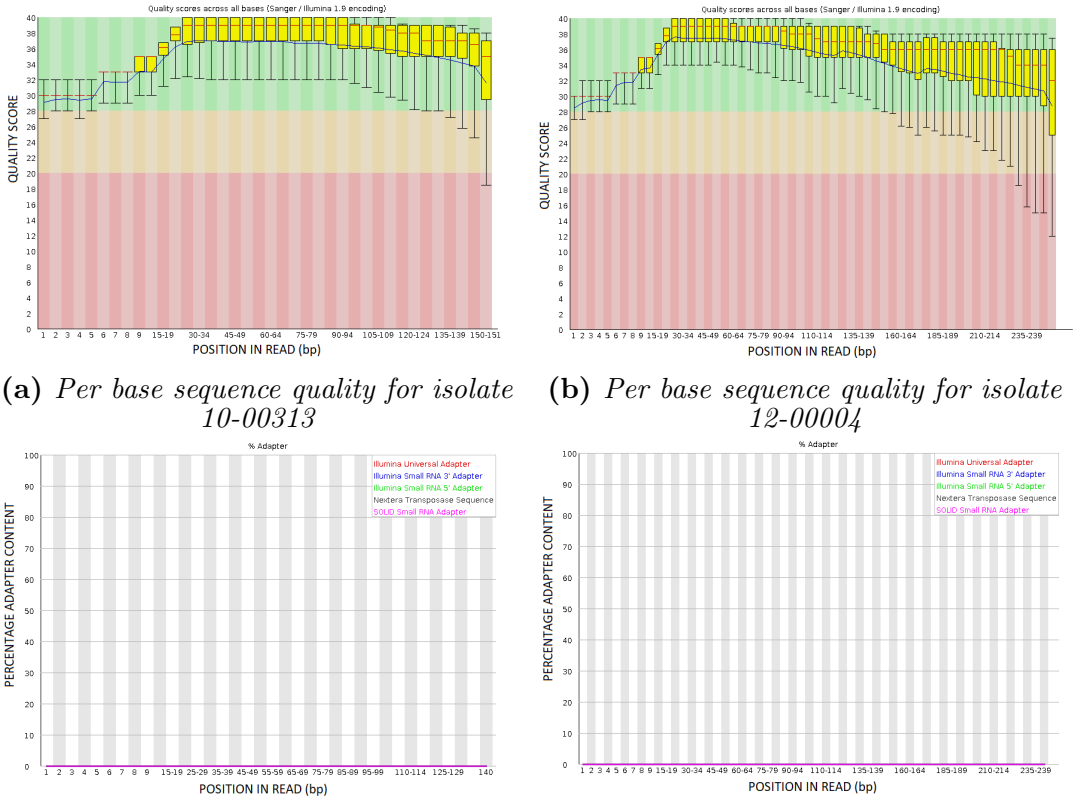
Phandango was used to produce figures.

3.5 RESULTS AND DISCUSSIONS

3.5.1 Quality of the raw data

Data extracted from the FastQC reports for each of the isolates on the total number of sequences, the number of sequences flagged as poor quality, and the percentage GC content are shown in table 3.4. Two examples of the per base sequence quality and adapter content graphs are shown in figure 3.4. These results show good quality of the raw data, with quality scores mainly in the green

region, no adapters present, and no sequences flagged as poor quality.



(a) *Per base sequence quality for isolate 10-00313*

(b) *Per base sequence quality for isolate 12-00004*

(c) *Adapter content for isolate 10-00313*

(d) *Adapter content for isolate 12-00004*

Figure 3.4 ***Example graphical output from FastQC for two samples.*** *Graphs a and b show the per base sequence quality as a function of position in read for isolates 10-00313 (a) and 12-00004 (b). Quality scores above 28 are good. Graphs c and d show the percentage of adaptors present as a function of the position in read for isolates 10-00313 (c) and 12-00004 (d). The lower the percentage adapter content, the better the quality of the data.*

ISOLATE	TOTAL NUMBER OF SEQUENCES	POOR QUALITY SEQUENCES	% GC	ISOLATE	TOTAL NUMBER OF SEQUENCES	POOR QUALITY SEQUENCES	% GC
07-00080	3714816	0	32	07-00089	2029453	0	32
08-00070	439050	0	29	08-00201	1486518	0	30
08-00233	591550	0	30	08-00267	4000000	0	31
08-00411	703015	0	31	08-00495	672303	0	30
08-00669	1123687	0	31	09-00022	427836	0	29
09-00072	778240	0	31	09-00077	418463	0	29
09-00133	581894	0	29	09-00161	763447	0	29
09-00211	602617	0	29	09-00274	572308	0	29
09-00286	965629	0	29	09-00300	588349	0	29
09-00313	728636	0	29	09-00350	762644	0	29
09-00361	672305	0	29	09-00385	700931	0	29
09-00414	1157543	0	29	10-00071	874535	0	30
10-00078	949235	0	29	10-00253	1418945	0	31
10-00313	1329639	0	29	10-00327	1577819	0	29
10-00331	851345	0	29	10-00371	1102866	0	29
10-00391	1755378	0	29	10-00412	1619346	0	29
10-00454	1366304	0	29	10-00484	1203978	0	29
12-00001	1641643	0	29	12-00002	683187	0	30
12-00003	1055257	0	29	12-00004	1485696	0	30
12-00005	1234450	0	30	12-00006	1503213	0	30
12-00007	1105920	0	30	12-00008	1886149	0	30
12-00009	1729371	0	30	12-00010	1266537	0	30
12-00011	1368116	0	30	12-00012	1470338	0	30
12-00013	1985224	0	30	12-00014	533733	0	30
12-00015	653908	0	30	12-00016	643695	0	30
12-00017	564671	0	30	12-00018	662771	0	31
12-00019	438424	0	31	12-00020	531622	0	30
12-00021	526559	0	31	12-00022	511252	0	31

Table 3.4 ***Important information on the raw data****. Important data (number of sequences per isolate; number of sequences flagged as poor quality; percentage of bases that were G or C) was extracted from FastQC analysis.*

3.5.2 Mapping the genome

The genetic sequences of each sample were mapped to a common reference sequence to produce a phylogenetic tree (figure 3.5). The reference sequence used in this report is different to that used by the original paper [85]. This produces a tree similar to that of the original paper (see appendix A.1) when 09-00072 was used as an outgroup for rooting the tree. The 2 main clades formed aligned with the main clades of the published phylogenetic tree. In the original paper, these clades were assigned to the two international fluoroquinolone-resistant lineages (FQR1 and FQR2) using comparisons to previously published data, however this was not done as part of this report.

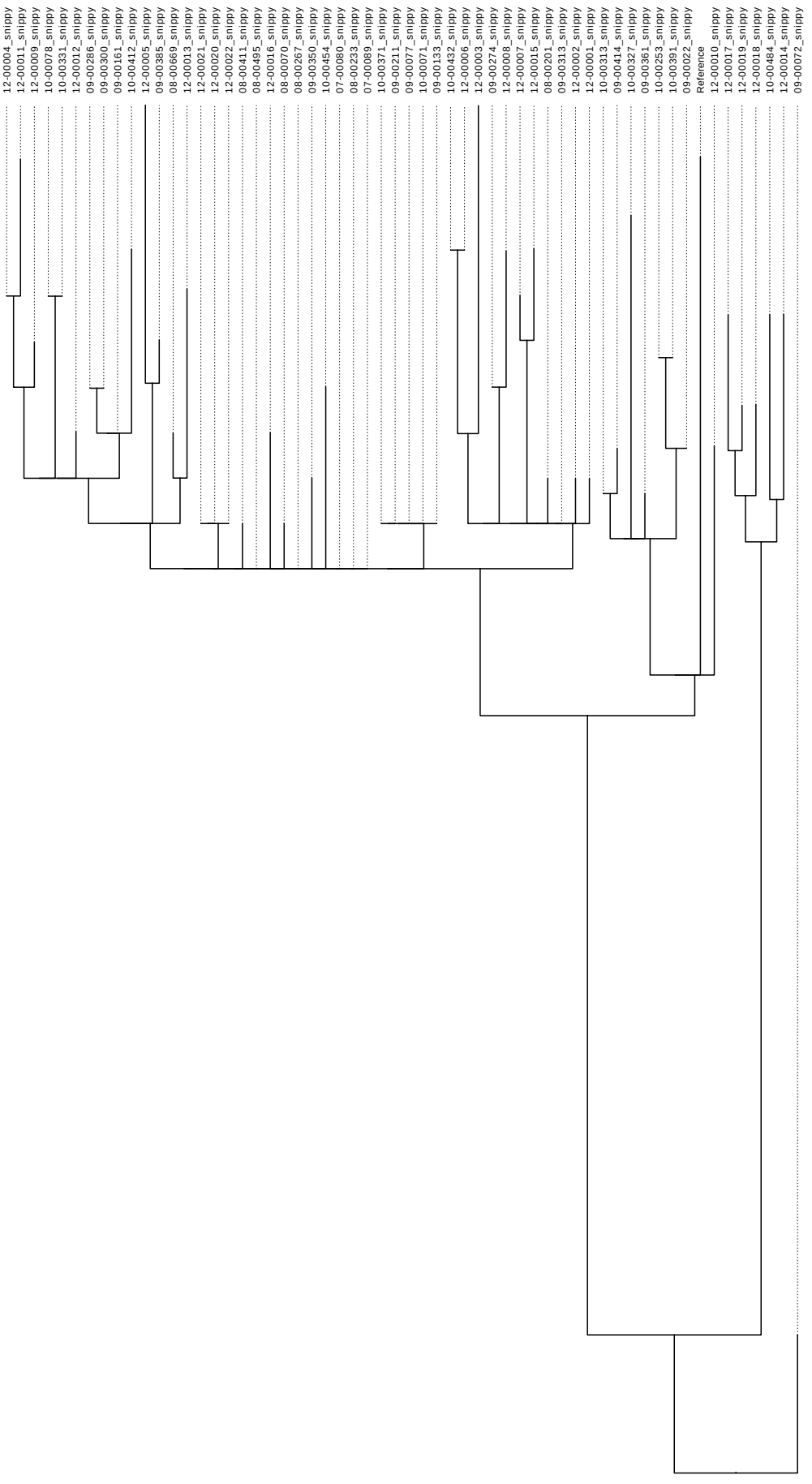


Figure 3.5 ***Maximum-likelihood phylogenetic tree produced from mapped genomes using SNIPPY core.*** *Bootstrap=100.*

3.5.3 *De novo* assembly

De novo assembly of the genomes was also conducted, with the quality of these assembled genomes being shown in figure 3.6.

Assembly	08_00233_scaffolds
# contigs (>= 0 bp)	553
# contigs (>= 1000 bp)	55
# contigs (>= 5000 bp)	49
# contigs (>= 10000 bp)	43
# contigs (>= 25000 bp)	32
# contigs (>= 50000 bp)	25
Total length (>= 0 bp)	4121420
Total length (>= 1000 bp)	4064558
Total length (>= 5000 bp)	4049402
Total length (>= 10000 bp)	4008060
Total length (>= 25000 bp)	3799511
Total length (>= 50000 bp)	3555865
# contigs	63
Largest contig	424393
Total length	4069783
GC (%)	28.44
N50	146964
N75	89114
L50	9
L75	18
# N's per 100 kbp	25.01

(a) *08-00233*

Assembly	09_00022_scaffolds
# contigs (>= 0 bp)	454
# contigs (>= 1000 bp)	42
# contigs (>= 5000 bp)	37
# contigs (>= 10000 bp)	32
# contigs (>= 25000 bp)	26
# contigs (>= 50000 bp)	23
Total length (>= 0 bp)	4138331
Total length (>= 1000 bp)	4081164
Total length (>= 5000 bp)	4067847
Total length (>= 10000 bp)	4035674
Total length (>= 25000 bp)	3925006
Total length (>= 50000 bp)	3821143
# contigs	49
Largest contig	425874
Total length	4086133
GC (%)	28.47
N50	218358
N75	113538
L50	7
L75	14
# N's per 100 kbp	24.18

(b) *09-00022*

Assembly	10_00484_scaffolds
# contigs (>= 0 bp)	483
# contigs (>= 1000 bp)	41
# contigs (>= 5000 bp)	38
# contigs (>= 10000 bp)	32
# contigs (>= 25000 bp)	27
# contigs (>= 50000 bp)	24
Total length (>= 0 bp)	4161434
Total length (>= 1000 bp)	4092878
Total length (>= 5000 bp)	4085370
Total length (>= 10000 bp)	4044853
Total length (>= 25000 bp)	3948348
Total length (>= 50000 bp)	3840368
# contigs	48
Largest contig	407691
Total length	4097732
GC (%)	28.47
N50	151102
N75	114128
L50	8
L75	15
# N's per 100 kbp	28.70

(c) *10-00484*

Figure 3.6 ***Example quality control outputs from QUAST****. The QUAST outputs for three samples (08-00233 (a), 09-00022 (b), and 10-00484 (c)) are shown. The output includes the number of contigs above set lengths, the total length of contigs, and the percentage of the bases that are G or C.*

An alternative tree was produced using the *de novo* core genome alignment (figure 3.7). Although this tree looks very different, the major clades can be seen to be the same. The difference between the two phylogenetic trees is likely to be due to the more accurate alignment of reads when mapped to a known genome over the accuracy of a *de novo* assembly. Although the QUAST quality control results (see figure 3.6) are good for a whole genome assembly, there are multiple contigs for each sample (as is expected), leading to the *de novo* core genome alignment likely being less accurate than the mapped genome.

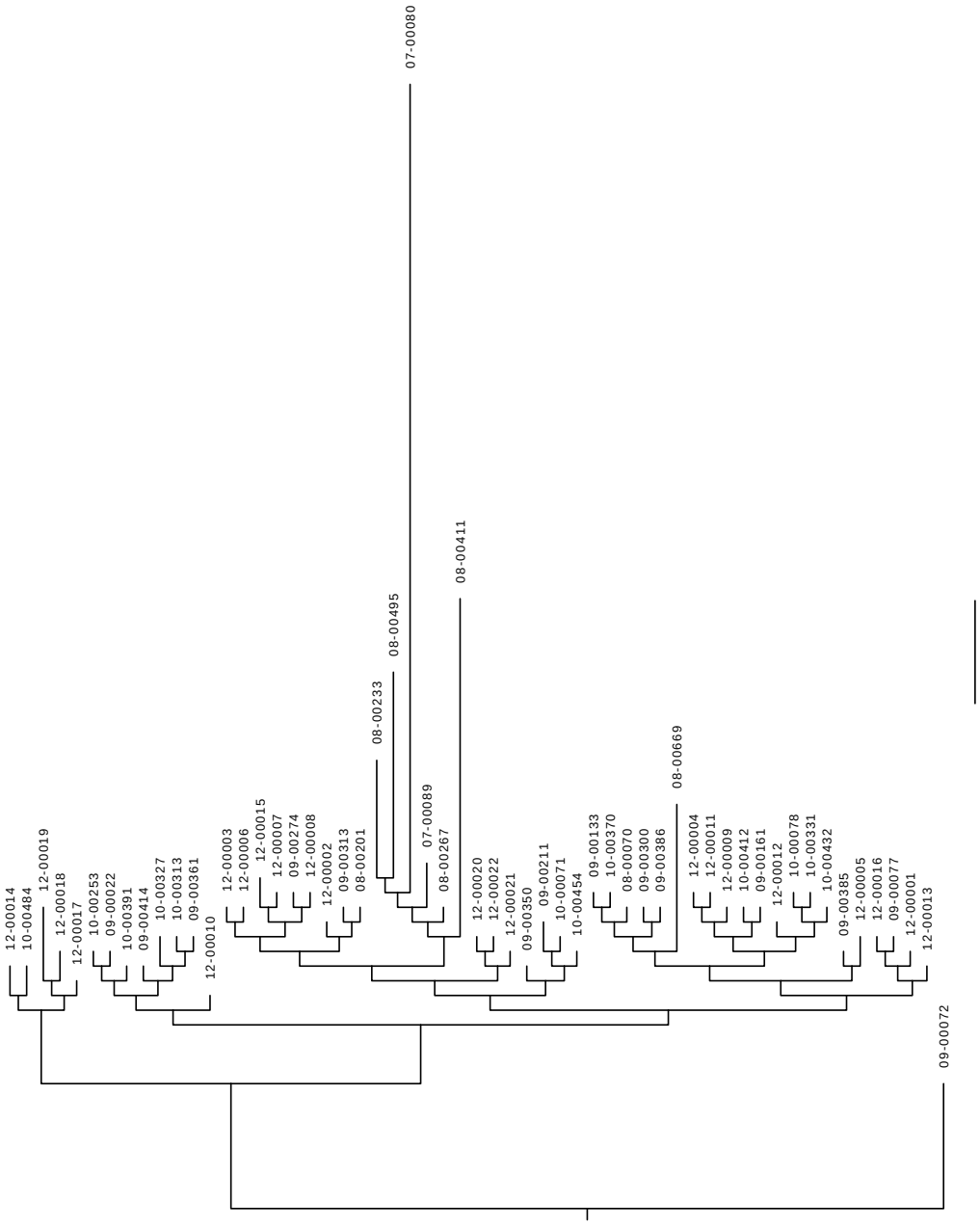


Figure 3.7 ***Maimum likelihood phylogenetic tree produced from*** de novo ***aligned genomes using ROARY****. Bootstrap=100.*

3.5.4 MLST results

From the multi-locus sequence typing (MLST), it can be seen that all of the samples are of the same species and sequence type (figure 3.8). All of the samples have correctly been identified as being *C. difficile*. The paper this analysis is based on focuses exclusively on *C. difficile* ribotype 027, a sufficient (although not necessary) condition for being of sequence type 1. It is therefore as expected that all of the samples should be of sequence type 1, as shown by the MLST analysis.

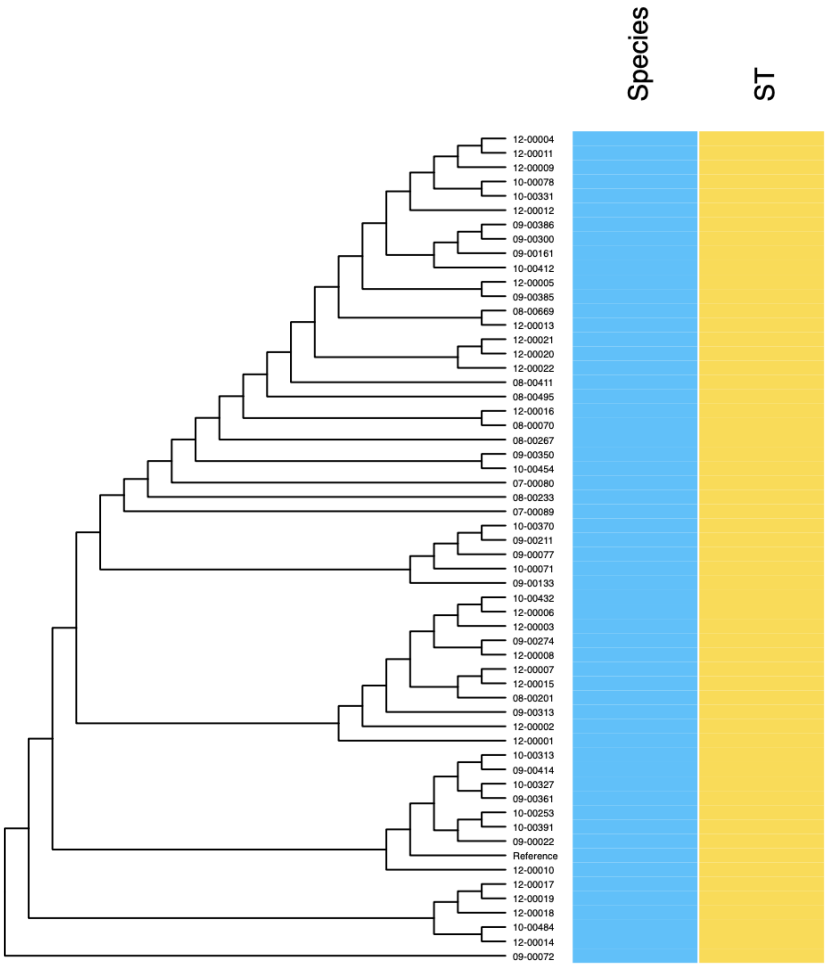


Figure 3.8 ***The species and sequence type of each isolate identified by mlst.*** *Phylogenetic cladogram (left) is produced using SNIPPY core and the mapped genomes. A cladogram is used for ease of reading; the corresponding phylogenetic tree is shown in figure 3.5. Blue represents that the identified species is* C. difficile*. Yellow represents that the sequence type of the given isolate is sequence type 1.*

3.5.5 SNPS

The number of SNPs present between each isolate, based on the mapped genomes are shown in figure 3.9. In the same way as the original paper, core genome analysis of the mapped genomes found a number of isolates with no differences in their core genome. In contrast, the SNP matrix for the *de novo* assembled genomes (figure 3.10) showed no isolates with identical core genomes. By comparing the SNP distances between the isolates using the mapped and *de novo* assembled genomes, it can be seen that the *de novo* assembled genomes contained many more SNPs than the mapped genomes.

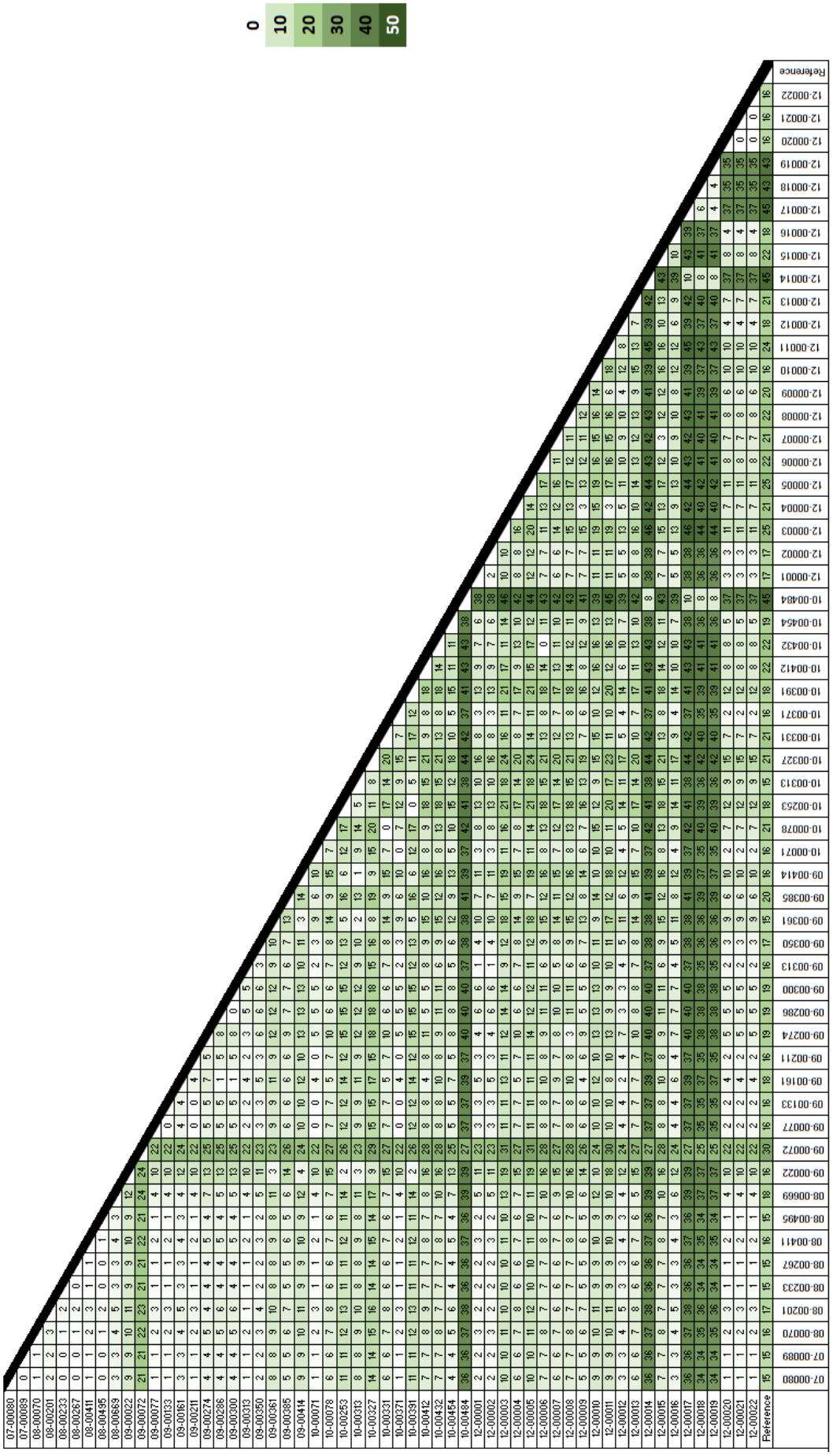


Figure 3.9 ***SNP distance matrix between isolates based on mapping.*** *The table has been colour-coded based on the number of SNPs between the isolates using to the scale on the right.*

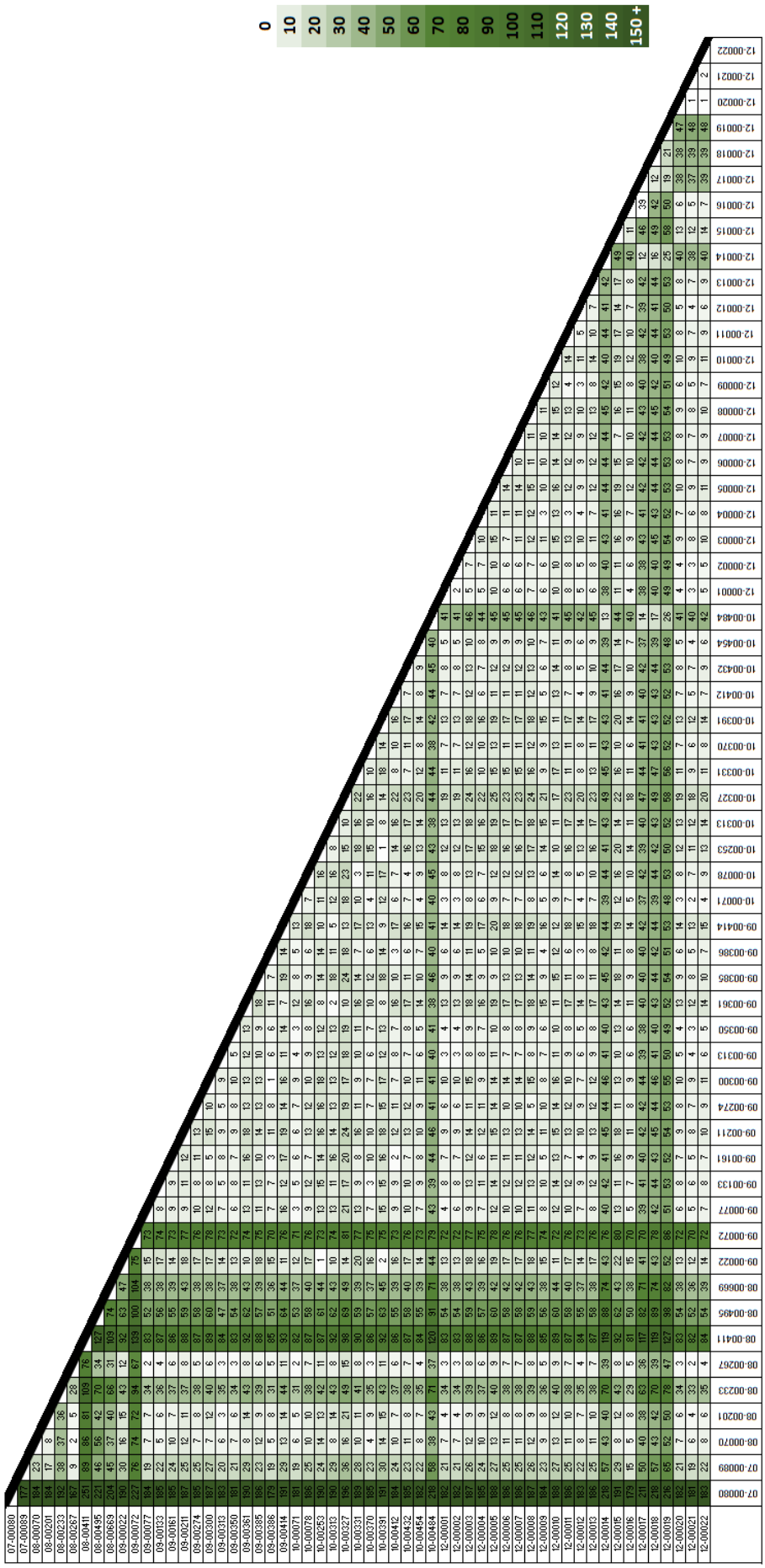


Figure 3.10 ***SNP distance matrix between isolates based on* de novo *assembly.*** *The table has been colour-coded based on the number of SNPs between the isolates using to the scale on the right.*

3.5.6 Isolate 07-00080

Of note in the SNP distance matrices is isolate 07-00080, which showed the largest number of SNPs compared to all of the other isolates based on the *de novo* assembled genomes, however this was not the case for the mapped genomes. This difference is also highly noticeable in the phylogenetic tree produced from the *de novo* assembled genomes (figure 3.7). When the quality of the *de novo* assembly of this isolate is looked at (figure 3.11), it can be seen that there are a large number of contigs in comparison to the other isolates, and that the largest contig is much shorter than for the other isolates. This indicates that the difference seen between this isolate and the other isolates in the *de novo* assembled phylogenetic tree is likely caused by errors in the *de novo* assembly.

Assembly	07_00080_scaffolds
# contigs (>= 0 bp)	1621
# contigs (>= 1000 bp)	239
# contigs (>= 5000 bp)	178
# contigs (>= 10000 bp)	133
# contigs (>= 25000 bp)	58
# contigs (>= 50000 bp)	10
Total length (>= 0 bp)	4201988
Total length (>= 1000 bp)	4064286
Total length (>= 5000 bp)	3910828
Total length (>= 10000 bp)	3587044
Total length (>= 25000 bp)	2365920
Total length (>= 50000 bp)	733389
# contigs	261
Largest contig	106558
Total length	4079179
GC (%)	28.48
N50	27611
N75	16570
L50	46
L75	93
# N's per 100 kbp	52.95

Figure 3.11 ***The QUAST output of isolate 07-00080****. The quality control shows a large total number of contigs, and that the longest contig is shorter than for other isolates.*

3.5.7 Presence of common resistance genes

ABRicate was used to analyse the patterns of resistance within the samples (figure 3.12). Vancomycin resistance via several mechanisms is found in all of the samples, including the older sample 09-00072. This resistance is of major concern, as vancomycin is one of the first line drugs for the treatment of *C. difficile* infections [102].

In contrast to the frequent occurrence of vancomycin resistance, *dfrF*, *erm(B)* and *tet(M)* resistance genes are less common within the samples. *erm(B)* resistance is associated with a single clade [containing 10-00484, 12-00014, 12-00017, 12-00019, 12-00018]. Of particular concern within this clade is isolate 12-00019, which also shows *dfrF* and *tet(M)* resistance genes.

With the exception of sample 12-00019, *tet(M)* is only associated with the clade containing 12-00021, 12-00020, and 12-000022.

Fluoroquinolone resistance

Fluoroquinolone resistance could not be detected in any of the samples by ABRicate, due to being a mutational resistance rather than an acquired resistance [90]. By analysing the gene locations of the mutations in each isolate when compared against the reference genome, no mutations in genes for DNA gyrase can be seen for any of the isolates (Topoisomerases are not present in *C. difficile* cells, so DNA gyrase is the only target for fluoroquinolones). This is unexpected, as fluoroquinolone resistance in *C. difficile* isolates is usually a result of mutations in DNA gyrase [90].

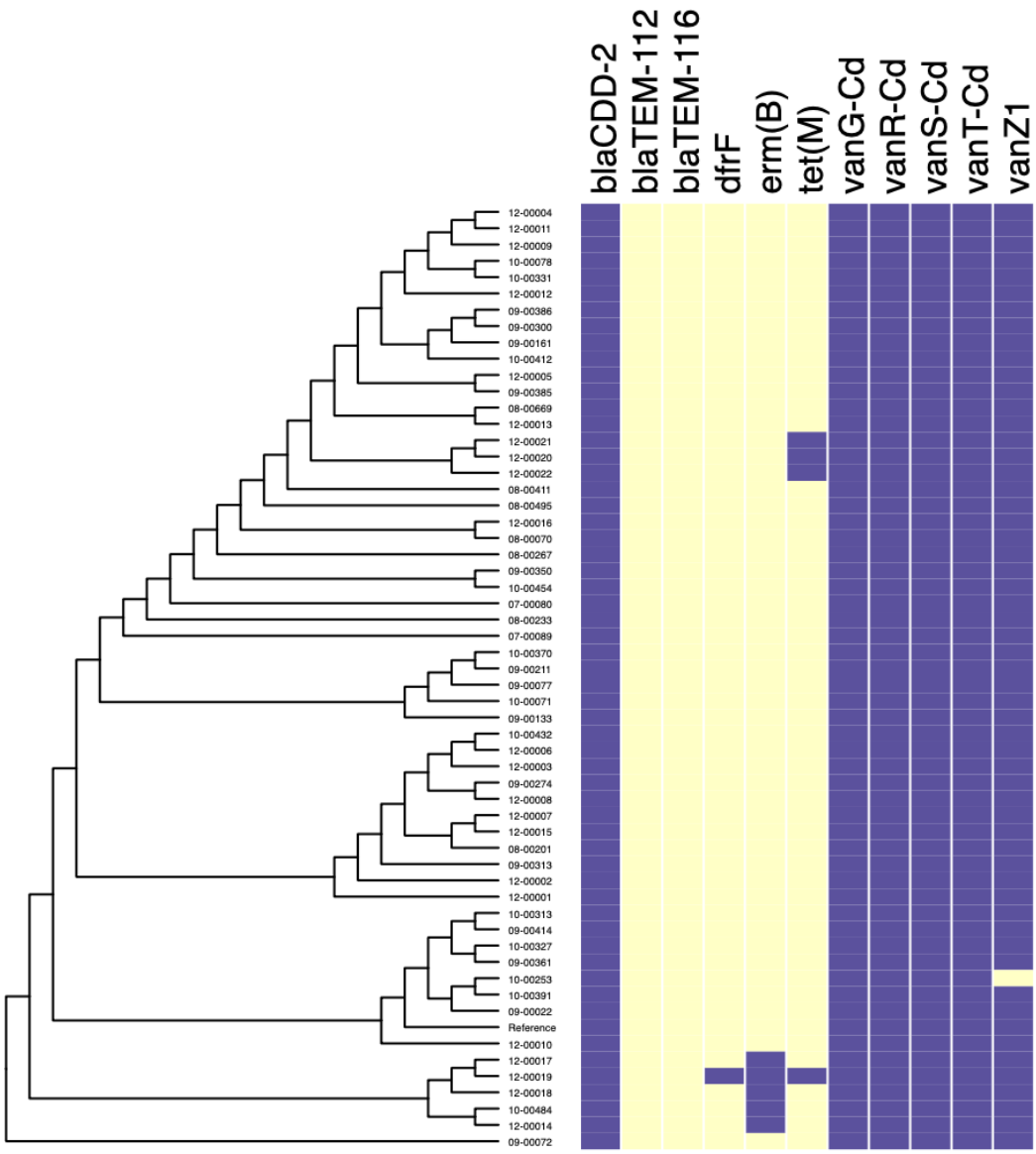


Figure 3.12 ***Presence of common resistance genes in the isolates.*** *Phylogenetic cladogram (left) is produced using SNIPPY core and the mapped genomes. A cladogram is used for ease of reading; the corresponding phylogenetic tree is shown in figure 3.5. The presence (purple) and absence (yellow) of common resistance genes (identified using ABRicate) are shown on the left.*

3.5.8 The pangenome

The pangenome produced by ROARY (figure 3.13) shows a large accessory genome in one isolate (10-00432) and smaller accessory genomes in all of the other isolates. The accessory genome of 10-00432 may be due to a mobile genetic element (MGE) being present, and includes genes related to spores (such as spore protein YabP, spore germination protein B1, and the sporulation inhibitor protein Soj). This isolate also contains additional DNA gyrase associated genes that are not present in any of the other samples.

The pangenome was derived from the *de novo* assembled genomes, so the phylogenetic tree produced from these assembled genomes was used in figure 3.13.

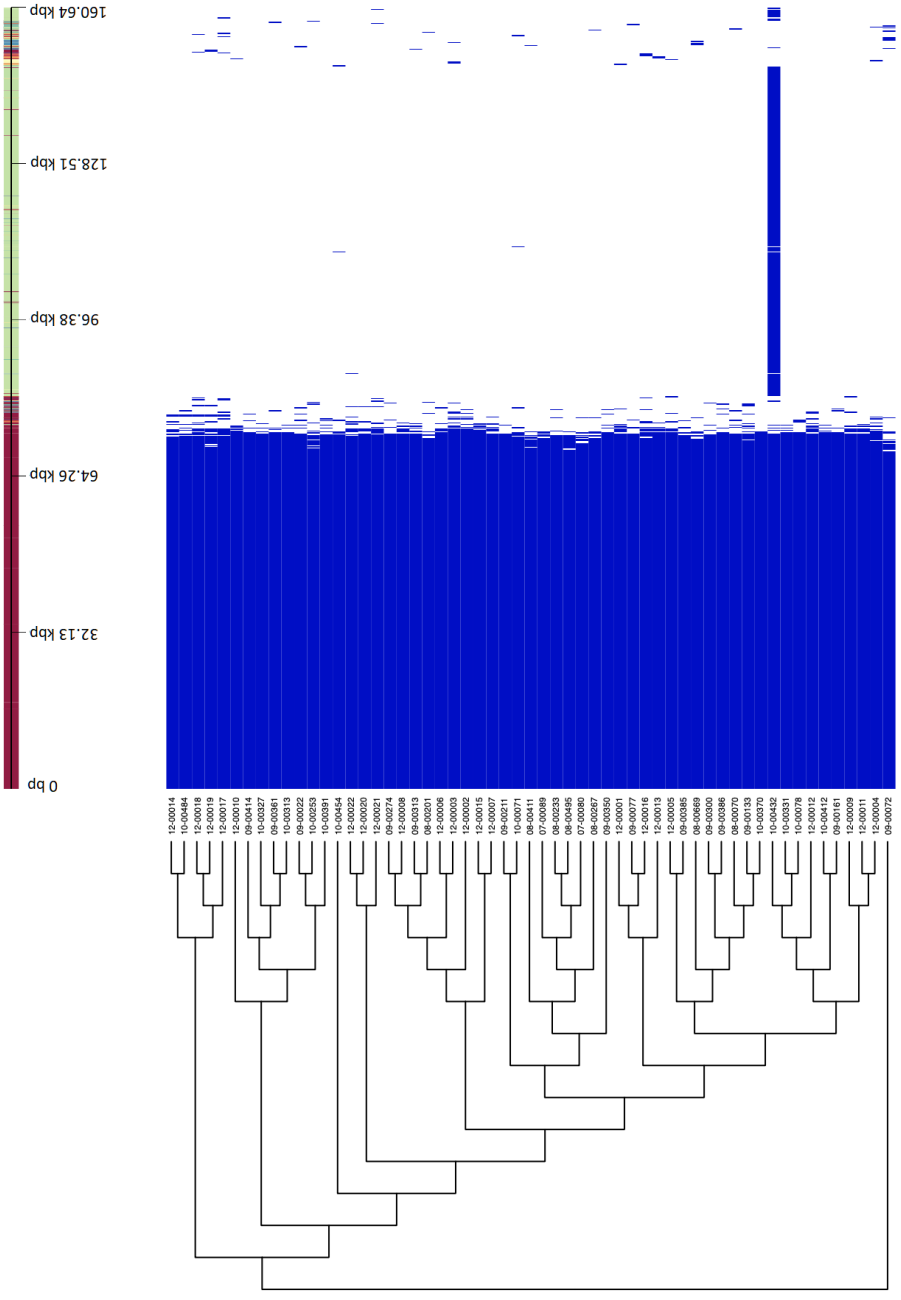


Figure 3.13 *Pangenome of the isolates.* *Phylogenetic cladogram (left) is produced using ROARY core and the* de novo *assembled genomes. A cladogram is used for ease of reading; the corresponding phylogenetic tree is shown in figure 3.7 . The pangenome (right) is produced using ROARY, with blue bars showing genes that are present in a given isolate.*

3.5.9 Toxin genes

A smaller subset of the pangenome, including only toxin-related genes, is shown in figure 3.14. It can be seen that the genes for toxin A and toxin B are present in all of the isolates, as is expected for the ribotype 027.

The antitoxin epsilon gene is only associated with a single clade, indicating that the acquisition of this gene occurred during the genomic separation of this clades from the rest of the phylogeny. The epsilon-zeta toxin-antitoxin system has been reported to be encoded both on plasmids of bacteria and within the chromosome [103]. Within *C. difficile* isolates, a mobile genetic element (MGE) called Tn6215 has been identified [104], which contains both the *erm(B)* resistance gene and genes associated with the epsilon-zeta toxin-antitoxin system. This paper also reports that, while the epsilon antitoxin gene is intact, the zeta toxin gene was truncated to only encode for 52 amino acids of the N-terminus region. It can be seen by comparing figure 3.14 and figure 3.12 that the presence of the epsilon antitoxin gene and *erm(B)* resistance gene occur for the same isolates. Most of these isolates also do not have a functioning zeta toxin gene, with the exception of 12-00017. It is reasonable to therefore hypothesises that it is the presence of the MGE Tn6215 that is responsible for these observations.

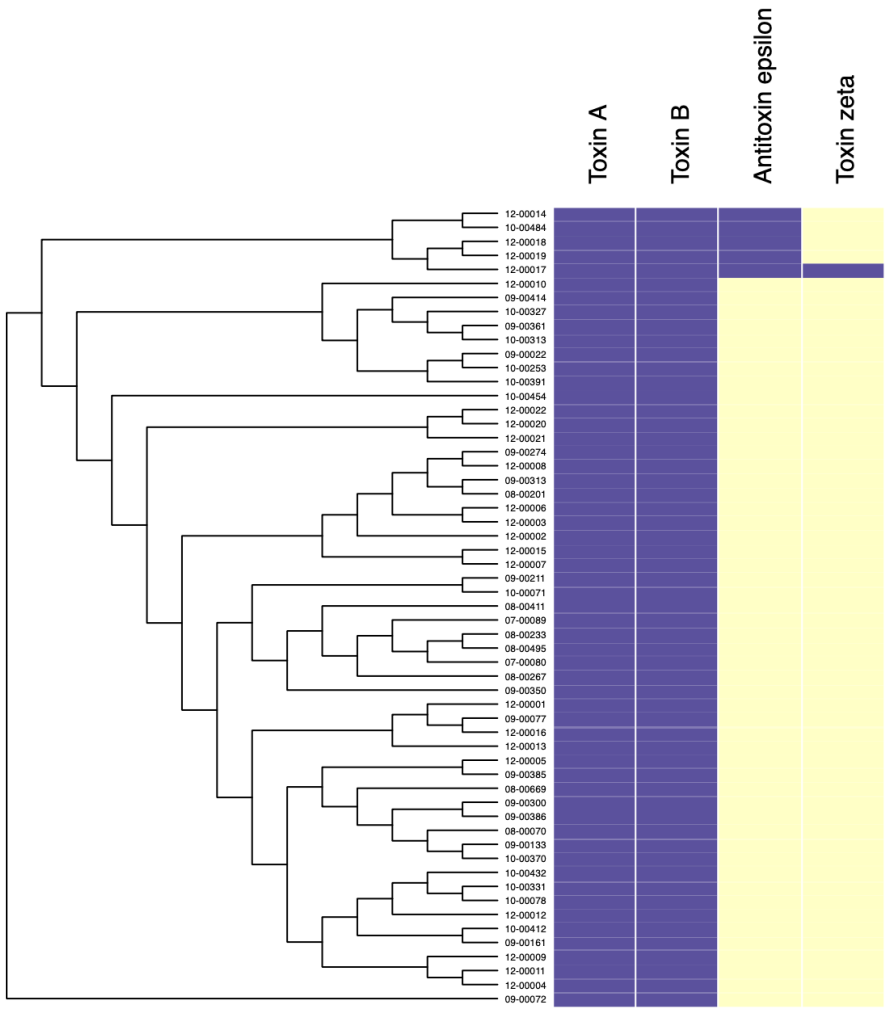


Figure 3.14 ***The presence (purple) or absence (yellow) of toxin related genes in the pangenome of the isolates.*** *Phylogenetic cladogram (left) is produced using ROARY core and the* de novo *assembled genomes. A cladogram is used for ease of reading; the corresponding phylogenetic tree is shown in figure 3.7. The gene presence/absence (right) is extracted from the pangenome produced using ROARY.*

3.6 CONCLUSIONS

In conclusion, although previous studies have shown these isolates to be fluoroquinolone resistant, the cause of this resistance could not be identified through the bioinformatics techniques used here. However, it has been shown that the presence of the Tn6215 MGE may have provided the *erm(B)* resistance gene and the epsilon anti-toxin gene to the isolates within a single clade.

Understanding the spread of antibiotic resistance in *C. difficile* isolates will allow future targeted treatments to prevent their spread, and therefore reduce the death rate caused by this pathogen.

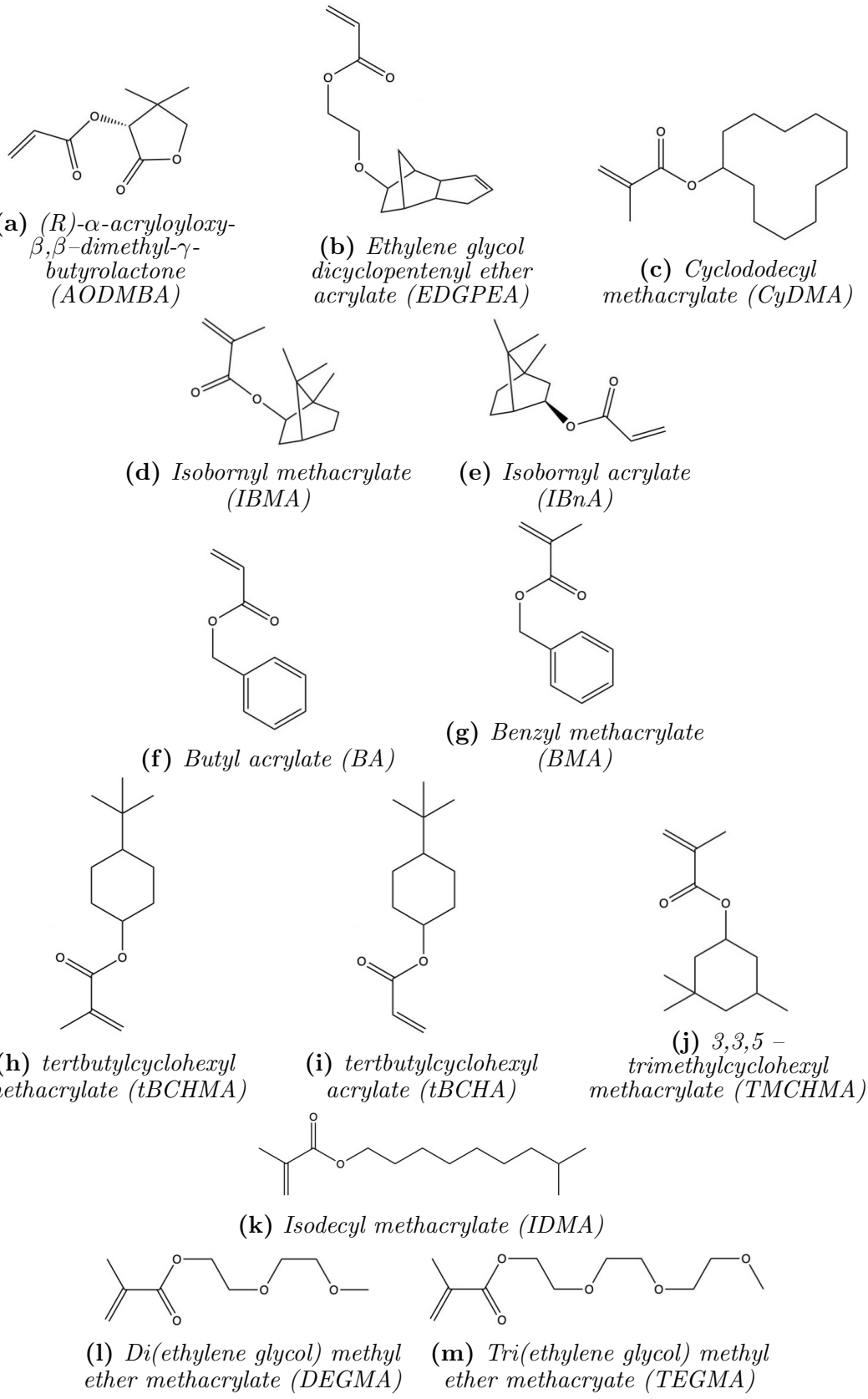
Chapter 4

THE NEXT 3 YEARS

Due to the detrimental effect of antibiotics, and the growing prevalence of antibiotic resistant bacteria, a beneficial method of antibiotic stewardship would be to prevent the formation of biofilms on catheter surfaces. Biofilms have increased tolerance to the host immune system. The prevention of biofilm formation therefore means that antimicrobials are not required as frequently because the host immune system can deal with the infection. In turn this reduces the selective pressure on pathogens which would otherwise promote antimicrobial resistance.

4.1 MONOMERS

Figure 4.1 shows the chemical structures, full chemical names, and contractions used throughout this chapter.



(a) *(R)-α-acryloyloxy-β,β–dimethyl-γ-butyrolactone (AODMBA)*

(b) *Ethylene glycol dicyclopentenyl ether acrylate (EDGPEA)*

(c) *Cyclododecyl methacrylate (CyDMA)*

(d) *Isobornyl methacrylate (IBMA)*

(e) *Isobornyl acrylate (IBnA)*

(f) *Butyl acrylate (BA)*

(g) *Benzyl methacrylate (BMA)*

(h) *tertbutylcyclohexyl methacrylate (tBCHMA)*

(i) *tertbutylcyclohexyl acrylate (tBCHA)*

(j) *3,3,5 – trimethylcyclohexyl methacrylate (TMCHMA)*

(k) *Isodecyl methacrylate (IDMA)*

(l) *Di(ethylene glycol) methyl ether methacrylate (DEGMA)*

(m) *Tri(ethylene glycol) methyl ether methacryate (TEGMA)*

Figure 4.1 ***Chemical structures, full names, and abbreviations used throughout this chapter****. Chemical structures were drawn using ChemDraw 19.0.*

4.2 BIOFILMS

Biofilms are multi-cellular communities of microbes that can form on both biotic and abiotic surfaces. The main stages of biofilm formation are shown in figure 4.2, however the main target for this project is the prevention of stages 1 and 2, before biofilms form.

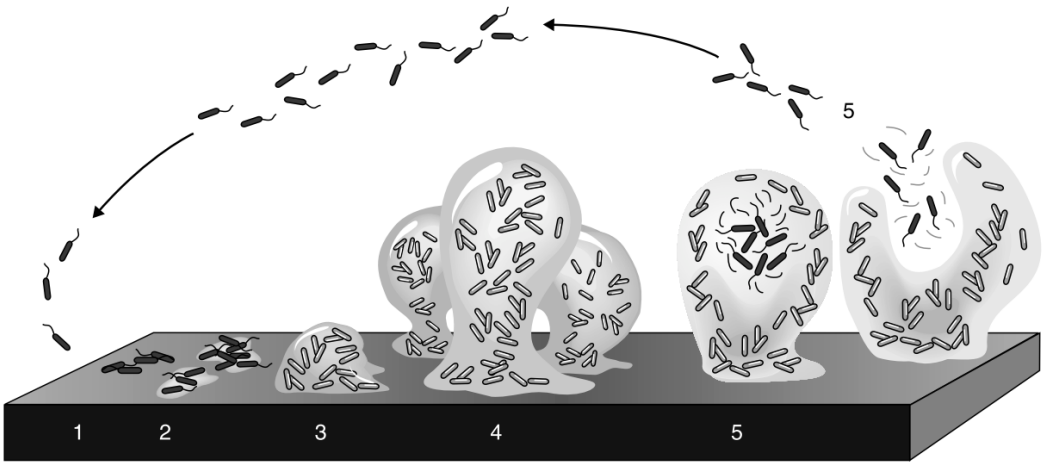


Figure 4.2 *The biofilm lifestyle [105].*

The initial attachment of bacteria to an abiotic surface can be through non-specific interactions (e.g. electrostatics, hydrophobic, or van der Waals) [106, p. 4-5], or by the specific interactions of bacteria with the surface conditioning layer that is rapidly formed on the abiotic surface once it is exposed to biological media (in this case blood). There are many surface structures on bacteria that are involved in the attachment process, including pili and flagella [107], and different bacteria display interactions with different surfaces [107].

Once a biofilm has formed, it increases the tolerance of the bacteria contained within it to antibiotics and to the host immune response. While antibiotic treatment will kill any remaining planktonic bacteria, the biofilm will remain and can disperse after antibiotic treatment has been ceased, 'reigniting' the symptoms of infection. The reasons for this increased tolerance include the inability of the antibiotic to penetrate into the biofilm matrix with sufficient concentration, zones of non-growing cells, and the presence of persister cells [108]. Biofilms are also

a suitable location for horizontal gene transfer of resistance to occur, as there is a high density of cells, and some studies have reported that conjugation is more efficient between cells within a biofilm compared to planktonic cells [109].

This increase in antibiotic resistance (both caused by the biofilm itself and by horizontal transfer of resistance genes) means that antibiotic treatment is often ineffective, and much higher doses may be required to treat the infection [110], increasing the risk of developing further antibiotic resistant strains of bacteria.

It is, therefore, of benefit to prevent the biofilm from forming initially, meaning that bacteria are more susceptible to antibiotic treatment and the host immune system. In some cases, this may only reduce the dose of antibiotic required, however in other cases the host immune system will be able to deal with the planktonic bacterial infection, eliminating the requirement for antibiotic treatment.

4.3 BACKGROUND SCIENCE – SOME IMPORTANT POLYMER PROPERTIES

4.3.1 Molecular weights

The molecular weight of a polymer is important in determining its mechanical properties, as the ends of polymer chains are only connected via weak intermolecular bonds. Further to this, entanglement is more prevalent at higher molecular weights, which further contributes to the strength of the polymer. Although higher molecular weights leads to improved mechanical properties, it also causes a higher melt viscosity, leading to more difficult processing conditions.

To create large numbers of polymer samples with consistent mechanical properties, it is necessary to ensure that the molecular weights produced are consistent

between samples. This requires careful control of the reaction conditions used and sample characterisation.

With the exception of biologically produced polymers, most polymers have a distribution of molecular weights across a sample. This leads to there being multiple ways of averaging the molecular weight (as seen in figure 4.3).

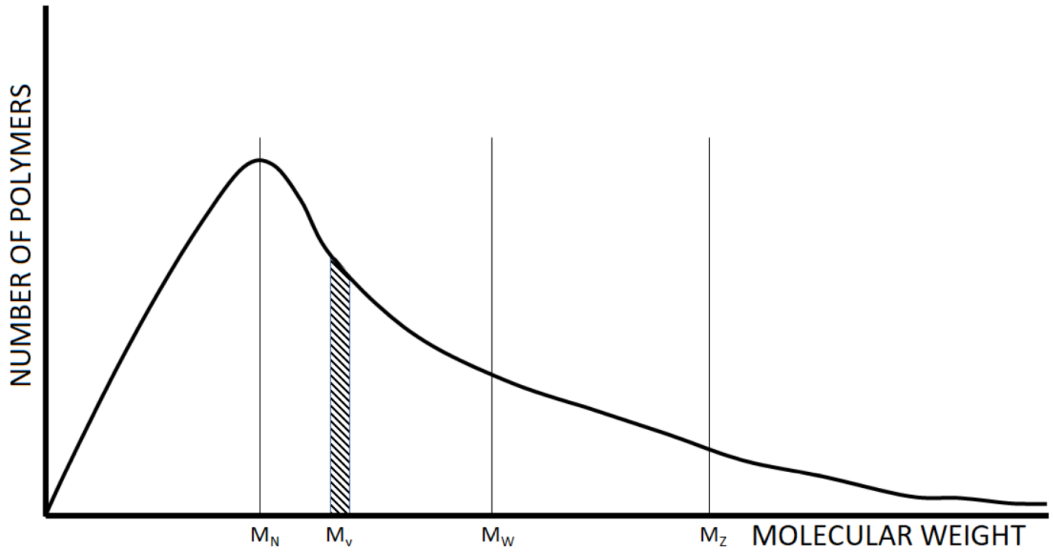


Figure 4.3 ***The distribution of molecular weights of individual polymer chains within a sample of polymer.*** *M_N = the number averaged molecular weight; M_ν = the viscosity averaged molecular weight; M_W = the weight averaged molecular weight; M_Z = the z averaged molecular weight.*

The most commonly determined weight averages are the number averaged molecular weight (M_N, determined by measuring the number of end groups in a specific mass of polymer) and the weight averaged molecular weight (M_W, determined by light scattering, SANS, or X-ray scattering). The ratio of these two averages gives the dispersivity of the polymer sample, which is a measure of how large the range of polymer molecular weights is. Two models that have been made of the molecular weight distribution are the Schultz molecular weight distribution and the Poisson molecular weight distribution [111]. Chromatography can be used to separate polymer samples into fractions based on their molecular weights, allowing the determination of the molecular weight distribution.

4.3.2 The glass transition

Polymers can be either partially or fully amorphous. Fully crystalline polymer samples are rare, due to the entanglements that form between the polymer chains. While the melting temperature is an important temperature for crystalline materials, it does not apply to fully amorphous polymers. For amorphous polymers, the glass transition temperature is of importance.

The glass transition is the point at which long range co-ordinated molecular motion begins to occur, and the polymer softens. Below the glass transition, only short range motions of the molecules is able to occur, so the polymer is stiff, brittle and 'glassy'. These changes can be seen for a non-cross-linked amorphous polymer in figure 4.4.

The response of a polymer to an applied stress is dependent on the time-duration over which the stress is applied, and also the temperature. This is referred to as the visco-elastic behaviour.

At temperatures below that of the glass transition, the polymer is glassy and brittle, as molecular motion is limited to vibrations and short range motion. The glass transition occurs over a range of temperatures (with the glass transition temperature usually being defined as the temperature at which there is the maximum change in modulus for quasi-static measurements). For temperatures above the glass transition region, an amorphous, non-crosslinked polymer exhibits long-range rubber elasticity, meaning that it can be stretched to high strains and will then relax back to its original state. In cross-linked polymers, this state of rubber elasticity exists at temperatures up until the polymer thermally decomposes. Cross-linking also has the effect of increasing the temperature at which the glass transition occurs.

In contrast, non-crosslinked polymers experience increased amounts of flow as the temperature is further increased. When the duration of the stress applied is

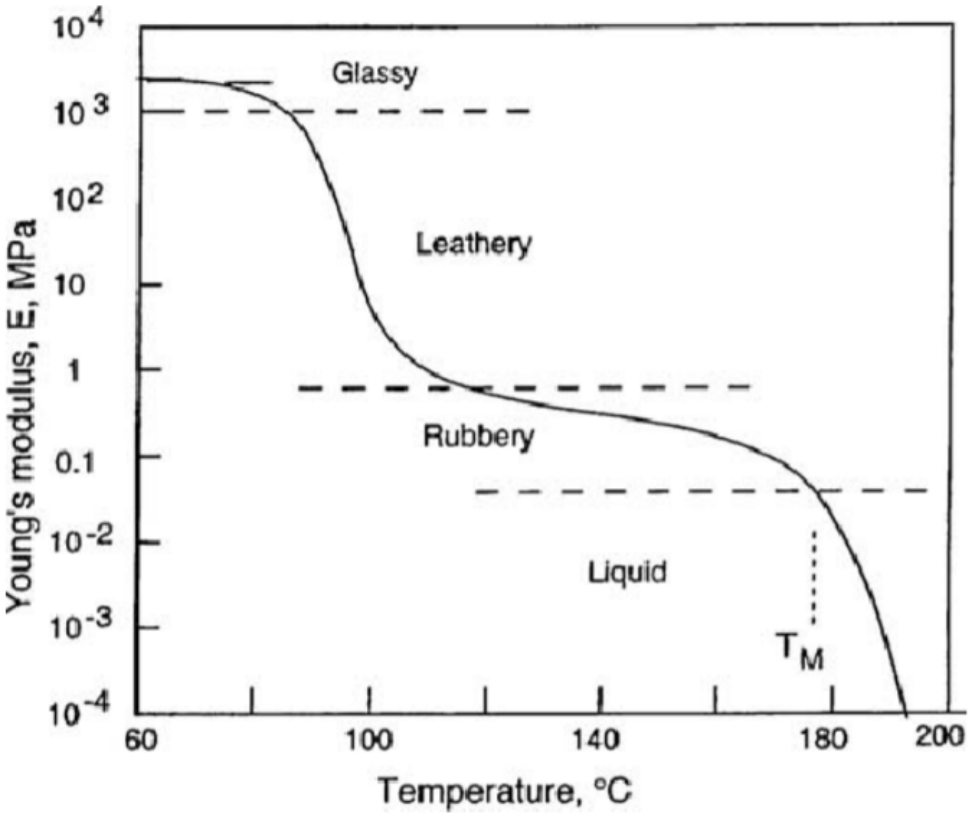


Figure 4.4 ***The variation in modulus with temperature for an amorphous, non-crosslinked polymer*** *[112].*

rapid, the physical entanglements between the polymer chains cannot relax, so the polymer behaves in a rubbery manner. If a longer duration of stress is used, the physical entanglements can relax, as the chains are able to move, resulting in flow being observed. As the temperature is further increased, flow of the polymer chains occurs for all stress rates.

In a semi-crystalline polymer, the glass transition only occurs in the amorphous regions. As these amorphous regions are linked by the crystalline regions, the change in behaviour is similar to that observed for cross-linked amorphous polymers. These polymers will also exhibit a melting temperature, at which the crystalline regions of the polymer will melt.

4.4 SUCCESS WITH URINARY CATHETERS

There is currently no theory linking the structure of a material with its ability to resist the formation of biofilms. The rational design of materials suitable for biofilm prevention is difficult, if not nearly impossible, due to the complex, and not fully understood, interactions between the substrate and bacteria. Modelling has been employed, but the use of microrrays still provides a rapid assessment of the suitability of materials for biofilm prevention. The use of microarrays within biomaterials discovery has proved to be of great importance, allowing the screening of hundreds of different materials for specific responses to biological environments. Early research using microarrays focused on adsorption of proteins and mammalian cells to the surfaces [113, 114].

Recent studies have shown that microarray testing can be used to discover poly(meth)acrylate monomers [115–117] that are resistant to bacterial attachment. Scaling up from microarrays to 'coupons' of promising candidate materials showed that the bacterial resistance was also seen in larger scale tests.

Mechanical properties are also of importance in medical devices, which must be able to withstand the stresses applied on insertion, during use, and on removal. One of the most important factors in determining the mechanical properties of a polymer is its glass transition temperature.

Adlington *et al* [118] modulated the mechanical properties of 5 promising (meth)acrylate monomers (called 'hit' monomers) detected by microarray testing [EDGPEA, BA, BMA, TMCHMA, and IBMA] by copolymerising with DEGMA, which has a glass transition temperature lower than room temperature. All 5 of the 'hit' monomers had a glass transition tempertature greater than room temperature, leading to brittle behaviour. The aim was to incorporate the DEGMA into the polymer so that the glass transition temperature of the copolymer was below room temperature, while maintaining the anti-attachment properties. The incorporation of

DEGMA (or TEGMA) into the copolymer formulations may also be beneficial due to their anti-biofouling properties (meaning that they resist the accumulation of proteins on the surface [119]).

The incorporation of DEGMA into the copolymer was shown to reduce the bacterial resistance of the polymer [118]. However, the incorporation of more than 50 mol% DEGMA still resulted in copolymer coatings that showed improved bacterial resistance in comparison to commercially available silicone catheters [118]. When 'hit' monomers were copolymerised with 25 mol% DEGMA, only EDGPEA and BA showed a glass transition temperature that was below room temperature [118], however BA did not show reduced bacterial coverage for all DEGMA compositions when compared to silver hydrogel coated catheters [118]. EDGPEA was therefore determined to be the most promising (meth)acrylate monomer in terms of both its mechanical properties and its bacterial resistance. Further mechanical work has also been carried out [120] into the adhesion of poly(EDGPEA-co-DEGMA) to catheter materials, with special consideration given to the adhesion promotor used, interfacial mechanical stressing, and chemical characterisation of the interface.

Success in the production of a biofilm-resistant polymer has led to the first-in-man trial [121], which has shown promising results, albeit in a small number of patients.

Differences have been reported between microarray results and larger scaled results, including the surface enrichment of some pendant groups [116], which may impact on the bacterial attachment. This impacts on the usefulness of microarray testing as a screening method because potentially 'good' materials in the large scale may only present these properties due to surface segregation of a specific pendant group, and may therefore not show up in the microarray testing.

Attempts have been made to computationally model the attachment of bacteria

to libraries of polymers, so that new structures can be proposed that prevent attachment of bacteria. A 2011 report [122] showed that the hydrophobicity and molecular rigidity were not individually correlated with bacterial attachment. It was, however, shown that the composite parameter, α, did correlate with bacterial attachment [122]. α was a function of the calculated partition coefficient (a measure of hydrophobicity) and the number of rotatable bonds for the monomer, and was shown to be a predictive indicator of bacterial attachment for low attachment poly(meth)acrylates with hydrocarbon pendant groups [122]. In 2019, the alpha parameter was used to predict that CyDMA would show good bacterial resistance [123]. Experiments showed that when CyDMA was thermally polymerised and dip coated onto silicone catheters, its biofilm resistance (to both mono-microbial biofilms and poly-microbial biofilms) was greater than that of the poly(EDGEPEA-co-DEGMA) discovered by microarray testing [123].

4.5 BLOOD CONTACTING CATHETERS

While the placement of a central line can enable healthcare workers to deliver potentially life-saving drugs, such as vasopressors, antiarrhythmia drugs, total parenteral nutrition (TPN), and antimicrobials [124], they are not without their complications. Complications may occur immediately on placement or may be delayed in their presentation [125]. A recent UK-based study has estimated that slightly more than 120,000 central venous catheters (CVCs) are being used annually in critical care units within the UK [124].

Complications that have been reported include:

- Pneumothorax [126]
- Artery puncture [124, 126]
- Heart Arrythmias [124, 126]
- Hematoma [126]

- Improper positioning of the catheter tip [125, 126]
- Vascular complications [125]
- Pulmonary complications [125]
- Dysfunction of the catheter [125]
- Infection [125]
- Venous puncture [124]

There are many reports indicating additional risk factors for the development of complications as a result of central line placement, including:

- The use of multi-lumen catheters [126]
- Multiple insertion attempts [124]
- The presence of multiple CVCs concurrently [127]

Wong *et al* [124] reports that across 117 procedures in 5 UK hospitals, the rate of complications immediately following catheterisation was 6.8%. These complications included puncture of a vein, puncture of the carotid artery, and significant arrhythmias.

Infections are a more delayed complication of placement. It has been reported that the presence of positive bacterial cultures on the tips of removed central lines is greater when the catheter has been in place for a longer duration [128], shown by the drop in cumulative survival in figure 4.5, especially after 10 days with the catheter present. Dube *et al* [127] have reported a similar effect, with a drop in the probability of a patient not having a central-line associated bloodstream infection (CLABSI) after $\sim$10days (figure 4.6).

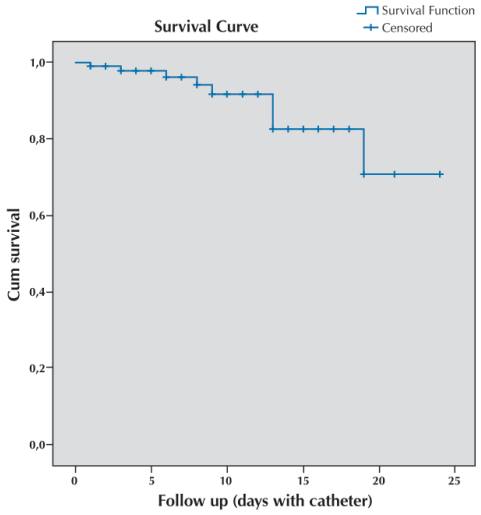


Figure 4.5 ***Cumulative survival curve showing the number of days between catheter insertion and the occurrence of infection*** *[128].*

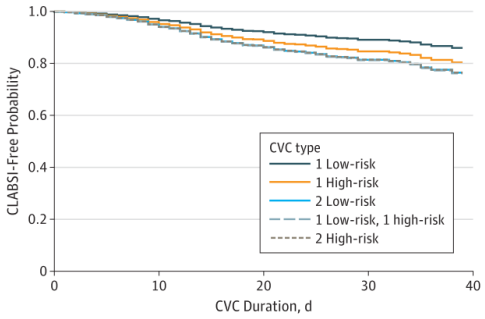


Figure 4.6 ***Probability of a patient being free from CLABSI as a function of duration of CVC placement.*** *[127] Different types of CVCs are shown by different coloured lines.*

The rates of CLABSI reported is highly variable between papers. The differences in these results is likely caused by the difference in patients analysed (including the reason for CVC placement, duration of CVC placement, and illness profile and wards of the patients) among other factors. Another possible explanation for the differences is due to potential differences in diagnosing the presence of a CLABSI. Nailon *et al* [129] reports a rate of CLABSI as 1.3 cases per 1000 device days for paediatric patients who have home-healthcare CVCs, and a lower rate of 0.21 cases per 1000 device days for adult patients who have home-healthcare CVCs. This figure is similar to the rate of CLABSI reported in intensive care units (ICUs) by Han *et al* [130] (0.284 cases per 1000 device days). Han *et al* also report a much lower rate of CLABSI in non-ICU units (0.082 cases per 1000 device days). A much higher rate of 17.04 cases per 1000 catheter days was reported for adult ICU patients by Mishra *et al* [131].

Dube *et al* [127] have reported that the treatment that is passed through a central line can affect the risk of developing an infection. In this study, TPN and

chemotherapy increased the risk of developing a CLABSI (RR of 1.81 and 2.96 respectively) while the difference caused by haemodialysis was closer to unity [RR = 0.89; 95% CI of the RR = 0.65-1.22].

Derderian *et al* [132] have reported that the anatomical site of insertion (figure 4.7) does not affect the rates of CLABSI infection, however the rate of venous thromboembolism was found to be significantly affected by the anatomical location of insertion. This is in contrast to research by Schwanke *et al* [128] who reports that insertion of the catheter into the left femoral vein instead of the jugular vein significantly increased the risk of infection. Another study, by Gowardman *et al* [133], reported that there was no statistically significance difference in the number of CVCs that were colonised when the CVCs were inserted into the internal jugular or femoral veins, however the insertion of a CVC into the subclavian vein did significantly decrease the risk of the CVC becoming colonised. In the same way as for the variations in reported rates of CLABSI, this is likely due to variations in the patients and in definitions of CLABSI. It is also worth noting that while colonisation of a CVC can be used as a surrogate end point when studying CLABSI [134], it is not a perfect surrogate – for example a patient with a compromised immune system is more likely to develop a CLABSI as a result of colonisation of their CVC in comparison to a patient who is not immunocompromised.

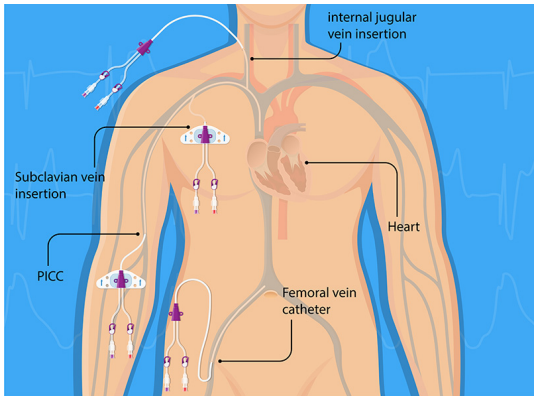


Figure 4.7 ***The locations at which central venous catheters can be placed*** *[135].*

A study in intensive care units (ICUs) [136] reported that there was no reduction in the incidence density of CVC-bloodstream infections (CVC-BSIs) in adult or paediatric ICUs or mortality of CVC-BSIs in adult ICUs (no data was provided for the mortality of CVC-BSIs in paediatric ICUs) after the implementation of a bundle of preventative methods. It is likely that, even if all reasonable methods of preventing infection are taken, there will be some risk of infection occurring because it is not reasonable to assume that there will be a completely sterile field, due to the presence of bacteria within the stratum corneum of the skin and the hair follicles [137]. However, this study also showed that there was not complete compliance to the bundle of preventative methods implemented (especially with regards to methods during catheter insertion and removing the catheter as soon as medically able/when there are signs or symptoms of catheter-related infections), and the reasons behind this were not looked into. With regards to the later of these factors, there is difficulty in knowing when a central line is no longer needed - premature removal may lead to additional procedures being needed to place another line, leading to an increased risk of complications. Lack of compliance to the former factor was significantly worse in the paediatric ICU in comparison to the adult ICU, and may be a result of the speed at which the devices are required to be placed. From these results, it can be seen that additional preventative methods are required that do not rely on alterations in the method of insertion. Methods of prevention that could be used include:

- Antibiotic-impregnated catheter [137],
- Chelating agents to remove metal cations that are involved in the structure of the biofilms [138],
- Lock treatments with antibiotics, biofilm dispersants, or ethanol [138],
- Coatings with polymers that prevent stage 1 or 2 of biofilm formation,
- Incorporation of zwitterionic compounds [139].

The advantages of polymers that prevent bacterial attachment is that no selection pressure is applied to the bacteria [116], reducing the spread of resistance. This

method of preventing infection will be the focus of the proposed PhD.

Given the success shown for urinary catheters, currently unpublished research by Singh *et al* [140] used microarrays to investigate the use of poly(meth)acrylates to prevent biofilm formation on blood contacting catheters. These have additional challenges over urinary catheters, due to the presence of proteins in the blood.

The first blood-material interaction that occurs is the adsorption of blood proteins onto the material [141]. These proteins can act as receptors for adhesion molecules on *staphylococcal* cell surfaces, encouraging the adhesion of the *staphylococcal* cells onto the surface [142]. The covering of the surface with host proteins may also 'mask' the carefully designed surface coating, resulting in the elimination of any beneficial effects obtained by the coating.

Oligo(ethylene glycol) [OEG] (such as DEGMA or TEGMA) can be used to prevent the binding of biological substances to a surface. When a protein molecule adsorbs to an OEG surface, the water molecules that are associated with the OEG chains will be released, reducing the entropy and increasing the enthalpy. Both of these thermodynamic changes are unfavourable, meaning that the surface thermodynamically favours the adsorption of water over the adsorption of proteins [143]. The effect of OEG on protein adsorption can be seen in figures 4.8 and 4.9. The protein resistance provided by OEG has a critical temperature, above which resistance is no longer seen, due to the transition from a hydrated, highly swollen state to a collapsed state [144]. The resistance to protein adsorption is dependent on the thickness of an OEG coating, with increased dry thickness of the surface being linked to decreased irreversible attachment of proteins [144]. The presence of side groups on poly(OEG) surfaces also contributes to preventing protein adsorption by causing steric hindrance, see figure 4.10. It is hoped that the incorporation of DEGMA or TEGMA into the copolymers will have the effect of limiting adsorption of proteins onto the surface.

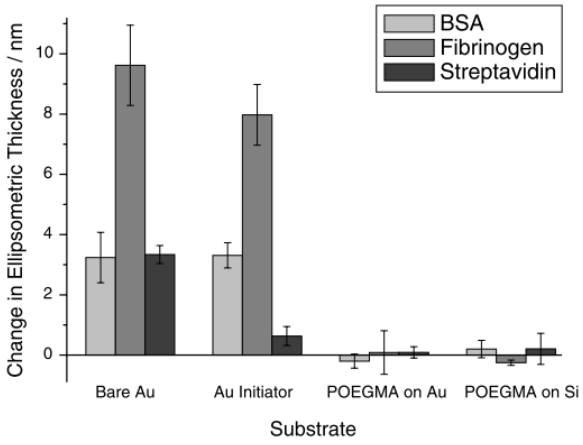


Figure 4.8 ***The effect on protein adsorption of Poly(oligeo ethylene glycol methacrylate) (POEGMA) on surfaces*** *[143]. The change in the ellipsometric thickness is a result of protein adsorption onto the surface.*

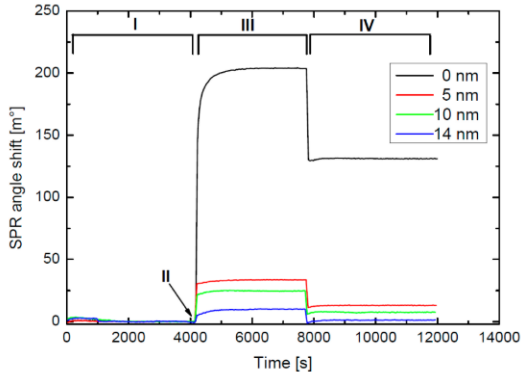


Figure 4.9 ***The variation in surface plasmon resonance (SPR) angle shift against time for different thicknesses of poly(di ethylene glycol methacrylate) (PDEGMA) coatings*** *[144]. The variation in SPR angle shift is proportional to the thickness of the layer of protein that is adsorbed to the surface. In region I, the surface is allowed to interact with PBS to form a baseline when no protein is present. In region II, BSA solution is injected, and in region III the BSA is allowed to interact with the surface under 'no flow' conditions. In region IV, the surface is washed with PBS. Any protein that remains bound to the surface after rinsing with PBS is considered to be irreversible adsorbed.*

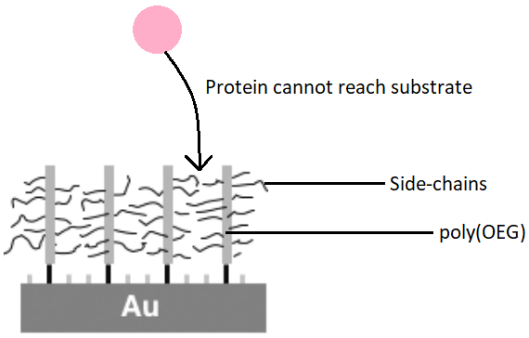


Figure 4.10 ***The structure of poly(OEG) on a gold surface, adapted from [145], showing the steric hindrance to protein adsorption.*** *The protein (pink) is prevented from reaching the substrate (and therefore cannot bind to the substate) as a result of steric hinderance caused by the side-chains of the poly(OEG).*

Later effects of contact of blood are the binding of complement products to the material, and the activation of neutrophils and monocytes, which cause immune reactions to occur.

Differences have been observed between the structures typically linked to low biofouling in protein-free media (cyclic structures [115–117]) and to low biofouling in whole human blood (branched long hydrocarbons [140]). In scaled up testing of 6 promising copolymer formulations (for blood contacting applications) found in microarray testing, poly(iBnA-co-TEGMA) (75:25 vol%) achieved the lowest thrombogenic and immune/inflammatory responses (figure 4.11) and the lowest *Pseudomonas aeruginosa* and *Staphylococcus aureus* biofilm formation on coated catheter segments in an *in vitro* model [140] (figure 4.12).

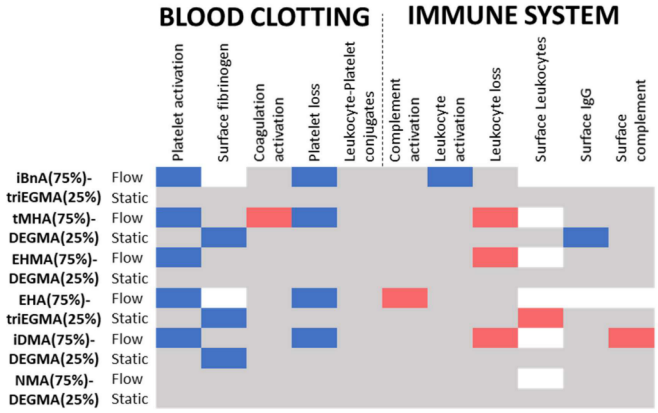


Figure 4.11 ***The blood clotting and immune system activation of the 6 'hit' copolymers*** *[140]. Blue squares indicate a statistically significant decrease compared to PTFE. Red squares indicate a statistically significant increase compared to PTFE. Grey squares indicate no statistically significant difference compared to PTFE*

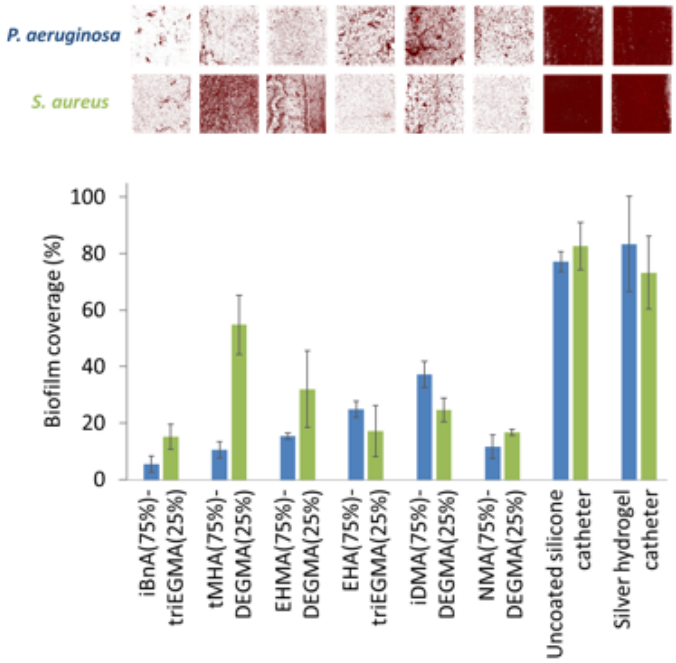
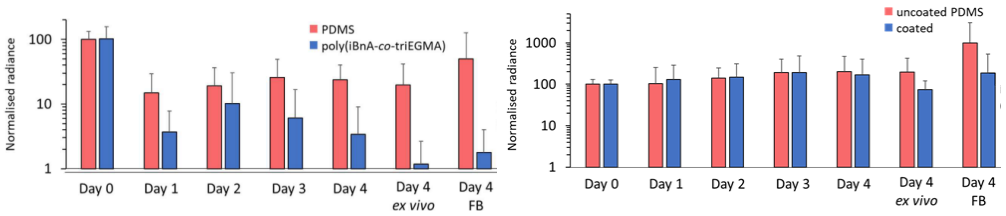


Figure 4.12 ***The bacterial surface coverage of the 6 'hit' copolymers*** *[140]. Catheters were coated with each of the 6 hit copolymers and conditioned for 2 hours in blood prior to 72 hours of incubation with* P. aureginosa *(blue) or* S. aureus *(green). The top panel shows confocal images of the biofilm; the lower panel shows the percentage of biofilm coverage.*



(a) *P. aeruginosa* **(b)** *S. aureus*

Figure 4.13 ***The results of a murine foreign body infection with* P. aeruginosa *and* S. aureus *to test the in vivo performance of silicone catheter segments coated with the 'hit' copolymer formulation poly(iBnA-co-TEGMA)(75:25)*** *[140]. Coated and uncoated catheter segments were implanted subcutaneously and inoculated with bioluminescent* P. aeruginosa *or* S. aureus*, and the radiance was measured daily for 4 days. After 4 days, the catheter segments (day 4 FB) and surrounding tissue (day 4 ex vivo) were removed and imaged also.*

While an *in vivo* mouse study of poly(iBnA-co-TEGMA) (75:25 vol%) showed a large reduction in *P. aeruginosa* biofilm formation compared to uncoated catheters, no difference was seen in *S. aureus* biofilm formation between coated and uncoated catheters [140] (figure 4.13). This may be due to surface receptors on *S. aureus* which target proteins laid down during the foreign body response.

It is not only bacterial species that colonise central lines and cause CLABSIs. A review of 20 studies of patients on home parenteral nutrition has reported that *Candida spp* infections accounted for 9.8% of CRBSIs within paediatric patients, and 11.9% of CRBSIs in adult patients [146]. The *Candida* species that was causing the greatest amount of these candida infections was *Candida albicans* for both the paediatric (46.2% of all *Candida spp* infections) and adult (37.3% of all *Candida spp* infections) patients. The results of this paper are also supported by the results of Yoshida *et al* [136].

A similar microarray process has been used to determine potential polymer coatings for the prevention of fungal biofilm formation [147], which showed promising results for a number of fungal species. However, polymer structures that appear beneficial to the prevention of fungal attachment are not the same as those that are beneficial to the prevention of bacterial attachment. Eight polymers were shown to be of interest in the prevention of fungal attachment whilst not in-

hibiting the growth of the fungi, however none of these formed suitable coatings when dip coating was used. When 3D printing was used, only a single polymer (AODMBA) formed solid and stable geometries. This 3D printed polymer showed $\sim$ 100% reduction in *C. albicans* attachment in comparison to a positive attachment control when 3D printed coupons were used, and a mean 84% reduction in biofilm biomass in comparison to standard silicone manufactured valve flaps for voice prostheses when 3D printed AOBMBA valve flaps were used. Other polymers found to be resistant to attachment by *C. albicans*, without inhibiting the growth of *C. albicans* were polymers of DEGMA, TEGMA, tBCHMA, tBCHA and iDMA.

4.6 THE AIM OF THE PHD

The following objectives are proposed:

1. Conduct polymer microarray screening to expand the (meth)acrylate library that has been tested in blood to date(Singh et al. 2020). This is expected to identify additional promising candidate polymers.

2. Determine, through polymer microarray screening, if the copolymers resist fungal attachment (Vallieres et al. 2020) in the presence of blood.

3. Incorporate the copolymerising agents di(ethylene glycol) methyl ether methacrylate and tri(ethylene glycol) methyl ether methacrylate to modulate mechanical properties and prevent protein biofouling into bacterial resistant and blood compatible polymer [including the previously identified isobornyl acrylate (Singh et al. 2020), cyclododecyl methacrylate (Dundas et al. 2019; Sanni et al. 2015), ethylene glycol dicyclopentenyl ether acrylate (Adlington et al. 2016; Hook et al. 2013)].

4. Assess immune and blood clotting reactions of candidate polymers through in vitro screening.

5. Assess biocompatibility of polymers in an in vivo foreign body infection model.

This project aims to extend the work of Singh (Singh et al. 2020) by expanding the number of (meth)acrylates that have been screened for bacterial attachment in the presence of blood. Promising candidates, along with 3 candidates already identified (isobornyl acrylate, cyclododecyl methacrylate, and ethylene glycol dicyclopentenyl ether acrylate) will be copolymerised in varying ratios with di(ethylene glycol) methyl ether methacrylate or tri(ethylene glycol) methyl ether methacrylate and the bacterial and fungal attachments to copolymer-coated catheter segments will be determined. In vitro testing will also be conducted to determine the adsorption of various relevant components of blood to the polymers. This will include the detection of adsorbed blood proteins (by disassociating the proteins and using a BCA assay to determine their concentration), adsorbed leukocytes (using DNA staining dye Sytox green and Saponin (Singh et al. 2020)), and surface attached platelets (using anti-human Cd41A FITC (Singh et al. 2020)). The detection of adsorbed macrophages and their polarisation will also be determined, using the methodology of Rostam et al (Rostam et al. 2020). Mechanical properties such as rolls/bends to delamination of the coating will also be determined. Microarray testing of (meth)acrylates resistance to fungal attachment may also be conducted in the presence of blood. The incorporation of these into the copolymer may impart fungal attachment resistance to the copolymer, although the balance between monomer content and the simultaneous bacterial and fungal control has not yet been tested.

For *in vivo* work conducted in the presence of blood, the blood will be taken from healthy human volunteers selected from the school of Pharmacy, with permission obtained prior to blood-letting. No personal data will be acquired. The university of Nottingham Medical School Ethics Committee will assess and review the ethics of this proposal, and the application will be submitted within the first 2 months of the project. Approval may also be required to use the facilities in the Queen's Medical Centre to use space within the phlebotomy department. Risks to patients are limited to minor discomfort as a result of the needle penetrating the skin, and potential, but minor, adverse reactions to blood-letting e.g.

fainting, nausea, and/or vomiting. Promising candidate materials will be tested in vivo in a foreign body sub-cutaneous infection model. In this model, coated catheters (treatment) and uncoated catheters (control) will be inoculated with a fluorescent pathogenic bacteria and inserted subcutaneously into mice. Live animal imaging will be used to monitor the development of the biofilm on a daily basis. Mice will then be euthanised at a humane end point and the catheter and surrounding tissue removed so that pathogenic burden can be determined. The project licence has completed the internal process by AWERB, and has had a first read at the Home Office. This licence will be for a subcutaneous model, intra-peritoneal implantation, and wound healing both with and without bacteria (infection and sterile responses). It will look at both single microbial infections and poly-microbial infection. It is hoped that the licence will be acquired by the beginning of 2021. The main outcome of this research will be a copolymer that can be coated onto blood-contacting catheters to prevent the formation of biofilms. The project will also provide a series of copolymer formulations supplemented with information on their fungal and bacterial resistance. All of the knowledge gained on the attachment of cells to different surfaces may aid in understanding the theory of cell attachment to surfaces.

4.6.1 Impact of this project

The primary aim of this project is to develop a new polymer coating for blood contacting catheters which will prevent the attachment of microbes to the surface, therefore reducing infection rates. If successful, patients with blood-contacting catheters will experience fewer infections, and infections will not require potentially painful replacement of the devices. In a wider context, the project will also provide further data on bacterial attachment to polymers that have not currently been tested in the presence of blood.

Knowledge gained through this project regarding whether materials resist microbial attachment in the presence of blood may also be of use in creating coatings for other blood contacting devices. For example, a coating on artificial heart valves (to prevent the formation of biofilms on the surface) may reduce the risk

of endocarditis.

Appendices

Chapter A

Phylogenetic tree produced by the original paper

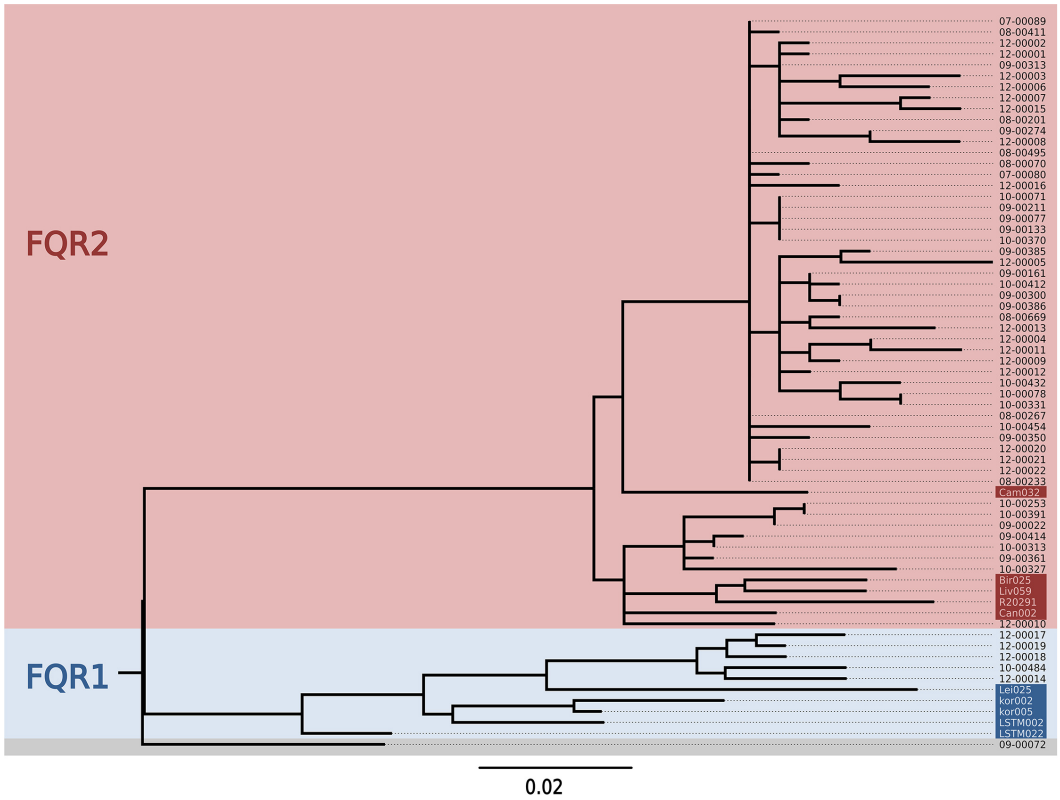


Figure A.1 ***Phylogenetic tree from [85] which was produced base on core genome SNPs***. *Shaded genome names show isolates that had been published before the publication of this tree, and these were used to identify the clades assciated with the lineages of FQR1 and FQR2.*

Bibliography

[1] Chiagozie I. Pickens and Richard G. Wunderink. Principles and Practice of Antibiotic Stewardship in the ICU. *Chest*, 156(1):163–171, 2019.

[2] Everett J. Bassett, Margaret S. Keith, George J. Armelagos, Debra L. Martin, and Antonio R. Villaneuva. Tetracycline-Labeled Human Bone from Ancient Sudanese Nubia (A.D. 350. *Science*, 209:1532–1534, 1980.

[3] Kate Gould. Antibiotics: From prehistory to the present day. *Journal of Antimicrobial Chemotherapy*, 71:572–575, 2016.

[4] Rustam I. Aminov. A brief history of the antibiotic era: Lessons learned and challenges for the future. *Frontiers in Microbiology*, 1(DEC), 2010.

[5] Nicholas C. Lloyd, Hugh W. Morgan, Brian K. Nicholson, and Ron S. Ronimus. The composition of Ehrlich's Salvarsan: Resolution of a century-old debate. *Angewandte Chemie - International Edition*, 44(6):941–944, 2005.

[6] Alexander Fleming. On the Antibacterial Action of Cultures of a Penicillium, with Special Reference to Their use in the Isolation of B. Influenzae. *British Journal of Experimental Pathology*, 10(3):226–236, 1929.

[7] Matt Hutchings, Andrew Truman, and Barrie Wilkinson. Antibiotics: past, present and future. *Current Opinion in Microbiology*, 51:72–80, 2019.

[8] Elias J Anaissie, Michael R. McGinnis, and Michael A. Pfaller. *Clinical Mycology*. 2009.

[9] Gerard D. Wright. Something old, something new: Revisiting natural products in Antibiotic drug discovery. *Canadian Journal of Microbiology*, 60:147–154, 2014.

[10] Contained and controlled: The UK's 20-year vision on antimicrobial resistance. *HM Government*, 2019.

[11] Tackling antimicrobial resistance 2019–2024 – The UK's five-year national action plan. *HM Government*, 2019.

[12] Tackling Drug-Resistant Infections Globally. *The review of Antimicrobial Resistance*, 2016.

[13] J. Ignacio Barrasa-Villar, Carlos Aibar-Remón, Purificación Prieto-Andrés, Rosa Mareca-Doñate, and Javier Moliner-Lahoz. Impact on Morbidity, Mortality, and Length of Stay of Hospital-Acquired Infections by Resistant Microorganisms. *Clinical Infectious Diseases*, 65:644–652, 2017.

[14] Esmita Charani and Alison Holmes. Antibiotic stewardship—twenty years in the making. *Antibiotics*, 8(7), 2019.

[15] Ilyas Alav, J. Mark Sutton, and Khondaker Miraz Rahman. Role of bacterial efflux pumps in biofilm formation. *Journal of Antimicrobial Chemotherapy*, 73:2003–2020, 2018.

[16] NHS - antibiotics.

[17] Mariya Morar and Gerard D. Wright. The Genomic Enzymology of Antibiotic Resistance. *Annual Review of Genetics*, 44(1):25–51, 2010.

[18] Xiao Su Pan and L. Mark Fisher. Streptococcus pneumoniae DNA gyrase and topoisomerase IV: Overexpression, purification, and differential inhibition by fluoroquinolones. *Antimicrobial Agents and Chemotherapy*, 43(5):1129–1136, 1999.

[19] A. S. Wagman and M. P. Wentland. *Comprehensive Medicinal Chemistry II: Volume 7*. Elsevier, Oxford, 2007.

[20] Rebecca Beyer, Ekaterina Pestova, John J. Millichap, Valentina Stosor, Gary A. Noskin, and Lance R. Peterson. A convenient assay for estimating the possible involvement of efflux of fluoroquinolones by Streptococcus

pneumoniae and Staphylococcus aureus: Evidence for diminished moxifloxacin, sparfloxacin, and trovafloxacin efflux. *Antimicrobial Agents and Chemotherapy*, 44(3):798–801, 2000.

[21] P. L. Ho, W. C. Yam, T. L. Que, D. N. C. Tsang, W. H. Seto, T. K. Ng, and W. S. Ng. Target site modifications and efflux phenotype in clinical isolates of Streptococcus pneumoniae from Hong Kong with reduced susceptibility to fluoroquinolones. *Journal of Antimicrobial Chemotherapy*, 47:655–658, 2001.

[22] Luis Martínez-martínez, Alvaro Pascual, and George A Jacoby. Quinolone resistance from a transferable plasmid. *Lancet*, 351:797–99, 1998.

[23] Jacob Strahilevitz, George A. Jacoby, David C. Hooper, and Ari Robicsek. Plasmid-mediated quinolone resistance: A multifaceted threat. *Clinical Microbiology Reviews*, 22(4):664–689, 2009.

[24] Peter C Fuchs, A L Barry, and Steven D Brown. Susceptibility of multiresistant Streptococcus pneumoniae to ciprofloxacin, ofloxacin and levofloxacin. *Journal of Antimicrobial Chemotherapy*, 39(5):671–672, 1997.

[25] F W Goldstein and J F Acar. Antimicrobial resistance among lower respiratory tract isolates of Streptococcus pneumoniae : results of a 1992-93 Western Europe and USA collaborative surveillance study. *Journal of Antimicrobial Chemotherapy*, 28(Supplement A):71–84, 1996.

[26] Adela G De Campa, Luz Balsalobre, Carmen Ardanuy, Asunción Fenoll, Emilio Pérez-trallero, and Josefina Linares. Fluoroquinolone Resistance in Penicillin-resistant Streptococcus pneumoniae Clones, Spain. *Emerging Infectious Diseases*, 10(10):1751–1759, 2004.

[27] P. L. Ho, R.W.H Yung, D.N.C. Tsang, T.L. Que, M. Ho, W.H. Seto, T.K. Ng, W.C. Yam, and Wilson W. S. Ng. Increasing resistance of Streptococcus pneumoniae to fluoroquinolones: results of a Hong Kong multicentre study in 2000. *Journal of Antimicrobial Chemotherapy*, 48:659–665, 2001.

[28] Guillermo Martín-Gutiérrez, Germán Peñalva, Maite Ruiz-Pérez de Pipaón, Manuela Aguilar, María Victoria Gil-Navarro, José Luis Pérez-Blanco, María Antonia Pérez-Moreno, Rosario Amaya-Villar, Carmen Ferrándiz-Millón, María L. Gascón, Walter A. Goycochea-Valdivia, Manuel E. Jiménez-Mejías, María Dolores Navarro, José A. Lepe, Rocío Alvarez-Marín, Olaf Neth, Ana B. Guisado-Gil, Carmen Infante-Domínguez, José Molina, and José M. Cisneros. Efficacy and safety of a comprehensive educational antimicrobial stewardship program focused on antifungal use. *Journal of Infection*, 80:342–349, 2020.

[29] Rachel A. Miller. A Case for Antifungal Stewardship. *Current Fungal Infection Reports*, 12:33–43, 2018.

[30] Michail S. Lionakis. New insights into innate immune control of systemic candidiasis. *Medical Mycology*, 52(6):555–564, 2014.

[31] Antibiotic resistance threats in the united states, 2013. *U.S. Department of Health and Human Services; Centers for Disease Control and Prevention.*

[32] Matthew C. Fisher, Nichola J. Hawkins, Dominiqe Sanglard, and Sarah J. Gurr. Worldwide emergence of resistance to antifungal drugs challenges human health and food security. *Science*, 360:739–742, 2018.

[33] David S. Perlin, Riina Rautemaa-Richardson, and Ana Alastruey-Izquierdo. The global problem of antifungal resistance: prevalence, mechanisms, and management. *The Lancet Infectious Diseases*, 17:e383–e392, 2017.

[34] Kemal Kazan and Donald M Gardiner. Targeting pathogen sterols : Defence and counterdefence ? *PLoS Pathogens*, 13(5), 2017.

[35] Gordon D Brown, David W Denning, Neil A R Gow, Stuart M Levitz, Mihai G Netea, and Theodore C White. Hidden Killers : Human Fungal Infections. *Medical Mycology*, 4(165), 2012.

[36] Laboratory surveillance of candidaemia in England, Wales and Northern Ireland: 2016. *Public Health England - Health Protection Report*, 11(32), 2017.

[37] Andrea K. Nash, Thomas A. Auchtung, Matthew C. Wong, Daniel P. Smith, Jonathan R. Gesell, Matthew C. Ross, Christopher J. Stewart, Ginger A. Metcalf, Donna M. Muzny, Richard A. Gibbs, Nadim J. Ajami, and Joseph F. Petrosino. The gut mycobiome of the Human Microbiome Project healthy cohort. *Microbiome*, 5(153), 2017.

[38] Keisha Findley, Julia Oh, Joy Yang, Sean Conlan, Clayton Deming, Jennifer A. Meyer, Deborah Schoenfeld, Effie Nomicos, Morgan Park, Heidi H. Kong, and Julia A. Segre. Topographic diversity of fungal and bacterial communities in human skin. *Nature*, 498:367–370, 2013.

[39] Keisha Findley, Julia Oh, Joy Yang, Sean Conlan, Clayton Deming, Jennifer A Meyer, Deborah Schoenfeld, Effie Nomicos, Morgan Park, Heidi H. Kong, and Julia A. Segre. Human Skin Fungal Diversity. *Nature*, 498(7454):367–370, 2013.

[40] Matteo Bassetti, Enrico Maria, Elda Righi, Maurizio Sanguinetti, Francesca Bisio, Brunella Posteraro, Ornella Soro, Roberto Cauda, Claudio Viscoli, and Mario Tumbarello. Incidence, risk factors, and predictors of outcome of candidemia. Survey in 2 Italian university hospitals. *Diagnostic Microbiology and Infectious Diseases*, 58:325–331, 2007.

[41] Rainer Isenmann, Michael Schwarz, Bettina Rau, Matthias Trautmann, Wolfgang Schober, and Hans G. Beger. Characteristics of infection with Candida species in patients with necrotizing pancreatitis. *World Journal of Surgery*, 25:372–376, 2002.

[42] Hitesh S. Deshmukh, Yuhong Liu, Ogechukwu R. Menkiti, Junjie Mei, Ning Dai, Claire E. O'Leary, Paula M. Oliver, Jay K. Kolls, Jeffray N. Welser, and G. Scott Worthen. The microbiota regulates neutrophil homeostasis and host resistance to Escherichia coli K1 sepsis in neonatal mice. *Nature medicine*, 20(5):524–30, 2014.

[43] Sameer Kalghatgi, Catherine S. Spina, James C. Costello, Marc Liesa, J. Ruben Morones-Ramirez, Shimyn Slomovic, Anthony Molina, Orian S.

Shirihai, and James J. Collins. Bactericidal antibiotics induce mitochondrial dysfunction and oxidative damage in mammalian cells. *Science Translational Medicine*, 5(192), 2013.

[44] B. F. Farber and R. C. Moellering. Retrospective study of the toxicity of preparations of vancomycin from 1974 to 1981. *Antimicrobial Agents and Chemotherapy*, 23(1):138–141, 1983.

[45] Barbara E. Murray. Vancomycin-Resistant Enterococcal Infections. *The New England Journal of Medicine*, 342(10):710–721, 2000.

[46] Michail S. Lionakis and Mihai G. Netea. Candida and Host Determinants of Susceptibility to Invasive Candidiasis. *PLoS Pathogens*, 9(1), 2013.

[47] P. C. J. Leijh, M. T. Van Den Barselaar, and R. Van Furth. Kinetics of phagocytosis and intracellular killing of Candida albicans by human granulocytes and monocytes. *Infection and Immunity*, 17(2):313–318, 1977.

[48] M. Baccarini, F. Bistoni, P. Puccetti, and E. Garaci. Natural Cell-Mediated Cytotoxicity Against Candida albicans Induced by Cyclophosphamide : Nature of the In Vitro Cytotoxic Effector. *Infection and Immunity*, 42(1):1–9, 1983.

[49] E. Blasi, L. Pitzurra, M. Puliti, L. Lanfrancone, and F. Bistoni. Early differential molecular response of a macrophage cell line to yeast and hyphal forms of Candida albicans. *Infection and Immunity*, 60(3):832–837, 1992.

[50] Jennifer Martinez. LAP it up, fuzz ball: a short history of LC3-associated phagocytosis. *Current Opinion in Immunology*, 55:54–61, 2018.

[51] Jennifer Martinez, R. K.Subbarao Malireddi, Qun Lu, Larissa Dias Cunha, Stephane Pelletier, Sebastien Gingras, Robert Orchard, Jun Lin Guan, Haiyan Tan, Junmin Peng, Thirumala Devi Kanneganti, Herbert W. Virgin, and Douglas R. Green. Molecular characterization of LC3-associated phagocytosis reveals distinct roles for Rubicon, NOX2 and autophagy proteins. *Nature Cell Biology*, 17(7):893–906, 2015.

[52] Sophie Dupré-Crochet, Marie Erard, and Oliver Nüβe. ROS production in phagocytes: why, when, and where? *Journal of Leukocyte Biology*, 94:657–670, 2013.

[53] Erika Rendra, Vladimir Riabov, Dieuwertje M. Mossel, Tatyana Sevastyanova, Martin C. Harmsen, and Julia Kzhyshkowska. Reactive oxygen species (ROS) in macrophage activation and function in diabetes. *Immunobiology*, 224:242–253, 2019.

[54] Sarah Fischer and Ludwig Eichinger. Dictyostelium discoideum and autophagy – a perfect pair. *International Journal of Developmental Biology*, 63:485–495, 2019.

[55] Isei Tanida. Autophagy basics. *Microbiology and Immunology*, 55:1–11, 2011.

[56] Karim C. EL Kasmi and Kurt R. Stenmark. Contribution of metabolic reprogramming to macrophage plasticity and function. *Seminars in Immunology*, 27:267–275, 2015.

[57] Jan Van den Bossche, Jeroen Baardman, Natasja A. Otto, Saskia van der Velden, Annette E. Neele, Susan M. van den Berg, Rosario Luque-Martin, Hung Jen Chen, Marieke C.S. Boshuizen, Mohamed Ahmed, Marten A. Hoeksema, Alex F. de Vos, and Menno P.J. de Winther. Mitochondrial Dysfunction Prevents Repolarization of Inflammatory Macrophages. *Cell Reports*, 17:684–696, 2016.

[58] Luke A. J. O'Neill, Rigel J. Kishton, and Jeff Rathmell. A Guide to immunometabolism for immunologists. *Nature Reviews Immunology*, 16(9):553–565, 2016.

[59] Masakuni Fukuzumi, Hiroto Shinomiya, Yasutake Shimizu, Kazuhito Ohishi, and Sayaka Utsumi. Endotoxin-induced enhancement of glucose influx into murine peritoneal macrophages via GLUT 1. *Infection and Immunity*, 64(1):108–112, 1996.

[60] Calum C. Bain and Allan Mci Mowat. Macrophages in intestinal homeostasis and inflammation. *Immunological Reviews*, 260:102–117, 2014.

[61] Anja A. Kühl, Ulrike Erben, Lea I. Kredel, and Britta Siegmund. Diversity of intestinal macrophages in inflammatory bowel diseases. *Frontiers in Immunology*, 6(613), 2015.

[62] Louise Basmaciyan, Fabienne Bon, Tracy Paradis, Pierre Lapaquette, and Frédéric Dalle. Candida Albicans Interactions With The Host: Crossing The Intestinal Epithelial Barrier. *Tissue Barriers*, 7(2), 2019.

[63] Arti Parihar, Timothy D. Eubank, and Andrea I. Doseff. Monocytes and macrophages regulate immunity through dynamic networks of survival and cell death. *Journal of Innate Immunity*, 2:204–215, 2010.

[64] Michail S. Lionakis, Jean K. Lim, Chyi Chia Richard Lee, and Philip M. Murphy. Organ-specific innate immune responses in a mouse model of invasive candidiasis. *Journal of Innate Immunity*, 3:180–199, 2011.

[65] Heather R. Conti, Anna R. Huppler, Natasha Whibley, and Sarah L. Gaffen. Animal models for candidiasis. *Current protocols in Immunology*, 105, 2014.

[66] Young Eun Ha, Kyoung Hye Kong, Mi Hyang Cho, Dong Hou Kim, Young Sup Song, and Seung Yong Yoon. Vancomycin blocks autophagy and induces interleukin-1β release in macrophages. *Journal of Antibiotics*, 68:76–80, 2015.

[67] André Moraes Nicola, Patrícia Albuquerque, Luis R. Martinez, Rafael Antonio Dal-Rosso, Carolyn Saylor, Magdia De Jesus, Joshua D. Nosanchuk, and Arturo Casadevall. Macrophage autophagy in immunity to Cryptococcus neoformans and Candida albicans. *Infection and Immunity*, 80(9):3065–3076, 2012.

[68] Marlène Sauget, Benoît Valot, Xavier Bertrand, and Didier Hocquet. Can MALDI-TOF Mass Spectrometry Reasonably Type Bacteria? *Trends in Microbiology*, 25(6):447–455, 2017.

[69] Anton Y. Peleg, Deborah A. Hogan, and Eleftherios Mylonakis. Medically important bacterial-fungal interactions. *Nature Reviews Microbiology*, 8:340–349, 2010.

[70] Eric F. Kong, Christina Tsui, Sona Kucharikova, David Andes, Patrick Van Dijck, and Mary Ann Jabra-Rizk. Commensal Protection of Staphylococcus aureus against antimicrobials by Candida albicans Biofilm Matrix. *mBio*, 7(5), 2016.

[71] Brian M. Peters and Mairi C. Noverra. Candida albicans-staphylococcus aureus polymicrobial peritonitis modulates host innate immunity. *Infection and Immunity*, 81(6):2178–2189, 2013.

[72] Tomoari Kuriyama, Kiyomasa Nakagawa, Shuichi Kawashiri, Etsuhide Yamamoto, Shinichi Nakamura, and Tadahiro Karasawa. The virulence of mixed infection with Streptococcus constellatus and Fusobacterium nucleatum in a murine orofacial infection model. *Microbes and Infection*, 2:1425–1430, 2000.

[73] Dilys T.H. Leung and Simon Chu. Measurement of oxidative stress: mitochondrial function using the seahorse system. In *Preeclampsia: Methods in Molecular Biology*, volume 1710, chapter 22, pages 285–293. Humana Press, New York, 2018.

[74] Zhimin Duan, Qing Chen, Leilei Du, Jianbo Tong, Song Xu, Rong Zeng, Yuting Ma, Xu Chen, and Min Li. Phagocytosis of Candida albicans inhibits autophagic flux in macrophages. *Oxidative Medicine and Cellular Longevity*, 2018.

[75] Melanie Wellington, Kristy Dolan, and Damian J. Krysan. Live Candida albicans suppresses production of reactive oxygen species in phagocytes. *Infection and Immunity*, 77(1):405–413, 2009.

[76] Brad Spellberg, Ashraf S. Ibrahim, John E. Edwards Jr., and Scott G. Filler. Mice with Disseminated Candidiasis Die of Progressive Sepsis. *The Journal of Infectious Diseases*, 192:336–343, 2005.

[77] Yu Kyong Shin, Ki Young Kim, and Young Ki Paik. Alterations of protein expression in macrophages in response to Candida albicans infection. *Molecules and Cells*, 20(2):271–279, 2005.

[78] Taj Ali Khan, Humaira Mazhar, Shamim Saleha, Hamid Nawaz Tipu, Niaz Muhammad, and Muhammad Nasser Abbas. Interferon-Gamma Improves Macrophages Function against M. tuberculosis in Multidrug-Resistant Tuberculosis Patients. *Chemotherapy Research and Practice*, 2016, 2016.

[79] Michael Heming, Sandra Gran, Saskia L. Jauch, Lena Fischer-Riepe, Antonella Russo, Luisa Klotz, Sven Hermann, Michael Schäfers, Johannes Roth, and Katarzyna Barczyk-Kahlert. Peroxisome proliferator-activated receptor-γ modulates the response of macrophages to lipopolysaccharide and glucocorticoids. *Frontiers in Immunology*, 9(893), 2018.

[80] Antonio José Ruiz-Alcaraz, Violeta Carmona-Martínez, María Tristán-Manzano, Francisco Machado-Linde, María Luisa Sánchez-Ferrer, Pilar García-Peñarrubia, and María Martínez-Esparza. Characterization of human peritoneal monocyte/macrophage subsets in homeostasis: Phenotype, GATA6, phagocytic/oxidative activities and cytokines expression. *Scientific Reports*, 8(12794), 2018.

[81] Stanley J. Stachelek, Ivan Alferiev, James Fulmer, Harry Ischiropoulos, and Robert J. Levy. Biological stability of polyurethane modified with covalent attachement of di-tert-butyl-phenol. *Journal of Biomedical Materials Research Part A*, 82A(4):1004–11, 2007.

[82] Nathalie Uwamahoro, Jiyoti Verma-Gaur, Hsin Hui Shen, Yue Qu, Rowena Lewis, Jingxiong Lu, Keith Bambery, Seth L. Masters, James E. Vince, Thomas Naderer, and Ana Traven. The pathogen Candida albicans hijacks pyroptosis for escape from macrophages. *mBio*, 5(2), 2014.

[83] Timothy M. Tucey, Jiyoti Verma, Paul F. Harrison, Sarah L. Snelgrove, Tricia L. Lo, Allison K. Scherer, Adele A. Barugahare, David R. Powell, Robert T. Wheeler, Michael J. Hickey, Traude H. Beilharz, Thomas Naderer, and Ana Traven. Glucose Homeostasis Is Important for Immune

Cell Viability during Candida Challenge and Host Survival of Systemic Fungal Infection. *Cell Metabolism*, 27:988–1006, 2018.

[84] Andrew L. Croxford and Thorsten Buch. Cytokine reporter mice in immunological research: Perspectives and lessons learned. *Immunology*, 132:1–8, 2010.

[85] Matthias Steglich, Andreas Nitsche, Lutz Von Müller, Mathias Herrmann, Thomas A. Kohl, Stefan Niemann, and Ulrich Nübel. Tracing the spread of clostridium difficile ribotype 027 in Germany based on bacterial genome sequences. *PLoS ONE*, 10(10), 2015.

[86] Benoit Guery, Tatiana Galperine, and Frédéric Barbut. Clostridioides difficile: Diagnosis and treatments. *British Medical Journal*, 366(l4609), 2019.

[87] F. Barbut and J. C. Petit. Epidemiology of Clostridium difficile-associated infections. *Clinical Microbiology and Infection*, 7(8):405–410, 2001.

[88] Evelyn Balsells, Ting Shi, Callum Leese, Iona Lyell, John Burrows, Camilla Wiuff, Harry Campbell, Moe H. Kyaw, and Harish Nair. Global burden of Clostridium difficile infections: A systematic review and meta-analysis. *Journal of Global Health*, 9(1), 2019.

[89] Carl Suetens, Katrien Latour, Tommi Kärki, Enrico Ricchizzi, Pete Kinross, Maria Luisa Moro, Béatrice Jans, Susan Hopkins, Sonja Hansen, Outi Lyytikäinen, Jacqui Reilly, Aleksander Deptula, Walter Zingg, Diamantis Plachouras, and Dominique L. Monnet. Prevalence of healthcare-associated infections, estimated incidence and composite antimicrobial resistance index in acute care hospitals and long-term care facilities: Results from two european point prevalence surveys, 2016 to 2017. *Eurosurveillance*, 23(46):1–17, 2018.

[90] Patrizia Spigaglia, Paola Mastrantonio, and Fabrizio Barbanti. *Antibiotic Resistances of Clostridium difficile*, pages 137–159. Springer International Publishing, Cham, 2018.

[91] Nada Khazal Kadhim Hindi, Zainab H. Alsaadi, Aalaa Fahim Abbas, and Aamal Ghazi Mahdi Al-Saadi. The emergence of multidrug-resistant and hypervirulent Clostridium difficile clinical isolates. *Meta Gene*, 24, 2020.

[92] Wiep Klaas Smits, Dena Lyras, D. Borden Lacy, Mark H. Wilcox, and Ed J. Kuijper. Clostridium difficile infection. *Nature Reviews Disease Primers*, (16020), 2016.

[93] Scott R. Curry, Carlene A. Muto, Jessica L. Schlackman, A. William Pasculle, Kathleen A. Shutt, Jane W. Marsh, and Lee H. Harrison. Use of multilocus variable number of tandem repeats analysis genotyping to determine the role of asymptomatic carriers in Clostridium difficile transmission. *Clinical Infectious Diseases*, 57(8):1094–1102, 2013.

[94] Philippe Bidet, Frédéric Barbut, Valérie Lalande, Béatrice Burghoffer, and Jean Claude Petit. Development of a new PCR-ribotyping method for Clostridium difficile based on ribosomal RNA gene sequencing. *FEMS Microbiology Letters*, 175:261–266, 1999.

[95] J Freeman, J Vernon, S Pilling, K Morris, S Nicholson, S Shearman, C Longshaw, and M H Wilcox. The ClosER study : results from a three-year pan-European longitudinal surveillance of antibiotic resistance among prevalent Clostridium difficile ribotypes, 2011-2014. *Clinical Microbiology and Infection*, 24:724–731, 2018.

[96] Kristina Rizzardi, Thomas Åkerlund, Torbjörn Norén, and Andreas Matussek. Impact of ribotype on Clostridioides difficile diagnostics. *European Journal of Clinical Microbiology and Infectious Diseases*, 39:847–853, 2020.

[97] D. Lachowicz, H. Pituch, D. Wultańska, E. Kuijper, and P. Obuch-Woszczatyński. Surveillance of antimicrobial susceptibilities reveals high proportions of multidrug resistance in toxigenic Clostridium difficile strains in different areas of Poland. *Anaerobe*, 62, 2020.

[98] Clostridium difficile Ribotyping Network (CDRN) for England and Northern Ireland 2015-2018. *Public Health England*.

[99] Anne J. Gonzales-Luna, Travis J. Carlson, Kierra M. Dotson, Kelley Poblete, Gabriela Costa, Julie Miranda, Chris Lancaster, Seth T. Walk, Shawn Tupy, Khurshida Begum, M. Jahangir Alam, and Kevin W. Garey. PCR ribotypes of Clostridioides difficile across Texas from 2011 to 2018 including emergence of ribotype 255. *Emerging Microbes and Infections*, 9(1):341–347, 2020.

[100] David Griffiths, Warren Fawley, Melina Kachrimanidou, Rory Bowden, Derrick W. Crook, Rowena Fung, Tanya Golubchik, Rosalind M. Harding, Katie J.M. Jeffery, Keith A. Jolley, Richard Kirton, Tim E. Peto, Gareth Rees, Nicole Stoesser, Alison Vaughan, A. Sarah Walker, Bernadette C. Young, Mark Wilcox, and Kate E. Dingle. Multilocus sequence typing of Clostridium difficile. *Journal of Clinical Microbiology*, 48(3):770–778, 2010.

[101] Andrew J. Page, Carla A. Cummins, Martin Hunt, Vanessa K. Wong, Sandra Reuter, Matthew T. G. Holden, Maria Fookes, Daniel Falush, Jacqueline A. Keane, and Julian Parkhill. Roary: Rapid large-scale prokaryote pan genome analysis. *Bioinformatics*, 31(22):3691–3693, 2015.

[102] Zhong Peng, Dazhi Jin, Hyeun Bum Kim, Charles W. Stratton, Bin Wu, Yi-Wei Tang, and Xingmin Sun. Update on antimicrobial resistance in Clostridium difficile: Resistance mechanisms and antimicrobial susceptibility testing. *Journal of Clinical Microbiology*, 55(7):1998–2008, 2017.

[103] Hannes Mutschler and Anton Meinhart. ϵ/ζ systems: Their role in resistance, virulence, and their potential for antibiotic development. *Journal of Molecular Medicine*, 89:1183–1194, 2011.

[104] Shan Goh, Haitham Hussain, Barbara J. Chang, Warren Emmett, Thomas V. Riley, and Peter Mullany. Phage C2 mediates transduction of Tn6215, encoding erythromycin resistance, between Clostridium difficile strains. *mBio*, 4(6), 2013.

[105] Karin Sauer. The genomics and proteomics of biofilm formation. *Genome Biology*, 4(219), 2003.

[106] Mark E. Rupp, Roger G. Finch, and John L. Pace. *Biofilms, Infection, and Antimicrobial Therapy*. Taylor & Francis, first edition, 2005.

[107] Hannah H. Tuson and Douglas B. Weibel. Bacteria-surface interactions. *Soft Matter*, 9(18):4368–4380, 2013.

[108] Philip S. Stewart. Mechanisms of antibiotic resistance in bacterial biofilms. *International Journal of Medical Microbiology*, 292:107–113, 2002.

[109] Divakar Sharma, Lama Misba, and Asad U. Khan. Antibiotics versus biofilm: An emerging battleground in microbial communities. *Antimicrobial Resistance and Infection Control*, 8(76), 2019.

[110] Gebreselema Gebreyohannes, Andrew Nyerere, Christine Bii, and Desta Berhe Sbhatu. Challenges of intervention, treatment, and antibiotic resistance of biofilm-forming microorganisms. *Heliyon*, 5, 2019.

[111] L. H. Sperling. *Introduction to Physical Polymer Science*. John Wiley & Sons, Inc., second edition, 1992.

[112] Mustafa Fincan. *Assessing Viscoelastic Properties of Polydimethylsiloxane (PDMS) Using Loading and Unloading of the Macroscopic Compression Test*. PhD thesis, 2015.

[113] Michael Taylor, Andrew J. Urquhart, Daniel G. Anderson, Philip M. Williams, Robert Langer, Morgan R. Alexander, and Martyn C. Davies. A methodology for investigating protein adhesion and adsorption to microarrayed combinatorial polymers. *Macromolecular Rapid Communications*, 29:1298–1302, 2008.

[114] Ying Mei, Sharon Gerecht, Michael Taylor, Andrew J. Urquhart, Said R. Bogatyrev, Seung-Woo Cho, Martyn C. Davies, Morgan R. Alexander, Robert S. Langer, and Daniel G. Anderson. Mapping the interactions among biomaterials, adsorbed proteins, and human embryonic stem cells. *Advanced Materials*, 21(27):2781–2786, 2009.

[115] Salvatore Pernagallo, Mei Wu, Maurice P. Gallagher, and Mark Bradley. Colonising new frontiers - Microarrays reveal biofilm modulating polymers. *Journal of Materials Chemistry*, 21:96–101, 2011.

[116] Andrew L Hook, Chien-yi Chang, Jing Yang, Jeni Luckett, Alan Cockayne, Steve Atkinson, Ying Mei, Roger Bayston, Derek J Irvine, Robert Langer, Daniel G Anderson, Paul Williams, Martyn C Davies, and Morgan R Alexander. Combinatorial discovery of polymers resistant to bacterial attachment. *Nature Biotechnology*, 30(9):868–875, 2012.

[117] Andrew L. Hook, Chien Yi Chang, Jing Yang, Steve Atkinson, Robert Langer, Daniel G. Anderson, Martyn C. Davies, Paul Williams, and Morgan R. Alexander. Discovery of novel materials with broad resistance to bacterial attachment using combinatorial polymer microarrays. *Advanced Materials*, 25:2542–2547, 2013.

[118] Kevin Adlington, Nam T Nguyen, Elizabeth Eaves, Jing Yang, Chien-yi Chang, Jianing Li, Alexandra L. Gower, Amy Stimpson, Daniel G. Anderson, Robert Langer, Martyn C. Davies, Andrew L Hook, Paul Williams, Morgan R Alexander, and Derek J Irvine. Application of Targeted Molecular and Material Property Optimization to Bacterial Attachment-Resistant (Meth)acrylate Polymers. *Biomacromolecules*, 17(9):2830–2838, 2016.

[119] Seung Pyo Jeong, Bong Soo Lee, Sung Min Kang, Sangwon Ko, Insung S Choi, and Jungkyu K Lee. Binding behaviors of protein on spatially controlled poly[oligo(ethylene glycol) methacrylate] brushes grafted from mixed self-assembled monolayers on gold. *Chemical Communications*, 50:5291–5293, 2014.

[120] Bonnie J. Tyler, Andrew Hook, Andreas Pelster, Paul Williams, Morgan Alexander, and Heinrich F. Arlinghaus. Development and characterization of a stable adhesive bond between a poly(dimethylsiloxane) catheter material and a bacterial biofilm resistant acrylate polymer coating. *Biointerphases*, 12(2), 2017.

[121] N. Jeffery, K. Kalenderski, J. Dubern, A. Lomiteng, M. Dragova, A. Frost, B. Macrae, A. Mundy, M. Alexander, P. Williams, and D. Andrich. A new bacterial resistant polymer catheter coating to reduce catheter associated urinary tract infection (CAUTI): A first-in-man pilot study. *European Urology Supplements*, 18(1):e377, 2019.

[122] Olutoba Sanni, Chien-yi Chang, Daniel G Anderson, Robert Langer, Martyn C Davies, Philip M Williams, Paul Williams, Morgan R Alexander, and Andrew L Hook. Bacterial Attachment to Polymeric Materials Correlates with Molecular Flexibility and Hydrophilicity. *Advanced healthcare materials*, 4:695–701, 2015.

[123] Adam A. Dundas, Olutoba Sanni, Jean-Frédéric Dubern, Georgios Dimitrakis, Andrew L. Hook, Derek J. Irvine, Paul Williams, and Morgan R. Alexander. Validating a predictive structure-property relationship by discovery of novel polymers which reduce bacterial biofilm formation. *Advanced Materials*, 31(49), 2019.

[124] Adrian V.K. Wong, Nitin Arora, Olusegun Olusanya, Ben Sharif, Robert M. Lundin, A. Dhadda, S. Clarke, R. Siviter, M. Argent, Gavin Denton, Anna Dennis, Angela Day, and Tamas Szakmany. Insertion rates and complications of central lines in the UK population: A pilot study. *Journal of the Intensive Care Society*, 19(1):19–25, 2018.

[125] Craig Kornbau, Kathryn C Lee, Gwendolyn D Hughes, and Michael S Firstenberg. Central line complications. *International Journal of Critical Illness and Injury Science*, 5(3):170–178, 2015.

[126] Samir Hodzic, Darko Golic, Jasmina Smajic, Selma Sijercic, Sekib Umihanic, and Sefika Umihanic. Complications Related to Insertion and Use of Central Venous Catheters (CVC). *Medical archives*, 68(5):300–303, 2014.

[127] William C. Dube, Jesse T. Jacob, Ziduo Zheng, Yijian Huang, Chad Robichaux, James P. Steinberg, and Scott K. Fridkin. Comparison of Rates of Central Line-Associated Bloodstream Infections in Patients With 1 vs 2 Central Venous Catheters. *JAMA network open*, 3(3), 2020.

[128] Alessandra Amaral Schwanke, Mitzy Tannia Reichembach Danski, Letícia Pontes, Solena Ziemer Kusma, and Jolline Lind. Central venous catheter for hemodialysis: incidence of infection and risk factors. *Revista brasileira de enfermagem*, 71(3):1115–1121, 2018.

[129] Regina E. Nailon and Mark E. Rupp. Surveillance of home health central venous catheter care outcomes: Challenges and future directions. *American Journal of Infection Control*, 47:1382–1387, 2019.

[130] Jingjing Han, Jun Wan, Yujia Cheng, Dan Li, Min Deng, Xuefen Wang, Jiarui Feng, Yuhong He, Qing Ye, Li Wang, Yourong Lei, and Jianmiao Wang. A hospital-wide reduction in central line–associated bloodstream infections through systematic quality improvement initiative and multidisciplinary teamwork. *American Journal of Infection Control*, 47:1358–1364, 2019.

[131] S. B. Mishra, R. Misra, A. Azim, A. K. Baronia, K. N. Prasad, T. N. Dhole, M. Gurjar, R. K. Singh, and B. Poddar. Incidence, risk factors and associated mortality of central line-associated bloodstream infections at an intensive care unit in Northern India. *International Journal for Quality in Health Care*, 29(1):63–67, 2017.

[132] S. Christopher Derderian, Ryan Good, Raphael N. Vuille-dit Bille, Todd Carpenter, and Denis D. Bensard. Central venous lines in critically ill children: Thrombosis but not infection is site dependent. *Journal of Pediatric Surgery*, 54:1740–1743, 2019.

[133] John R. Gowardman, Iain K. Robertson, Scott Parkes, and Claire M. Rickard. Influence of insertion site on central venous catheter colonization and bloodstream infection rates. *Intensive Care Medicine*, 34(6):1038–1045, 2008.

[134] Bart J. A. Rijnders, Eric Van Wijngaerden, and Willy E. Peetermans. Catheter-Tip Colonization as a Surrogate End Point in Clinical Studies on Catheter-Related Bloodstream Infection: How Strong Is the Evidence? *Clinical Infectious Diseases*, 35(9):1053–1058, 2002.

[135] LPN IV Series: Central Venous Catheters and Arterial Catheters.

[136] Thais Yoshida, Ana Elisa Bauer De Camargo Silva, Luciana Leite Pineli Simões, and Rafael Alves Guimarães. Incidence of central venous catheter-related bloodstream infections: Evaluation of bundle prevention in two intensive care units in central Brazil. *Scientific World Journal*, 2019, 2019.

[137] Anika C. Jahns and Oleg A. Alexeyev. Microbial colonization of normal skin: Direct visualization of 194 skin biopsies. *Anaerobe*, 38:47–49, 2016.

[138] Rodney M. Donlan. Biofilm elimination on intravascular catheters: Important considerations for the infectious disease practitioner. *Clinical Infectious Diseases*, 52(8):1038–1045, 2011.

[139] Priyadarshini Singha, Marcus J. Goudie, Qiaohong Liu, Sean Hopkins, Nettie Brown, Chad W. Schmiedt, Jason Locklin, and Hitesh Handa. Multipronged Approach to Combat Catheter-Associated Infections and Thrombosis by Combining Nitric Oxide and a Polyzwitterion: A 7 Day in Vivo Study in a Rabbit Model. *ACS Applied Materials and Interfaces*, 12(8):9070–9079, 2020.

[140] Taranjit Singh, Andrew L Hook, Jeni Luckett, Manfred F Maitz, Claudia Sperling, Carsten Werner, Martyn C Davies, Derek J Irvine, Paul Williams, and Morgan R Alexander. Discovery of Hemocompatible Bacterial Biofilm-Resistant Copolymers. *UNPUBLISHED*.

[141] Henk J. Busscher, Henny C. Van Der Mei, Guruprakash Subbiahdoss, Paul C. Jutte, Jan J.A.M. Van Den Dungen, Sebastian A.J. Zaat, Marcus J. Schultz, and David W. Grainger. Biomaterial-associated infection: Locating the finish line in the race for the surface. *Science Translational Medicine*, 4(153), 2012.

[142] F Fitzpatrick, H Humphreys, and J P O Gara. The genetics of staphylococcal biofilm formation — will a greater understanding of pathogenesis lead to better management of device-related infection ? 2005.

[143] Lingyan Li, Shengfu Chen, Jie Zheng, Buddy D Ratner, and Shaoyi Jiang. Protein Adsorption on Oligo (ethylene glycol) -Terminated Alkanethiolate Self-Assembled Monolayers : The Molecular Basis for Nonfouling Behavior. pages 2934–2941, 2005.

[144] Ekram Wassel, Siyu Jiang, Qimeng SOng, Stephan Vogt, Gilbert Noll, Sergey I. Druzhinin, and Holger Schonherr. Thickness Dependence of Bovine Serum Albumin Adsorption on Thin Thermoresponsive Poly(diethylene glycol) Methyl Ether Methacrylate Brushes by Surface Plasmon Resonance Measurements. *Langmuir*, 32(36):9360–9370, 2016.

[145] Hongwei Ma, Matthew Wells, Thomas P Beebe, and Ashutosh Chilkoti. Surface-Initiated Atom Transfer Radical Polymerization of Oligo (ethylene glycol) Methyl Methacrylate from a Mixed Self-Assembled Monolayer on Gold. *Advanced Functional Materials*, 16:640–648, 2006.

[146] Andrew Ian Hong Phua, Kay Yee Hon, Andrew Holt, Margie O'Callaghan, and Shailesh Bihari. Candida catheter-related bloodstream infection in patients on home parenteral nutrition - Rates, risk factors, outcomes, and management. *Clinical Nutrition ESPEN*, 31:1–9, 2019.

[147] Cindy Vallieres, Andrew L Hook, Yinfeng He, and Valentina Cuzzucoli Crucitti. Discovery of (Meth) Acrylate Polymers that Resist Colonization by Fungi associated with Pathogenesis and Biodeterioration. pages 1–34.